Characterization of Spontaneous Motor Recovery and Changes in Plasticity-Limiting Perineuronal Nets Following Cortical and Subcortical Stroke

Sai Sudarshan Karthikeyan

Thesis submitted to the
Faculty of Graduate and Postdoctoral Studies
in partial fulfillment of the requirements
for the Master of Science degree in Neuroscience

Department of Cellular and Molecular Medicine

Faculty of Medicine

University of Ottawa

Permission to Reprint Published Material

Figure 1 was adapted from ‘Stroke rehabilitation’ (Langhorne et al., 2011) with permission from Elsevier, license number 4090951017960.

Figure 2A was adapted from ‘The chemorepulsive protein semaphorin 3A and perineuronal net-mediated plasticity’ (de Winter et al., 2016) which is an open access article distributed under the Creative Commons Attribution License.

Figure 2B was adapted from ‘Very long-term memories may be stored in the pattern of holes in the perineuronal net’ (Tsien, 2013). Permission was not required from the Proceedings of the National Academy of Sciences to reproduce this figure.

Abstract

Stroke is a leading cause of neurological disability, often resulting in long-term motor impairments due to damage to the striatum and/or motor cortex. While both humans and animals show spontaneous recovery following stroke, little is known about how the injury location affects recovery and what causes recovery to plateau. This information is essential in order to improve current rehabilitation practice and develop new therapies to enhance recovery.

In this thesis, we used endothelin-1 (ET-1), a potent vasoconstrictor, to produce focal infarcts in the forelimb motor cortex (FMC), the dorsolateral striatum (DLS) or both the FMC and DLS in male Sprague-Dawley rats. In the first experiment, the spontaneous recovery profile of animals was followed over an 8-week period using multiple behavioural tasks assessing motor function and limb preference to identify how recovery varies depending on injury location. Infarct volumes were measured to determine the association between injury and behavioural outcome.

All three groups had significant functional impairments on the Montoya staircase, beam traversal, and cylinder tests following stroke, with the combined group having the largest and most persistent impairments. Importantly, spontaneous recovery was not simply dependent on lesion volume but on the lesion location and the behavioural test employed.

In the second experiment, we focused on a potential cellular mechanism thought to underlie post-stroke plasticity and functional recovery. In a separate cohort of animals, we assessed how plasticity-limiting perineuronal nets (PNNs) and associated parvalbumin-positive (PV) GABAergic interneurons change following similar ET-1 strokes as in the prior experiment.

A significant reduction in the density of PNNs was observed in the perilesional cortex of animals that received a cortical-only or combined stroke but not a striatal-only injury. Although

there were no significant differences in the density of PV interneurons between sham and stroked groups, a significant negative correlation existed between cortical infarct volume and the density of PV interneurons in the perilesional cortex.

Taken together these results demonstrate that lesion location influences motor recovery and neuroplastic changes following stroke. This supports the idea that a "one size fits all" approach for stroke rehabilitation may not be effective and treatment needs to be individualized to the patient.

Table of Contents

List of Figures

List of Tables

List of Abbreviations

AP	Anteroposterior
ANOVA	Analysis of variance
ChABC	Chondroitinase ABC
CNS	Central nervous system
CSPGs	Chondroitin sulfate proteoglycans
DLS	Dorsolateral striatum
DV	Dorsoventral
E/I	Excitatory/Inhibitory
ET-1	Endothelin-1
ECM	Extracellular matrix
FMC	Forelimb motor cortex
GABA	Gamma-Aminobutyric acid
HA	Hyaluronan
MCAO	Middle cerebral artery occlusion
ML	Mediolateral
MRI	Magnetic resonance imaging
PBS	Phosphate-buffered saline
PFA	Paraformaldehyde
PNN(s)	Perineuronal net(s)
PR	Pellets retrieved
PV	Parvalbumin
REGW-F	Ryan-Einot-Gabriel-Welch F
RT	Room temperature
SD	Sprague-Dawley rat

Acknowledgments

First, I would like to sincerely thank my supervisor Dr. Dale Corbett, for providing me with the environment, resources and the many opportunities to excel academically and grow as a researcher. I am very grateful for his constant support and encouragement over the past couple of years.

I would also like to thank Dr. Paul Albert and Dr. Diane Lagace for serving on my thesis advisory committee and for their invaluable feedback throughout this project.

A special thank you to Matthew Jeffers, lab manager extraordinaire for his dedicated involvement with every aspect of this thesis from the very beginning.

A huge thank you to my fellow lab mates, past and present for their advice, technical assistance and support with this thesis: Anthony Carter, Nicolay Hristozov, Sabina Antonescu, Mariana Gomez-Smith, Dr. Jessy Livingston-Thomas, Paul Nelson, Sarah Gasinzigwa and Amanda Nitschke. All of them made my graduate experience a lot more fun and memorable.

I am very grateful to the Canadian Institutes of Health Research, the Ontario Ministry of Training, Colleges and Universities and the University of Ottawa for providing me with scholarship support.

Last but not least, I would like to thank my parents and my brother for their never-ending support and encouragement.

Introduction

1.1 Stroke: Epidemiology and Pathophysiology

In Canada, over 62,000 strokes occur each year making it a leading cause of death and neurological disability [1]. With improvement in stroke prevention and acute stroke care, more individuals are surviving strokes; however, this has resulted in more living with long-term stroke-induced disabilities. Currently, over 405,000 Canadians are living with the after effects of stroke, and with an aging population this number is projected to double in the next two decades [2]. As a result, stroke imposes a major financial burden on patients, their families, and the health care system. It is estimated that the average cost of treating a stroke patient in Canada in the first year alone is $75,000 with an annual national cost of over $3.0 billion dollars [3]. Thus, these statistics demonstrate the urgent need for novel and effective treatment strategies to further improve independence and quality of life of stroke survivors.

There are two main types of strokes: hemorrhagic and ischemic. A hemorrhagic stroke results from weakened blood vessels rupturing and leaking in the brain, whereas ischemic strokes are caused by blockages (e.g. clots) of blood vessels in the brain. While hemorrhagic strokes are more likely to result in death [4], ischemic strokes are far more common and represent ~87% of all strokes [5]. This thesis focuses specifically on ischemic stroke.

Following a stroke, neurons become dysfunctional if deprived of oxygen for more than a few seconds, with structural damage occurring within minutes [6]. A lack of oxygen and glucose results in impaired ATP production, leading to the failure of energy-dependent processes that maintain ionic gradients across the cell membrane and are crucial for neuronal survival. This triggers a series of cell death cascades involving both apoptosis and necrosis, resulting in tissue loss and ultimately functional impairments [7, 8]. Surrounding the ischemic core is a region with

reduced blood flow, called the penumbra, which is supplied by collateral circulation. In contrast to the ischemic core, where neurons are rapidly lost, neurons in the penumbra remain structurally intact and are therefore potentially salvageable if blood flow is restored promptly [7, 9].

In the acute phase, ischemic stroke treatment focuses on restoring blood flow to the deprived brain regions to minimize the extent of tissue damage. Currently, treatment is limited to the use of the thrombolytic drug, tissue plasminogen activator (t-PA) and mechanical thrombectomy. Although effective, the narrow time window (3-4.5 hours after stroke onset) limits the use of t-PA to less than 10% of the stroke population [10, 11]. Similarly, mechanical thrombectomy must be performed within 6-7 hours after stroke onset in order for it to be beneficial, thereby restricting its use [12]. Therefore, for most stroke survivors, rehabilitation offers the greatest hope for improved functional outcome [13].

1.2 Stroke Location and Functional Outcome

Stroke can result in impairments to a wide range of neural systems; including motor, somatosensory, visual, linguistic, and cognitive domains. Stroke survivors often display more than one type of deficit [14]. The occurrence of a particular impairment is dependent on the region of the brain that has been affected. Motor impairments, including upper limb hemiparesis, are the most common deficits affecting ~80%-85% of all stroke patient [14, 15]. These impairments result from damage to specific cortical regions (e.g. primary motor cortex, primary somatosensory cortex, secondary sensorimotor cortical areas), subcortical structures (e.g. basal ganglia, thalamus, internal capsule), and/or the corticospinal tract [16]. This thesis focuses on post-stroke recovery of motor function.

Although several studies have attempted to examine the association between location of stroke injury and functional outcome of motor function, very few have directly compared recovery following a cortical and subcortical stroke. Some studies have shown that location of lesion does matter, and that patients with a cortical-only injury respond better to rehabilitation and show better motor recovery than those with a purely subcortical stroke (basal ganglia, internal capsule and/or thalamus) [17, 18]. Surprisingly, in one of the studies, stroke patients with a mixed cortico-subcortical injury showed better motor outcomes than those with purely subcortical stroke, despite having a larger total infarct volume [18]. This suggests that lesion location may be a more important predictor of recovery than the lesion size. The location of lesion has also been shown to influence the time course of recovery. Patients with subcortical strokes tend to take longer to recover than those with a cortical injury [19, 20]. Since subcortical strokes often affect both the primary and secondary motor pathways, they are thought to result in worsened outcomes compared to strokes isolated to the cortex [17]. In contrast to these studies, others have reported that the location of lesion (cortical/subcortical) does not affect functional outcome [21, 22]. Clearly, further research is needed to clarify the effect of lesion location on motor recovery following stroke.

Evidence from multiple large-scale prospective clinical studies indicate that strokes primarily affect subcortical structures such as the basal ganglia, white matter and/or the thalamus [23–25]. In these studies, cortical-only strokes accounted for less than ~15% of the total number of strokes (Table 1). The region of infarct (cortical, subcortical or cortico-subcortical) is dependent on the vascular territory that has been occluded. Occlusion of the middle cerebral artery (MCA) is the most common form of stroke in humans [26]. Occlusion of the distal branches of the MCA results in damage limited to cortical regions (e.g. sensory and motor

Study/Year	Sample Size	% Subcortical Injury	% Cortical Injury	% Cortico-Subcortical Injury
Kang, 2003	n=104	50%	16%	33%
Wessels, 2006	n=302	66%	14%	16%
Corbetta, 2015	n=132	39%	13%	23%

Table 1: Frequency of cortical and subcortical strokes in large-scale prospective studies. [23–25]

cortex) whereas occlusion of the proximal branches result in larger strokes affecting both cortical and subcortical regions. Isolated subcortical strokes (e.g. striatum or internal capsule) typically result from occlusion of the small perforating lenticulostriate branches that arise from the MCA [27].

Despite the high prevalence of subcortical strokes, pre-clinical stroke research has emphasized and continues to focus on investigating and treating cortical strokes. A recent study compared lesion profiles between pre-clinical studies and a clinical trial and found that current pre-clinical models result in either too large or superficial strokes and may not be representative of the clinical population. This mismatch in lesion characteristics between pre-clinical and clinical research could impair translational efforts [28].

An aim of this thesis was to capture the heterogeneity of human stroke, and investigate whether lesion location influences functional recovery in a rat model of stroke. Focal strokes were directed at the forelimb motor cortex (FMC; homologous to the human primary motor cortex) and/or the dorsolateral striatum (DLS; homologous to the human caudate and putamen; components of the basal ganglia) [29].

1.3 Animal Models of Stroke

Several animal models of stroke have been developed in order to study the complex pathophysiology of ischemia as well as to evaluate new interventions [30]. Rats are one of the most commonly used species for investigating neural plasticity and functional recovery after brain injury. They have a cerebral vasculature that is very similar to that of humans and their small brain size allows for easy histological analysis [31]. Importantly, rats exhibit similar limb movements to that of humans and several validated behavioural tests are available for assessing

upper limb function [32, 33]. The three most widely used stroke models in rats are middle cerebral artery occlusion (MCAO), photothromobosis (PT) and endothelin-1 (ET-1) administration. The advantages and disadvantages of each model are summarized below.

One approach for producing strokes is through the occlusion of the MCA which is a common cause of ischemic injury in humans [34]. Several variations of this model exist, however the intraluminal suture method is the most widely used model. This technique involves insertion of a suture or filament through the internal carotid artery into the MCA. Transient occlusion is achieved by retracting the suture after varying durations of time, allowing for reperfusion, whereas permanent occlusion is produced by leaving the suture in place permanently [35]. This model does not require craniotomy and can produce a combined cortical and striatal injury, which is characteristic of human stroke. However, the intraluminal suture model frequently produces very large infarcts that are similar to malignant infarctions in humans which are untreatable. Moreover, it also affects brain regions not typically affected in humans, thereby causing unintended behavioural and physiological effects [35]. For example, hypothalamic damage is often seen after long duration occlusions. Damage to the hypothalamus results in a hyperthermic response which exacerbates cell death, and therefore could complicate studies evaluating neuroprotective interventions [35, 36]. Other models of MCAO were developed to produce smaller injuries and avoid damage to the thalamus, hypothalamus and hippocampus typically seen with the suture model. However, these models involve invasive surgery, require a high degree of technical skill, and risk possible damage to autonomic nerve fibres [35, 37].

In the PT model of stroke, a photosensitive dye is administered and ischemia is induced by immediately illuminating the targeted brain region with a light source [38]. Irradiation causes

activation of the dye, generating free radicals that cause endothelial damage and platelet aggregation. This results in thrombus formation and disruption of local blood flow [39]. This model is non-invasive and produces small cortical strokes with well-defined infarct boundaries. However, it is difficult to produce subcortical injuries with this model. Another disadvantage of the PT model, particularly for neuroprotective studies, is that it lacks an ischemic penumbra region as limited reperfusion is observed following stroke [35]. Furthermore, the injury response and pattern of edema development observed following PT differs from human stroke and is more similar to that seen in traumatic brain injuries [35].

Another widely used method for producing focal strokes is the potent vasoconstricting agent endothelin-1; a peptide that can be applied topically or stereotaxically injected into specific regions of the brain [40–42]. ET-1 causes a rapid reduction in blood flow (~30%-50% of baseline level) followed by gradual reperfusion over several hours, modeling the blood flow changes seen in human stroke patients [43] and resulting in an ischemic penumbra region. An advantage of this model is the ability to produce focal infarcts in deep subcortical regions such as the dorsolateral striatum or the internal capsule [44, 45]. Furthermore, the size of injury can be easily controlled by changing the volume and concentration of ET-1 [46]. While this model works well in the rat, it is difficult to produce consistent injury in mice [47]. This may be due to interspecies difference in the distribution of ET_A and ET_B receptors that favor dilation over constriction [48]. Another complicating factor with this model is that ET-1 levels are naturally elevated following stroke and therefore could confound studies investigating neuroprotective strategies [49, 50].

As stroke is a complex and heterogeneous disorder, no single model can completely capture all aspects of it. Therefore when selecting a model, researchers need to carefully consider

the advantages and limitations of each model, and select one that best addresses their research question. This thesis was aimed at evaluating recovery following focal strokes to specific cortical and subcortical regions. The ET-1 model was the most suitable as it allowed for strokes to be induced in deep subcortical regions.

1.4 Spontaneous Recovery after Stroke

Spontaneous recovery refers to the amount of functional improvement after stroke that is determined by passage of time alone [51]. Both humans and animals demonstrate some degree of spontaneous recovery following stroke [8, 52, 53]. Since a vast majority of stroke survivors receive rehabilitation therapy it is very difficult to study this in humans. Moreover, due to heterogeneity among stroke patients in both severity of impairment and type of functions affected, it is challenging to characterize this process in detail. However, several trends in the pattern of recovery have been identified [52]. Evidence suggests that spontaneous recovery after stroke, follows a non-linear, logarithmic pattern [54] (Figure 1). In humans, most of the recovery typically occurs within the first three months following stroke, after which recovery reaches a plateau [55]. However, the pattern of recovery is different across functional domains [52]. For instance, recovery of language and cognitive function can continue well beyond the first three months [56, 57].

Recovery of motor function has been the most studied of all domains of stroke impairments [52]. In stroke patients with hemiplegia, first voluntary movements are observed starting from 6 to 33 days post-stroke [58]. Moreover, studies examining motor impairments have identified that the biggest gains in motor recovery occur within the first 30 days, although

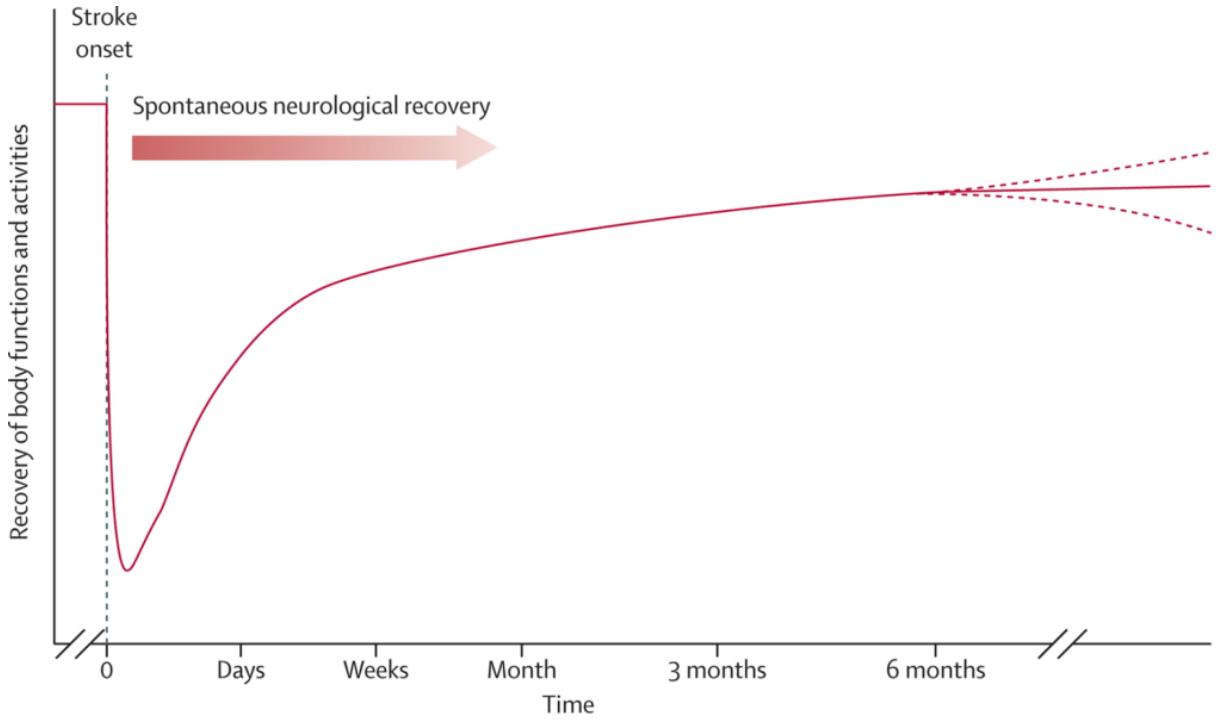

Figure 1: Spontaneous neurological recovery following stroke. Recovery follows a non-linear, logarithmic pattern. Most recovery occurs in the first three months after stroke. Reproduced from: Langhorne et al. (2011) [54]

in patients with more severe impairments, recovery may continue up to 90 days post-stroke [59–61]. Similar patterns of motor recovery have been observed in pre-clinical models of stroke, although within shorter time courses [53].

Interestingly, recent clinical work has shown that upper limb motor impairments in most stroke patients resolves by a fixed proportion (~70% of their maximum possible improvement) and can be predicted based on the initial level of impairment or corticospinal tract injury [62–65]. This phenomenon is referred to as the "proportional recovery rule" and has been found to also apply to other functional domains including language, visuospatial attention, and verbal/spatial memory [14, 66, 67]. Furthermore, the rule has been shown to hold true for patients across a range of demographics and even across countries with different rehabilitation practices [62, 63, 65, 68]. The existence of this rule implies that post-stroke functional improvement may be mostly due to spontaneous recovery and that current rehabilitation might not be providing any added benefits [69]. In clinical research, as it is unethical to withhold treatment including rehabilitation it is not possible to investigate true spontaneous recovery. Therefore, pre-clinical models of stroke provide a valuable tool to study spontaneous recovery of motor function.

1.5 Mechanisms of Spontaneous Recovery

Spontaneous functional recovery is thought to be mediated by the interaction of a number of mechanisms including resolution of diaschisis, behavioural compensation and cortical reorganization [70].

Diaschisis, refers to reduced blood flow and metabolism in remote and uninjured brain regions that are connected to the injured area [71]. It occurs due to sudden disruption of afferent

input from the injured area. Diaschisis begins to resolve as changes in blood flow, edema and inflammation improve over time [72]. Evidence suggests that resolution of this phenomenon may contribute to functional improvement after stroke [73].

In addition, behavioural compensation may also explain recovery in the absence of any interventions [74]. Both humans and animals often use compensatory movement patterns to accomplish tasks in a different manner than they did prior to stroke [75, 76]. Use of such strategies allow patients to show improvement on functional outcome measures in the absence of true recovery [70]. Kinematic analysis can be used to characterize movement patterns and differentiate true recovery from compensation [77].

Another mechanism that contributes to recovery is neuroplasticity that leads to neuroanatomical reorganization [78]. Following stroke, there is evidence for the existence a critical period of heightened plasticity that is somewhat analogous to developmental critical periods [8, 79]. Research in animal models have demonstrated that stroke triggers unique waves of molecular and cellular changes that influence cortical plasticity in the days to weeks following injury [80–82]. For example, immediately in the days after stroke, an increase in growth-promoting genes such as GAP43, MARCKS and CAP23 are observed in the peri-infarct cortex. These growth promoting factors induce a permissive environment for processes such as synaptogenesis, axonal sprouting and dendritic branching in the injured brain [8, 81]. It is thought that most of the spontaneous behavioural recovery occurs during this early repair phase [52]. However, with increasing time after stroke, growth-inhibiting factors such as the extracellular matrix (ECM) components, neurite outgrowth inhibitor (NOGO) and chondroitin sulfate proteoglycans (CSPGs) begin to be gradually upregulated [80]. Developmentally, these factors exist to prevent the formation of aberrant connections, however in the adult brain they

may limit plasticity and recovery [8]. Thus, this late upregulation and predominance of growth-inhibiting factors may explain why functional recovery is limited and plateaus in the weeks following stroke.

The second aim of my thesis focuses on investigating post-stroke changes in plasticity-limiting ECM structures, known as perineuronal nets (PNNs), which are largely composed of CSPGs.

1.6 Perineuronal Nets

Perineuronal nets (PNNs) are condensed, lattice-like, ECM structures that are found around cell bodies and proximal dendrites of certain types of neurons in the central nervous system (CNS) [83] (Figure 2A). Although their role in the CNS is not fully understood, evidence suggests that PNNs may serve several functions including regulation of synaptic plasticity, maintenance of ion homeostasis and protection against oxidative stress [83–87].

PNNs begin to appear late in development following the closure of different critical periods such as formation of ocular dominance columns in the visual cortex and plasticity in the barrel cortex [84, 88]. Their formation and maturation appears to be experience-dependent and requires neuronal activity. For example, sensory deprivation of animals through monocular deprivation or whisker trimming during these critical periods reduces PNN expression in the respective cortical regions and prolongs the critical period [84, 88]. Moreover, reduction of PNNs through the use of the bacterial enzyme chondroitinase ABC (chABC) restores juvenile states of plasticity in the adult brain [84, 89, 90]. In the visual system, treatment with chABC reinstates ocular dominance plasticity in the mature visual cortex of animals that were monocularly deprived [84, 91]. Furthermore, in animal models of stroke and spinal cord injury,

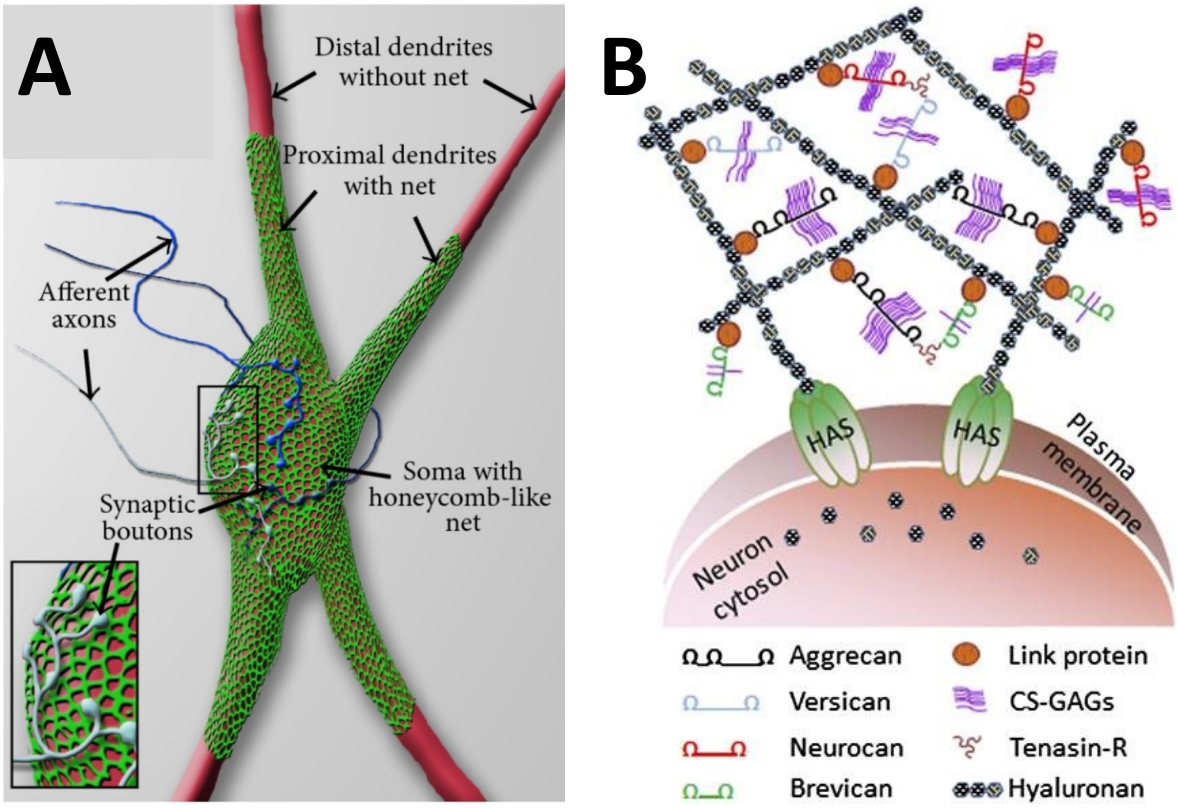

Figure 2: Structure and composition of PNNs. (A) PNNs are condensed mesh-like structures that surround the soma and proximal dendrites of specific neuronal types in the brain. **(B)** PNNs are largely composed of different chondroitin sulfate proteoglycans (e.g. aggrecan, versican, neurocan and brevican) that are bound to hyaluronan (the backbone of the matrix that is anchored to the neuronal surface). Link proteins and tenascin-R bind and stabilize the interaction between hyaluronan and CSPGs. Reproduced from: Winter et al. (2016) [97] and Tsien (2013) [98].

digestion of PNNs enhances neuronal plasticity and promotes functional recovery following injury [89, 92–94]. Together, these findings suggest that PNNs stabilize synaptic connections and restrict plasticity in the adult brain, and that their removal can restore plasticity.

PNNs are composed of four main components that are synthesized by neurons and glial cells: CSPGs, hyaluronan (HA), link proteins and tenascin-R [95] (Figure 2B). CSPGs are a family of molecules comprised of a core protein that is covalently attached to chondroitin sulfate glycosaminoglycan (CS-GAG) chains of varying lengths [96]. In the adult brain, CSPGs are known to inhibit neurite outgrowth as well as limit neuronal repair following injury [99, 100]. The link proteins in the ECM tightly bind different CSPGs to HA, the main backbone that is anchored to the neuron surface. The component tenascin-R forms crosslinks between CSPGs in different HA [95]. Together, these specific interactions between components help stabilize and form the dense and highly organized structure of PNNs.

PNNs have been observed in birds, mice, rats, monkeys and humans [101–105]. They are differentially expressed throughout the brain and spinal cord and also show variation in expression between species [106]. In the rodent brain, PNNs are found in abundance in motor and motor-related cortical regions, and also sensory regions such as the visual and somatosensory cortex [83, 104]. Immunohistochemistry studies have identified that PNNs are mainly associated with parvalbumin (PV)-positive GABAergic interneurons [107, 108]. However, PNNs are also found surrounding a population of glutamatergic excitatory pyramidal cells [108].

The mechanisms through which PNNs act to limit plasticity in the CNS is unclear, however several hypotheses have been proposed [109]: 1) PNNs may serve as a physical barrier around neurons and prevent formation of new synaptic connections. 2) The CSPG components

interact with growth-modulating molecules such as the axon guidance ligand, semaphorin [110]. Therefore, PNNs may serve as a scaffold for molecules that restrict plasticity. 3) PNNs limit the mobility of receptors such as AMPA on the cell surface, and could therefore influence synaptic plasticity (e.g. LTP) [111]. 4) Through their association with PV interneurons, PNNs may regulate the excitatory/inhibitory (E/I) balance in the brain.

1.7 Perineuronal Nets and Parvalbumin Interneurons

As previously mentioned, PNNs are primarily associated with GABAergic interneurons which contain the calcium-binding protein, parvalbumin [107]. PV interneurons account for approximately 40% of all cortical GABAergic interneurons and can be distinguished from other types by their unique fast-spiking activity [112]. In the cortex, there are two main subtypes of PV interneurons; basket cells, which synapse onto the soma and proximal dendrites of pyramidal cells, and chandelier cells, which target the initial axon segment of pyramidal cells [113]. Although PV interneurons are few in number relative to other inhibitory interneurons, the strategic placement of their synapses allows them to tightly control the generation and timing of action potentials of nearby pyramidal cells [114]. Moreover, a single PV interneuron can innervate large numbers of pyramidal cells, thereby having the ability to synchronize activity and generate powerful inhibition [115].

PV interneurons begin to appear in parallel with the onset of critical periods indicating their role in regulating plasticity in the brain [116, 117]. It is hypothesized that PNNs provide a stable microenvironment that facilitates the high metabolic demands of the PV interneurons [118]. The CSPG components of PNNs are highly anionic and therefore can bind to various cations in the microenvironment and serve as an ion buffering system [87]. Indeed, removal of

PNNs with chABC has been to shown to make mature PV neurons more susceptible to oxidative stress [86]. Moreover, degradation of PNNs around PV interneurons has been shown to reduce the excitability of these fast-spiking neurons, suggesting that PNNs help enhance synaptic inhibition [119]. Together, these findings suggest that PNNs, along with the PV interneurons they surround, play a critical role in regulating the E/I balance in the brain.

1.8 Changes in PNNs and PV following Stroke

PNNs are not static structures and can undergo remodeling in adulthood, such as following an injury [95]. To date, there have been a limited number of pre-clinical studies that have examined temporal changes in PNNs and PV following a permanent MCAO (pMCAO) or PT stroke [80, 120–125]. A summary of these findings are presented in Table 2 (changes in PNNs) and Table 3 (changes in PV).

It is clear that PNNs are permanently reduced in the infarct core [120–122]. However, there are conflicting findings as to whether or not PNNs are disrupted in the peri-infarct and contralesional cortices. Following pMCAO, striking and sustained reductions in PNNs have been observed in the peri-infarct region as late as 35 days post-stroke [121]. In comparison, using a PT stroke model, Karetko-Sysa and colleagues demonstrated that although there is a significant reduction in PNN density within the peri-infarct region immediately following stroke, they begin to re-emerge as early as 7 days post-stroke and continue to increase [122]. Others have reported no changes in PNNs in the peri-infarct cortex or only observed changes late (30 days) after stroke [120, 123].

As with PNNs, there is inconsistency in the current literature as to whether or not PV interneurons are affected in the peri-infarct cortex following stroke. Following pMCAO, an early

Study/Year	Stroke Model	Species	Infarct Core	Perilesional Cortex			Contralesional Cortex
				Distance *(μm)*	Early changes *(<7 days)*	Late changes *(>7 days)*	
Bidmon, 1997	PT	Wistar rats	↓	-	No changes		No changes
Carmichael, 2005	pMCAO	F344 rats	NA	200-500	↑ (3 dps)	↓ (14 dps)	NA
				2000	↓ (3 dps)	↑ (28 dps)	
Hobohm, 2005	pMCAO	SH rats	↓	400	↓ (permanent reduction)		No changes
Karetko, 2011	PT	Wistar rats	↓	250	↓ (24 hrs - 1 dps)	↑ (7-30 dps)	↓
Alia, 2016	PT	C57 mice	NA	200	No changes (7 dps)	↓ (30 dps)	No changes

dps = days post stroke; **pMCAO** = permanent middle cerebral artery; **PT** = photothrombosis; **SH** = spontaneously hypertensive

Table 2: Summary of previous literature examining changes in PNNs following stroke. [80, 120–123]

Study/Year	Stroke Model	Species	Infarct Core	Perilesional Cortex			Contralesional Cortex
				Distance *(μm)*	Early changes *(<7 days)*	Late changes *(>7 days)*	
Hobohm, 2005	pMCAO	SHR rats	↓	400	↓ (permanent reduction)		No changes
Cheatwood, 2008	pMCAO	Long–Evans rats	↓	-	↓ (7 dps)	↑ (30 dps)	No changes
Zeiler, 2013	PT	C57 mice	NA	-	No changes		NA
Alia, 2016	PT	C57 mice	NA	200	No changes (7 dps)	↓ (30 dps)	No changes

dps = days post stroke; **pMCAO** = permanent middle cerebral artery; **PT** = photothrombosis; **SH** = spontaneously hypertensive

Table 3: Summary of previous literature examining changes in PV interneurons following stroke. [121, 123–125]

and significant reduction in PV was observed in the peri-infarct cortex. While one study found this reduction to be permanent, the other found the density of PV to return back to control levels by 30 days post-stroke [125, 126]. In contrast to pMCAO models, no significant changes in PV cells were observed early (<7 days) following PT stroke [123, 124].

The discrepancies between studies make it difficult to evaluate changes observed in stroke models following different interventions targeting PNNs or PV (e.g. chABC). Previous studies have all examined changes in PV and PNNs independently. However, as PNNs are tightly associated with PV interneurons, it is important to understand how changes in one affect the other. Furthermore, no study to date has examined changes in PNNs following strokes to different locations in the brain. An aim of this thesis was to clarify previous findings and provide a baseline characterization of post-stroke changes in PNNs and PV interneurons following an ET-1 induced stroke to the cortex and/or the striatum.

Objective and Hypothesis

Strokes primarily target subcortical regions such as the striatum. However, much of the research in stroke recovery has focused on investigating and treating cortical injuries. Furthermore, while both humans and animals show spontaneous recovery following stroke, little is known about how injury location affects the recovery process. This information is important in order to develop new therapies to enhance functional recovery.

The **objective** of this thesis was to examine how the location of stroke injury (cortical/ subcortical) affects spontaneous recovery of motor function and engages plasticity in the injured brain. The following two aims were investigated:

Aim 1: Determine how lesion location affects spontaneous recovery following cortical and striatal stroke *(Experiment 1)*

Aim 2: Determine how plasticity-limiting PNNs and associated PV-interneurons change following cortical and striatal stroke *(Experiment 2)*

Hypothesis: I hypothesize that the location of stroke will influence the severity of initial impairments and the degree of motor recovery. Furthermore, stroke will trigger neuroplastic changes, such as modification of plasticity-limiting PNNs and PV interneurons, which will be determined by the stroke location.

Materials and Methods

2.1 Animals

All experimental procedures were approved by the University of Ottawa Animal Care Committee and complied with guidelines set by the Canadian Council on Animal Care. A total of 92 male Sprague-Dawley rats (Charles River Laboratories, Montreal, Canada) weighing between 200-250g on arrival were used in this study (experiment 1, n=30; experiment 2, n=62). All animals were pair-housed in standard Plexiglas cages on a reverse 12-hour light/dark cycle (8 am off/8 pm on). Upon arrival, animals were allowed to acclimate to the housing facilities for one week and then handled for 5 minutes per day for 5 days to familiarize them with the experimenters. Animals had ad libitum access to food and water except during behavioural training and testing periods.

2.2 Behaviour Training and Testing

General Procedures

Prior to stroke surgeries, animals were trained on a battery of behavioural tests (Montoya staircase, cylinder, beam traversal and adhesive strip removal task) over a 2-week period and their baseline performance was assessed. Subsequent behavioural testing was conducted at post-stroke weeks 1, 2, 4, 6 and 8. Testing was done over 3 days at each of these test points. During the training and testing days, animals were moved from their housing room to the testing room and allowed to habituate for 30 minutes prior to testing. All procedures were conducted during the dark cycle. All behaviour testing and analysis was performed by experimenters blinded to group identity.

Montoya Staircase Test

The Montoya staircase test was used to assess skilled reaching ability [127]. In this task animals use fine motor skills to extend their arm, grasp and retrieve small food pellets. Animals were food restricted to ~90% of their body weight during the training period. Rats were placed inside a clear box with 7-tiered descending steps on each side (Figure 3). Each step has a food well containing 3 small food pellets (45 mg TestDiet; Purified Rodent Tablet; 5TUL). The design of the staircase apparatus allows animals to only reach for pellets placed on steps on the same side as their paw. Forepaw dexterity was measured by counting the total number of pellets retrieved (PR) versus those that were left or dropped. In addition, the lowest step (maximum distance) from which the rats were able to retrieve pellets from was recorded.

Animals were trained on this task twice daily for 2 weeks to reach a minimum criterion of at least 14 ± 2 pellets. Each training and testing session was 15 minutes in duration and was separated by a 3 hour break. Baseline measure was calculated as the average of all trials over the last two days of training. Post-stroke testing was conducted over 3 days; animals were given one day to re-familiarize them with the task and their performance was tested on trials across the next 2 days. Percent improvement at 8 weeks was calculated as follow:

$$\% \text{ improvement} = ([PR_{Week\text{-}8}/ PR_{Pre\text{-}stroke}] - [PR_{Week\text{-}1}/ PR_{Pre\text{-}stroke}])$$

Cylinder Test

The cylinder test was used to assess asymmetrical limb use for postural support [128]. In contrast to the staircase test, this task relies on spontaneous use of the animals forelimb, therefore pre-training was not required prior to baseline assessment. Rats were placed inside a tall Plexiglas cylinder (20 cm diameter, 30 cm tall) on a glass tabletop and video-taped from below.

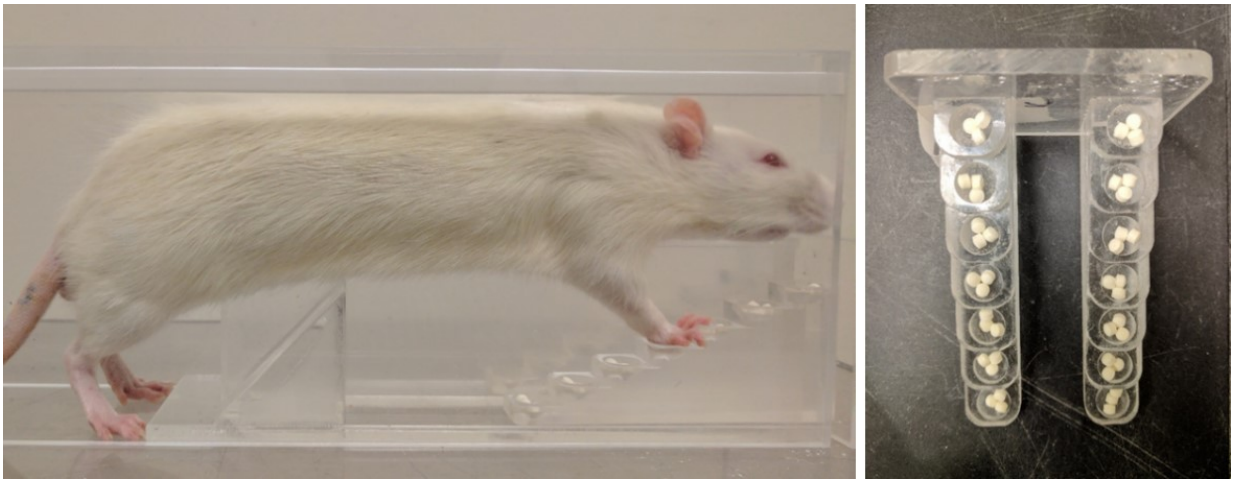

Figure 3: Montoya staircase test. Animals were placed into the staircase apparatus and the total number of pellets retrieved and the maximum step reached were recorded.

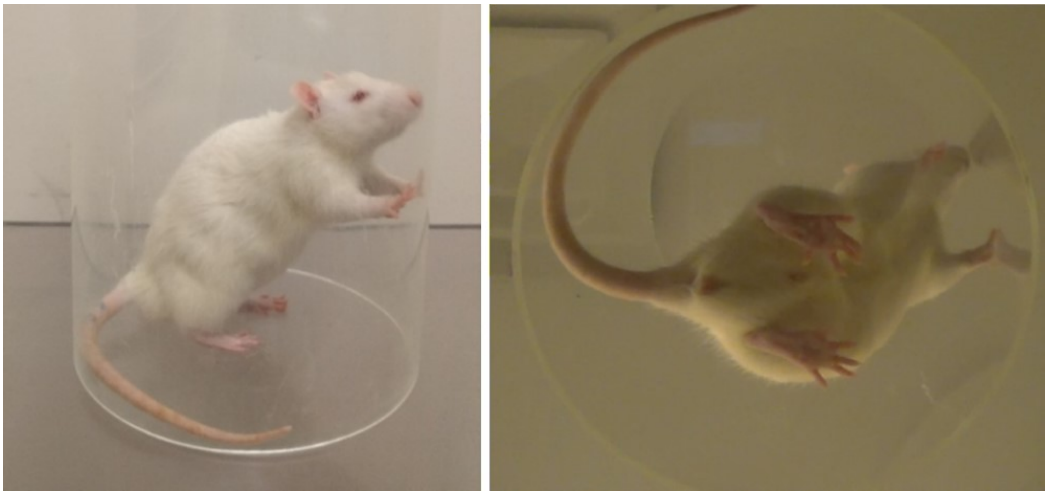

Figure 4: Cylinder test. Rats were placed inside a Plexiglas cylinder and filmed from below. The number of wall contacts with each forelimb as the animal reared was recorded.

Animals were allowed to freely move around and explore the cylinder (Figure 4). A trial continued until a rat performed a minimum of 20 independent rears and touched the walls of the cylinder using their forelimbs (~5 minutes/rat). One trial was conducted during each testing period. The number of independent (ipsilateral and contralateral) and bilateral wall contacts with the forelimbs was counted for each animal from recorded videos, and the percent use of their impaired forelimb was calculated as follow [128]:

% use of impaired paw = ([contralateral contacts +1/2 bilateral contacts]/total contacts) × 100%

Adhesive Strip Removal Task

The adhesive strip removal task was utilized to evaluate sensorimotor impairments following stroke [129]. Two rectangular pieces of adhesive tape of equal size (20 mm × 12.5 mm) were applied with equal pressure on the plantar surface of both forepaws, one per paw, of each animal. Animals were then placed in a Plexiglas cylinder and observed by two experimenters located on opposite sides of the cylinder (Figure 5). The time to initial contact (sensory component) and time to remove tape (motor component) were recorded for each forepaw. Each trial continued for 2 minutes or until the animals successfully removed the tape on both paws. Animals were trained on this task daily for 5 days and their performance on day 5 was used as the measure of baseline performance. For post-stroke assessment an average of 2 trials separated by a 3 hour break was used for each time point.

Tapered Beam Traversal Test

The beam traversal test was used to assess both forelimb and hindlimb placement accuracy [130, 131]. Rats were trained to cross a 160 cm long elevated/tapered beam (6 cm at the

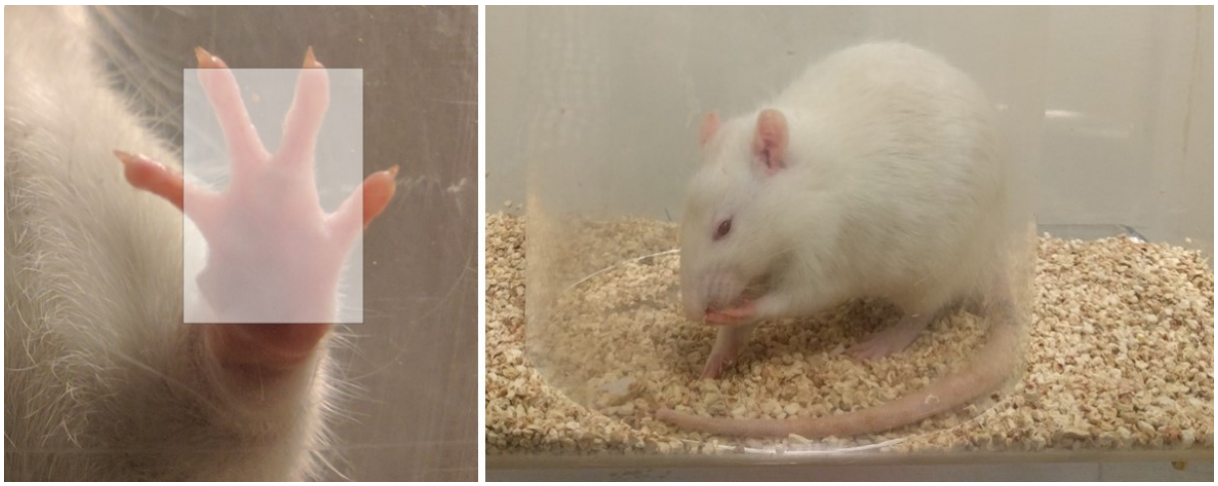

Figure 5: Adhesive strip removal test. A small piece of adhesive tape was applied to each animal's forepaws and both the time to initially contact and remove the tape was recorded.

Figure 6: Beam traversal test. Rats were trained to cross a tapered beam to reach a goal box. The number of foot faults made with both the fore- and hind-limbs were recorded.

wide end; 1.5 cm at the narrow end) to gain access to a dark goal box containing food pellets at the end (Figure 6). Training consisted of gradually placing the rats at increasing distances from the goal box until the animals were able to cross the full length of the beam without any pauses. Baseline performance was assessed on the very next day following training. Animals will normally cross the beam with very few foot faults and attempt to stay on the top level of the beam. However following stroke, animals slip off the top level onto the safety level below with increased frequency [131] (Figure 6). Trials were video recorded and the number of slips with both the left and right fore- and hindlimbs were assessed from video playback. During each test-point including baseline assessment, animals were required to cross the beam four times and data from all trials was averaged. The percentage of successful steps for each paw was calculated as [132]:

$$\% \text{ successful steps} = (1 - [\text{foot faults}/\text{total steps}]) * 100$$

2.3 Endothelin-1 Stroke Surgeries

Focal strokes were produced by intracerebral injections of the vasoconstricting peptide ET-1 as previously described [45, 132, 133]. After an overnight fast, animals were anesthetized with isoflurane (4% induction, in oxygen) and prepped for surgery. Briefly, the heads were shaved and cleaned with soap followed by chlorhexidine. To keep the animals hydrated during the duration of the surgery, saline was delivered subcutaneously. Tear-gel was applied to prevent drying of the eyes and a local anesthetic (Xylocaine) was applied to the ear canals to reduce any discomfort caused by ear bars.

After prepping, animals were secured onto a stereotaxic frame and a small incision was made in the scalp. During surgery isoflurane was maintained at 1.5%-2.0%. Body temperature

was closely monitored throughout the surgery and maintained at 36.5°C using a heating blanket. One (striatal-only), two (cortical-only) or three (combined and sham groups) small, ~1.0 mm diameter burr holes were drilled in the skull. In each model, stereotaxic injection coordinates targeted the forelimb motor cortex (FMC) and/or dorsolateral striatum (DLS; Table 4). All strokes were produced in the hemisphere opposite the animals' dominant forelimb as determined by their baseline performance on the staircase test.

ET-1 (Abcam, AB120471/Sigma-Aldrich, E7764) was thoroughly dissolved in sterile water at a concentration of 400 pmol/µl. At each injection site, a 0.485 mm inner diameter syringe (Hamilton, 80366) was slowly lowered into the brain and after a 1 minute delay, 1 µl of ET-1 was infused at a rate of 250 nl/min. Following injection, the needle was left in place for 2 min and then very slowly withdrawn to minimize backflow of ET-1. The sham injection rats were treated identically to the combined stroke group, except they received injections of sterile water instead of ET-1. Experiment 2, also included an anesthetic control group that consisted of anesthesia (isoflurane) for a similar duration of time as the other groups.

Following injections, the incision was sutured and a topical anesthetic (2% bupivacaine cream, Chiron) was applied. Animals were placed in an incubation chamber to recover from surgery and administered an analgesic, 0.05 mg/kg sub-cutaneous injection of buprenorphine (Chiron) once they woke up. Animals were then moved back to their home cages and monitored over the following 24 hours.

Group	Injection #	AP	ML	DV
Cortical	1	0.0	± 3.0	-1.7*
	2	+2.3	± 3.0	-1.7*
Striatal	1	+0.7	± 3.8	-7.0#
Combined	1	0.0	± 3.0	-1.7*
	2	+2.3	± 3.0	-1.7*
	3	+0.7	± 3.8	-7.0#

Table 4: Stereotaxic injection coordinates for ET-1 surgeries. Coordinates were relative to Bregma. All injections were 1 µl in volume.* = from brain surface, # = from skull surface.

2.4 Tissue Preparation and Immunohistochemistry

Perfusion

Rats were deeply anesthetized by an intraperitoneal injection of euthanyl (149.5 mg/kg, Bimeda-MTC Health Inc.). Animals were then transcardially perfused with 120 ml (20 ml/min) of cold 1x heparinized saline followed by 120 ml (20 ml/min) of cold 4% paraformaldehyde (PFA) in phosphate buffered saline (PBS; pH 7.4). Immediately following perfusion, brains were removed and post-fixed in 4% PFA overnight at 4°C and then transferred to a solution of 20% sucrose for cryoprotection.

Tissue samples were embedded in optimal cutting temperature compound (Sakura Finetek, 4583) and frozen in cold isopentane (-40°C to -50°C). Brains were sectioned into 20 µm thick coronal section at intervals of 1:24 (every 480 µm) using a cryostat (Leica Biosystems, CM1850) and were slide mounted onto chrome alum, gelatin-subbed, slides. Multiple series of sections was collected for each brain for immunohistochemistry and cresyl violet staining. Mounted sections were dried overnight and then stored at -20°C prior to staining.

Immunohistochemical Staining for PNNs and PV

One series of sections per animal was used to perform double immunofluorescence staining for PNNs and PV. To visualize PNNs we used Wisteria floribunda agglutinin (WFA), a lectin that binds to N-acetylgalactosamine residues of CSPGs [83, 107]. An anti-parvalbumin antibody was used to label PV interneurons. All materials used for staining are listed in Supplemental Table 1.

Prior to staining, slides were thawed at RT for an hour and then hydrated in PBS. To improve the detection of antibody, slides underwent heat induced epitope retrieval at 95ºC for 20

minutes in citric acid (0.01M, pH=6.0). After cooling to RT, slides were washed with PBS and a PAP pen (Super PAP Pen, Daido Sangyo Co.) was used to draw a water-repellent barrier around the sections. To reduce non-specific binding, sections were blocked in 10% normal donkey serum and 10% Carbo-Free blocking solution in PBS+0.3% triton x-100 for 60 min. Sections were then incubated in primary antibodies, 1:500 WFA and 1:600 anti-PV in blocking solution overnight at 4ºC.

The following day, slides were washed in triplicate with PBS+0.01% tween and then incubated with secondary antibodies conjugated to Alexa Fluor 594 (for PV; 1:250) and Alexa Fluor 488 (for PNNs; 1:250) in PBS+0.3% triton x-100 at RT for 3 hours. Finally, slides were washed in triplicate with PBS+0.01% tween, and coverslipped with Immu-Mount mounting medium (Thermo-Scientific, Shandon, SH9990402). Staining was performed in small batches and was randomized.

2.5 Infarct Volume Measurement

MRI Acquisition and Infarct Measurement

Magnetic resonance imaging (MRI) was performed at 72 hours following surgery to visualize and confirm infarcts in the animals post-stroke. Scans were obtained using a 7T General Electric/Agilent MR901 small-animal scanner. Animals were anesthetized with isoflurane (4% induction; 2% maintenance) during the 15 minute procedure, and respiratory and cardiovascular function was monitored throughout with a SA Instruments Inc. (SAII) physiological monitoring system. A localizer scan was first performed, during which routine adjustments were made. T2-weighted structural images were obtained using the following

parameters: 15 axial (transverse) slices; slice thickness = 800 microns; in-plane resolution = 78 microns; echo train length = 8; echo time = 27 ms; scan time = 5 minutes.

MRI image stacks were exported into ImageJ (National Institute of Health, Bethesda MD) to assess early infarct volumes in the animals. In each slice, any observable striatal and/or cortical damage was manually traced and the infarct area for each region was measured. Infarct volumes were calculated by multiplying the sum of infarcted area for all measured slices by the MRI slice thickness (0.80 mm).

Infarct Measurement from Cresyl Violet Staining

One series of sections per animal was stained with cresyl violet (0.25% solution) to visualize infarcted tissue and calculate infarct volume. Depending on the extent of damage, a minimum of 7 evenly-spaced sections, spanning the lesion was selected for analysis. Sections were imaged at 5x (Exp. 1) or 20x magnification (Exp. 2) using a Leica DMRXE microscope (Leica Microsystems) or Aperio CS2 digital pathology slide scanner (Leica Biosystems). Infarct volumes were calculated as previously described [8, 9]. In each section, the area of intact tissue in the striatum and cortex of both hemispheres (ipsilesional and contralesional) was manually traced and measured. The total volume of injury (in mm^3) was calculated for the cortex and striatum separately as follows [9]:

[(area of contralesional (cortex/striatum) − area of undamaged ipsilesional (cortex/striatum) × distance between sections × thickness of sections]

2.6 Microscopy and Cellular Quantification

Stereological Cell Counting

Unbiased stereological procedures were utilized to estimate the density of PNNs and PV cells. Digital images of co-labelled PNN and PV sections were acquired at 10x magnifications using a Leica DMR microscope (Leica Microsystems, Germany). Six to eight sections spanning the infarct were analyzed for each animal. Cell counting was performed in the lateral perilesional cortex, defined as a 1 mm wide profile adjacent to the infarct core, comprising all cortical layers (Figure 7A). An adjacent cresyl violet stained series was used to visualize the lesion and trace the infarct boundary. Counting was also performed in a 1 mm wide box in the contralesional cortex homotopic to the infarct core. The counting areas were manually traced and the Fractionator probe (Stereo Investigator V10.0; MicroBrightField Bioscience, Williston, VT) was used to estimate cell counts in the regions of interest [134]. All quantification was performed by a blinded experimenter.

A pilot counting study was initially conducted using the resample-oversample probe to determine the optimal stereological parameters in order to achieve a desired precision of sampling with minimal amount of sampling [135]. Based on this, a 400 μm × 400 μm spaced grid was superimposed onto the traced regions of interest, and counting was performed in randomly chosen 200 μm × 200 μm counting frames within each grid. An estimate of total number of cells per region sampled was extrapolated by multiplying the numbers of cells counted by the reciprocal of the volume fraction. The density per mm^3 for each marker was calculated by dividing the total estimated population by the volume sampled.

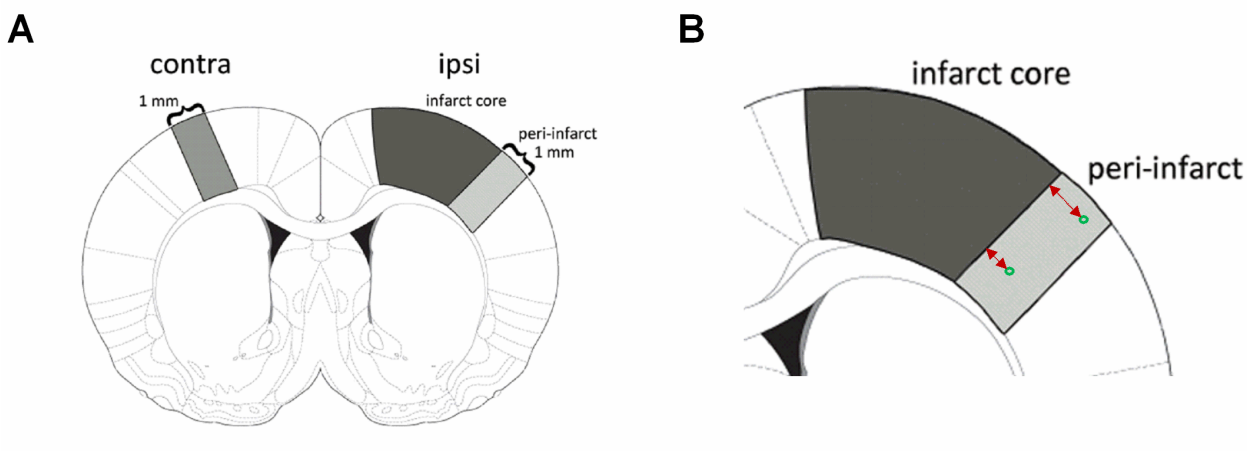

Figure 7: Stereological counting and locus analysis. (A) Representative image illustrating analyzed cortical regions in the ipsilesional and contralesional hemisphere. **(B)** Measurement of distance between counted cells and infarct border using the locus analysis probe.

Locus Analysis

In order to assess if the distribution of PNNs and PV cells varied as a function of distance, the locus analysis probe in Neurolucida explorer software (MicroBrightField Bioscience) was used. Briefly, the lateral infarct boundary was traced, and the distance of every counted PNN+ and PV+ cell in the perilesional cortex was measured from the infarct border (Figure 7B). Due to the complex shapes of the stroke, it was challenging to manually draw a peri-infarct box that was precisely 1 mm in width throughout from top to bottom. Therefore to account for this we analyzed the distribution of counted cells within the first 800 μm from the infarct border.

2.7 Statistical Analysis

All analyses were performed using IBM SPSS Statistics for Windows, version 24 (IBM Corp., Armonk, N.Y., USA). In experiment 1, all behavioural data were analyzed using one-way and repeated-measures ANOVA. The length of time that animals remained significantly impaired was analyzed using simple contrast comparison at each post-stroke test point using pre-stroke performance as control. Infarct volumes were analyzed using a one-way ANOVA with Ryan-Einot-Gabriel-Welsch (REGW-F) post-hoc. Forward regression analysis was utilized to evaluate the association between infarct volumes and functional outcome. In experiment 2, all behavioural and histological data was analyzed using a two-way (Surgery type x Time) ANOVA with REGW-F post-hoc. Post-hoc power analysis was performed using G*Power 3.1 [136]. Significance was set at $p \leq 0.05$ for all analyses and post-hoc multiple comparisons were corrected to the 0.05 level. All values reported are means ± SEM.

2.8 Excluded Animals/Outliers

In experiment 1, one rat in the combined group died due to surgical complications. A total of three animals were excluded; two animals in the striatal-only group had large non-targeted cortical injuries (~25 mm^3 and 47 mm^3) and were identified as being extreme outliers by SPSS (cortical infarct volumes that were 3 times the interquartile range). As the aim of this study was to characterize the effect of infarct location on functional outcome, it was necessary to have animals with a "pure" striatal or cortical injury. In addition, one animal from the cortical-only group was excluded due to having a small infarct (~3 mm^3) and failing to show any behavioural impairments following stroke surgery.

In experiment 2, two animals died due to surgical complications. In addition a few animals had to be removed from analysis due to the presence of a histological artifact known as "dark neurons" that affected immunohistochemical staining (Supp. Figure 1). In cresyl stained sections, these cells appear shrunken with a darkly stained nucleus [137, 138]. This artifact appeared to strongly affect staining for PV interneurons but did not affect PNN staining. In areas where "dark neurons" were present there was a clear reduction in immunoreactivity for PV. Thus, animals that had large areas of "dark neurons" were excluded from the analysis to avoid any confounding effects (n=12). Animals that had small patches of "dark neurons" were still included in the study but with sections containing the "dark neurons" removed from analysis. In addition a few animals in this study had irregularly shaped strokes with injury spanning the lateral cortex (n=3). These animals did not have a defined lateral perilesional area to count in, therefore analysis was only performed in their intact contralesional hemisphere.

Results

Experiment 1: Characterizing Spontaneous Recovery of Motor Function

In this experiment, animals received focal ET-1 strokes that targeted the FMC alone, the DLS alone or both the FMC and DLS. The spontaneous recovery profile of the animals was followed over an 8-week period using multiple behavioural tests to evaluate how lesion location influenced impairments and functional recovery (Figure 8). Impairments on each behavioural task were evaluated by comparing each group's performance at post-stroke test points with their pre-stroke level. Recovery on the tasks for each group was calculated as the difference in performance between the first and the last post-stroke time points (week 1 and 8).

3.1 Infarct Volumes

Quantification from Cresyl Violet Stained Sections

Following the last behavioural test point, rats were sacrificed and the amount of striatal and cortical damage was calculated from cresyl violet stained sections. Figure 9A depicts the typical injury profile seen in each of the three groups.

There was a significant difference in total hemispheric damage between the groups ($F=7.4$, $p<0.005$; Figure 9B). The combined group had the largest total damage (49.5 ± 10.0 mm^3) compared to the striatal-only (15.1 ± 2.2 mm^3) and cortical-only group (23.9 ± 3.8 mm^3; $p<0.05$). There was no significant difference in the amount of cortical damage between the cortical-only (23.1 ± 3.6 mm^3) and combined group (33.6 ± 9.0 mm^3). Similarly, there was no difference in the amount of striatal damage between the striatal-only (13.2 ± 1.9 mm^3) and the combined group (15.8 ± 1.7 mm^3). The striatal-only group had a small amount of cortical

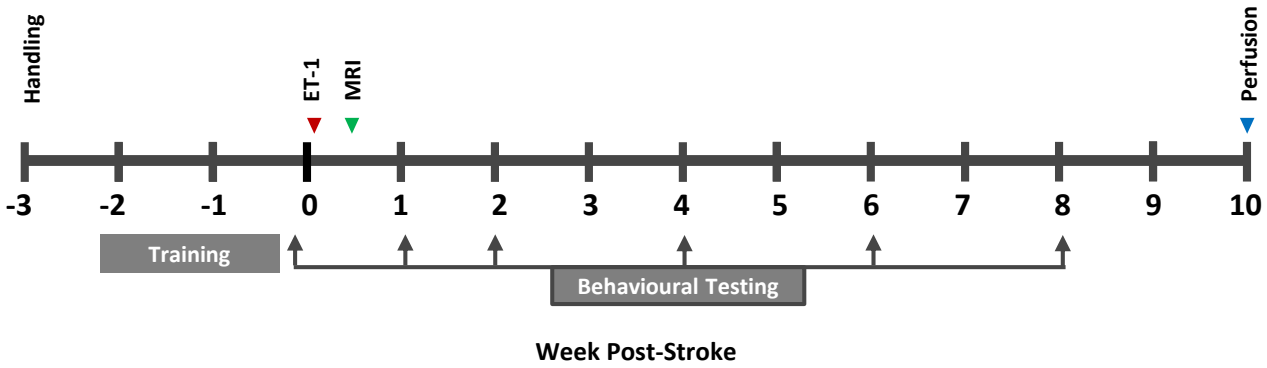

Figure 8: Timeline of experiment 1 to characterize spontaneous recovery of motor function. Animals were trained on a battery of behavioural tests over a period of two weeks and baseline performance was assessed. Following ET-1 induced strokes, behaviour testing was conducted at post-stroke week 1, 2, 4, 6, and 8. MRI imaging was performed at 72 hours post-stroke. Animals were perfused at 10 weeks.

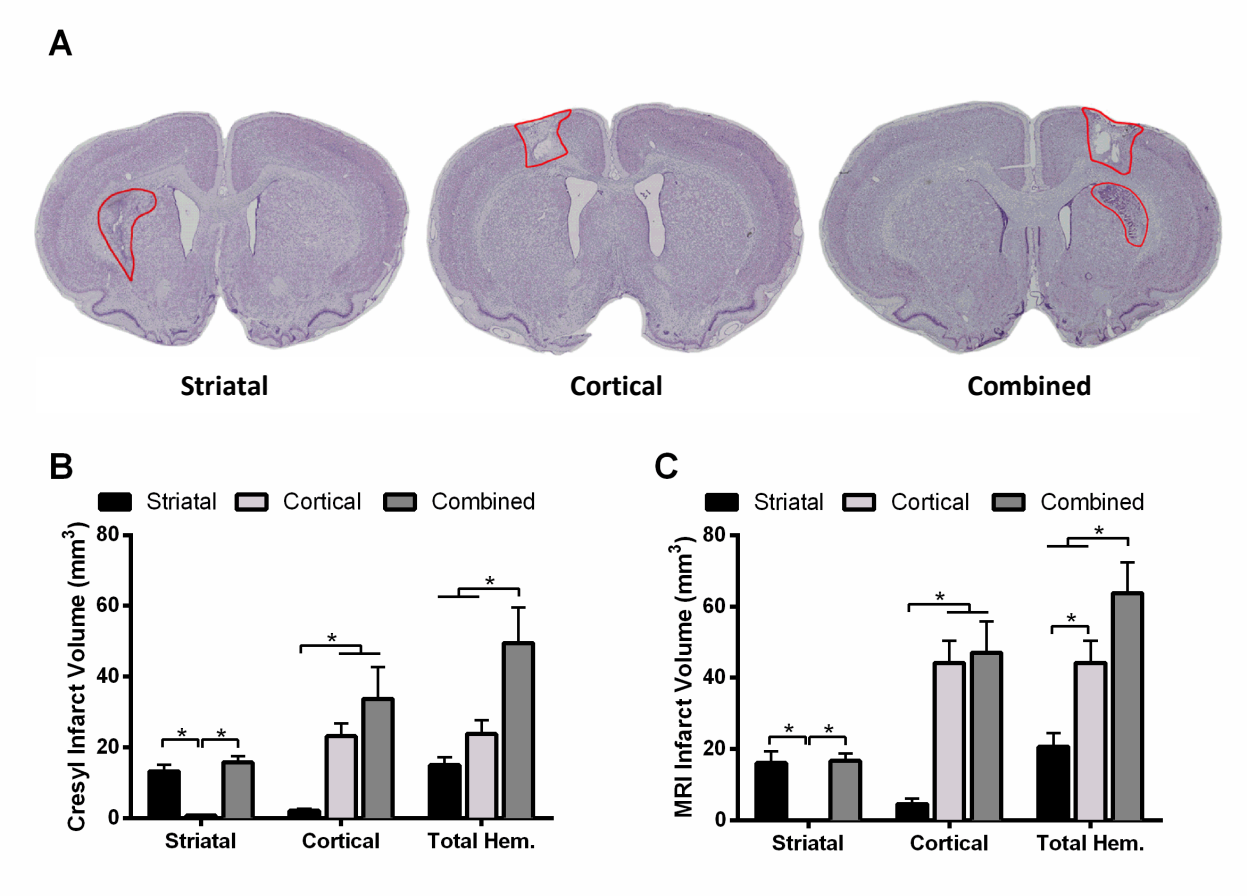

Figure 9: Infarct volumes following ET-1 induced stroke in the forelimb motor cortex and dorsolateral striatum. (**A)** Representative cresyl violet stained sections showing typical stroke lesion seen in the three groups. Quantification of infarct volumes from both **(B)** cresyl violet stained sections (10 weeks post-stroke) and **(C)** T2-weighted MRI (72 hours post-stroke). Infarct volumes estimated from early MRI were larger but correlated with that obtained from cresyl violet stained tissue. The combined group had the largest total hemispheric damage. The amount of cortical damage was similar in the cortical-only and combined group. There was no difference in striatal infarct volume between the striatal-only and combined group. n = 8; striatal-only, n = 9; cortical-only and n = 9; combined group. Values are means ± SEM. * = $p<0.05$. Total Hem. = total hemispheric infarct volume.

damage (1.8 ± 0.5 mm^3) that may have resulted from lowering of the needle through the cortex and also due to backflow of ET-1. Infarct volumes calculated from cresyl stained sections were used for all analyses examining the relationship between infarct volume and functional outcome.

Quantification from T2-Weighted MRI

T2-weighted MRI images obtained 72 hours post-stroke were used to estimate the extent of cortical and striatal injury in all groups. Infarct volumes calculated from MRI were significantly larger than those measured from corresponding cresyl violet stained sections ($t=4.30$, $p<0.001$ for total hemispheric damage; Figure 9C). For example, the amount of cortical damage estimated from T2 MRI images was 4.6 ± 1.5 mm^3 for the striatal-only, 44.2 ± 6.2 mm^3 for the cortical-only and 47.1 ± 8.8 mm^3 for the combined group. In comparison, cortical volumes measured from cresyl violet were 1.8 ± 0.5 mm^3 for the striatal-only, 23.1 ± 3.6 mm^3 for cortical-only and 33.6 ± 9.0 mm^3 for the combined group. The difference in volume measurement obtained from MRI and cresyl is likely due to edema and tissue swelling, which occur in the early days following stroke, leading to an overestimate in the MRI measure [139]. Despite the difference, the volume of cortical and striatal damage estimated from early MRI strongly correlated with cresyl infarct volumes measured from tissue obtained at 10 weeks post-stroke ($r=0.92$ and 0.90 for the cortex and striatum respectively, $p<0.001$ for both regions).

3.2 Performance on the Montoya Staircase Test

Pellet Retrieval

A one-way ANOVA indicated that all groups reached a similar number of pellets (17.1 ± 0.4 out of 21 pellets) with their dominant paw prior to stroke (Figure 10A). Following ET-1

surgeries, all three groups demonstrated a significant reduction in the average number of PR with the contralateral forelimb (PR: 14.2 ± 1.0 for striatal-only, 12.4 ± 0.9 for cortical-only and 8.8 ± 1.0 for the combined group), indicating deficits in the ability to perform skilled reaching movements ($p<0.005$). Repeated-measures ANOVA revealed a significant effect of group ($F=8.96$, $p<0.001$) and time ($F=5.93$, $p<0.01$) for all post-stroke weeks. Animals in all three groups remained significantly impaired relative to pre-stroke performance throughout the entire 8-week duration of the experiment. The combined group was significantly more impaired than both the cortical-only and striatal-only group ($p<0.05$).

The percentage of improvement was evaluated by taking the difference between performance at post-stroke week 8 and week 1. There was no significant difference in the amount of improvement in contralateral reaching performance between groups (16.6 ± 5.5% for the cortical-only, 13.7 ± 5.5% for the combined and 7.4 ± 6.3% for the striatal-only group; Figure 10E).

Assessment of the non-impaired ipsilateral forelimb revealed a difference in performance over time ($F=3.53$, $p<0.05$) but no difference between groups (Figure 10B). Animals did not exhibit any post-stroke impairments with their ipsilateral forelimbs. Both the striatal-only and cortical-only group performed significantly better with their ipsilateral forelimbs at week 6 and week 8 compared to their pre-stroke measure.

Lowest Step Reached

In addition to the total number of pellets eaten, the maximum reaching distance as indicated by the lowest step reached by the animals was examined. Rats from all groups performed similarly during baseline assessment, and the majority of animals reached for pellets

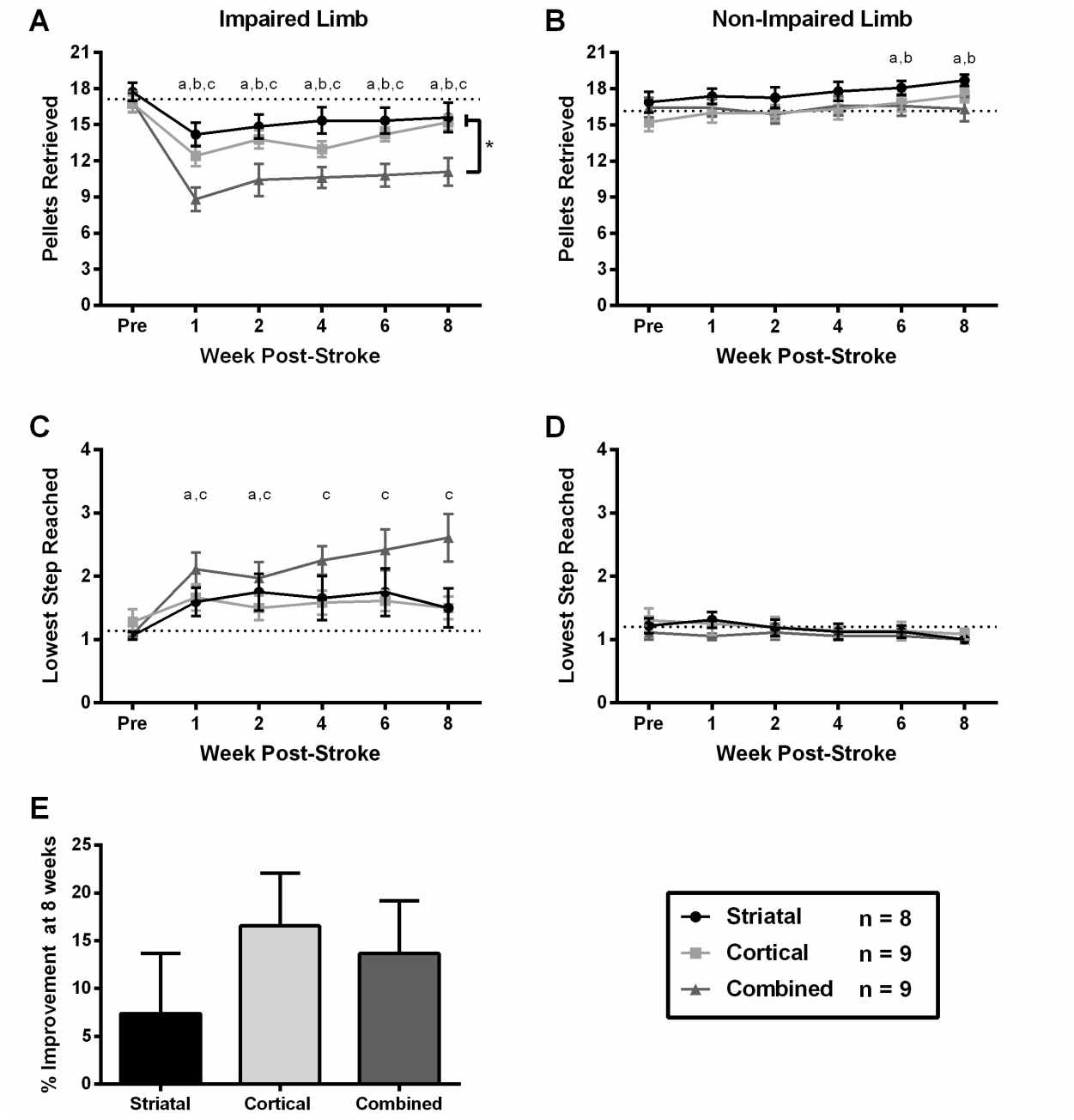

Figure 10: Post-ischemic performance on the Montoya staircase test for skilled reaching. (A) Animals in all three groups retrieved fewer pellets with their contralateral forelimb and remained significantly impaired for the entire 8-week period. Significant between-group differences were detected between the combined and both striatal- and cortical-only groups. **(B)** No post-stroke impairments in ipsilateral forelimb reaching were detected, and animals continued to improve over time. **(C)** Both the striatal-only and combined group displayed significant impairments in the ability to reach for pellets on lower steps up until week 2 and week 8 respectively. **(D)** Animals did not show impairments of the ipsilateral forelimb in the measure of maximum step reached. **(E)** Percent improvement in pellet retrieval with the contralateral limb between post-stroke week 1 and 8. Values are means ± SEM. Significance markers for pre-stroke vs. post-stroke within-group differences: a = striatal-only, b = cortical-only, c = combined; $p<0.05$. Between-group differences: * = $p<0.05$.

placed at the lowest step (step 1) with their dominant paw (Figure 10C). Following stroke, both the striatal-only and combined group showed a significant deficit in the ability to reach for pellets on the lower steps with the contralateral forelimb ($p \leq 0.028$). These impairments persisted for the duration of the experiment for the combined group, and up until week 2 for the striatal-only group. There was no significant effect of time or group for post-stroke time points.

Animals did not show any post-stroke deficits in the use of their non-impaired paw in the measure of maximum step reached (Figure 10D).

3.3 Performance on the Cylinder Test

Prior to stroke induction, animals tended to use both forelimbs equally for postural support on the cylinder task, and there were no differences between groups (Figure 11). After ET-1 surgery, rats in all three groups significantly reduced their use of the contralateral forelimb from ~50% to 28.4 ± 3.8% for the striatal-only, 21.3 ± 3.9% for the cortical-only and 21.7 ± 3.1% for the combined groups ($p<0.001$). Repeated-measures ANOVA verified a main effect of time ($F=13.26$, $p<.001$) and time by group interaction ($F=2.53$, $p<0.05$) for all post-stroke time points. On this task both the striatal-only and combined group had significant impairments that persisted throughout the 8-week period. In comparison, the cortical-only group remained significantly impaired only up until week 4.

Assessment of the degree of spontaneous recovery between post-stroke week 1 and 8 indicated a significant difference between groups ($F=4.14$, $p=0.03$). The cortical-only group demonstrated significantly greater improvement (24.3 ± 4.9%) than the striatal-only (7.8 ± 3.2%) and combined group (12.2 ± 3.9%; $p<0.05$).

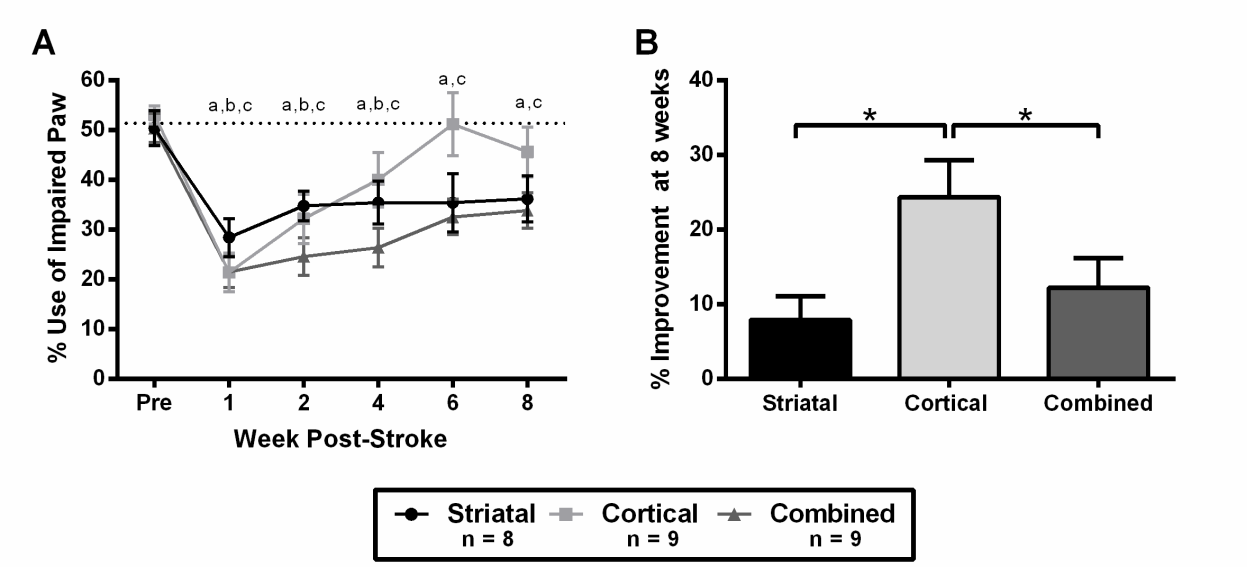

Figure 11: Post-ischemic performance on the cylinder task for forelimb asymmetry. (A) All groups displayed reduced reliance on their impaired forepaw after stroke. Both the striatal-only and combined groups were significantly impaired relative to pre-stroke for the entire 8-week testing period. The cortical-only group had significant impairments up until 4 weeks post-stroke. **(B)** The cortical-only group showed significantly greater recovery than the other groups. Values are means ± SEM. Significance markers for pre-stroke vs. post-stroke within-group differences: a = striatal-only, b = cortical-only, c = combined; $p<0.05$. Between-group differences: * = $p<0.05$.

3.4 Performance on the Beam Traversal Test

In the tapered beam traversal test the percentage of successful steps with the forelimbs and hindlimbs was calculated and analyzed. During baseline assessment, animals in all groups performed equally well and made few forelimb and hindlimb errors (~94% and ~96% successful steps respectively; Figure 12, 13).

Forelimb Performance

Following stroke, the cortical-only and combined group made significantly more contralateral forelimb foot faults ($p \leq 0.003$). Repeated-measures ANOVA revealed a main effect of both time ($F=5.04$, $p=0.006$) and group ($F=5.75$, $p=0.01$) for contralateral forelimb performance for all post-stroke time points (Figure 12A). The combined group showed significant forelimb impairments throughout the experiment and were significantly more impaired than the cortical-only and striatal-only group ($p<0.05$). The cortical-only group displayed significant impairments only on the first week following stroke, whereas the striatal-only group did not show any post-stroke impairments. There were no significant differences in the amount of improvement in contralateral forelimb performance between the groups (Supp. Figure 2A). Animals did not show significant deficits in the use of their ipsilateral forelimb following stroke (Figure 12B).

Hindlimb Performance

Analysis of contralateral hindlimb performance indicated that all three groups made significantly more hindlimb foot faults following stroke ($p \leq 0.016$). Repeated-measures ANOVA revealed a main effect of time ($F=8.01$, $p=0.001$) but not group for all post-stroke time points. The combined and striatal-only group remained significantly impaired throughout the 8-week

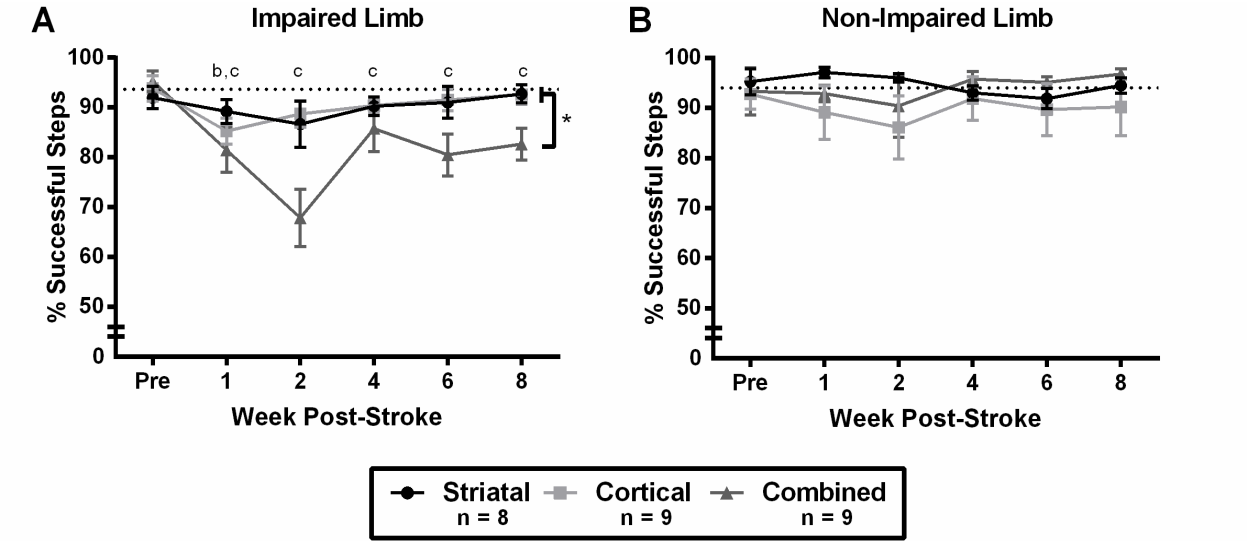

Figure 12: Post-ischemic performance on the beam-traversal test (forelimb accuracy). (A) The cortical group had significant contralateral impairments at week 1 post-stroke while the combined group had significant impairments that were apparent as late as 8 weeks post-stroke. Significant between-group differences were detected between the combined and both cortical- and striatal-only groups. **(B)** No impairments were observed in the use of the ipsilateral forelimb. Values are means ± SEM. Significance markers for pre-stroke vs. post-stroke within-group differences: a = striatal-only, b = cortical-only, c = combined; $p<0.05$. Between-group differences: * = $p<0.05$.

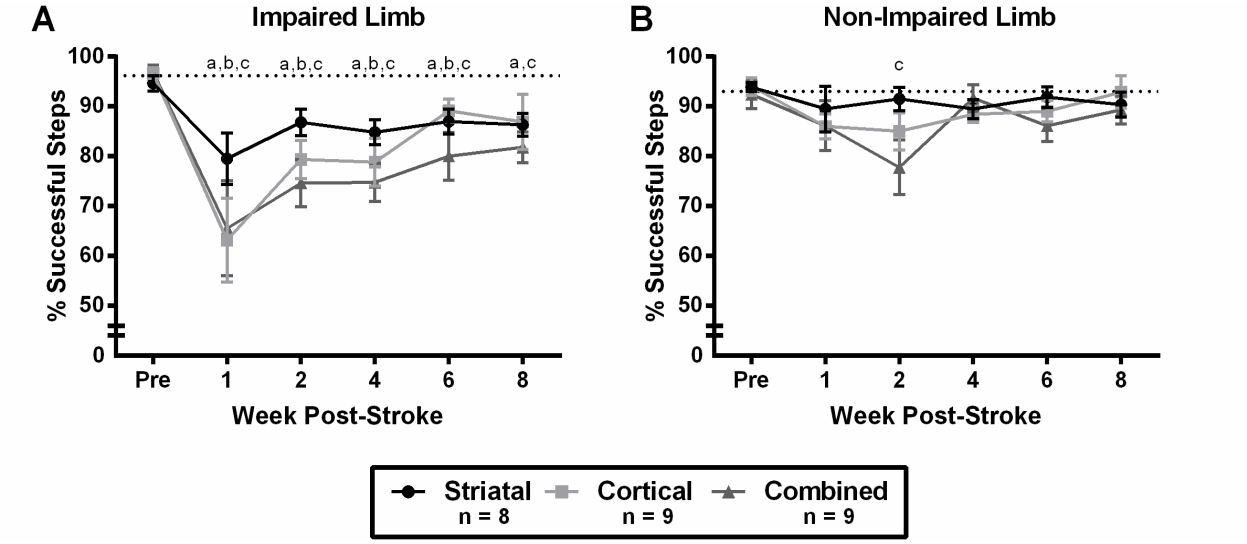

Figure 13: Post-ischemic performance on the beam-traversal test (hindlimb accuracy). (A) Rats in both the striatal-only and combined groups had significant contralateral hindlimb impairments for the entire 8-week testing period. The cortical-only group had significant impairments up until 6 weeks post-stroke. **(B)** Ipsilateral hindlimb impairments were not detected for the striatal- and cortical-only groups. The combined group demonstrated significant impairments at week 2 post-stroke. Values are means ± SEM. Significance markers for pre-stroke vs. post-stroke within-group differences: a = striatal-only, b = cortical-only, c = combined; $p<0.05$.

testing period, whereas the cortical-only group showed significant impairments until week 6 (Figure 13A). There were no significant differences in the amount of improvement in contralateral hindlimb performance between the groups (Supp. Figure 2B).

Assessment of ipsilateral hindlimb performance indicated a significant effect of time ($F=3.75$, $p<0.05$). The combined group made significantly more ipsilateral hindlimb foot faults at week 2 post-stroke compared to their pre-stroke level (Figure 13B).

3.5 Performance on the Adhesive Removal Test

In the adhesive test, both time to initially contact and time to remove tape were recorded and analyzed. Two animals in this experiment failed to learn the task (neglected and did not remove tape) during the training sessions and were therefore excluded from this analysis. Following training, the remaining animals took ~5 seconds to contact and ~24 seconds to remove the tape with their dominant paw and no differences existed between groups at pre-stroke.

Time to Contact Tape

After stroke, all groups took longer time to contact the tape with their contralateral forelimb (seconds taken: 9.4 ± 1.9 for striatal-only, 14.6 ± 5.1 for cortical-only and 38.4 ± 16.3 for the combined group); however significant post-stroke impairments could only be detected in the striatal-only group ($p<0.046$; Figure 14A). These impairments were observed the first week following stroke. Repeated-measures ANOVA indicated an effect of time ($F=6.74$, $p=0.005$) but not group for post-stroke time points.

Assessment of the time to contact with the non-impaired ipsilateral limb revealed a significant effect of time ($F=6.70$, $p<0.005$; Figure 14B). The cortical- and striatal-only groups

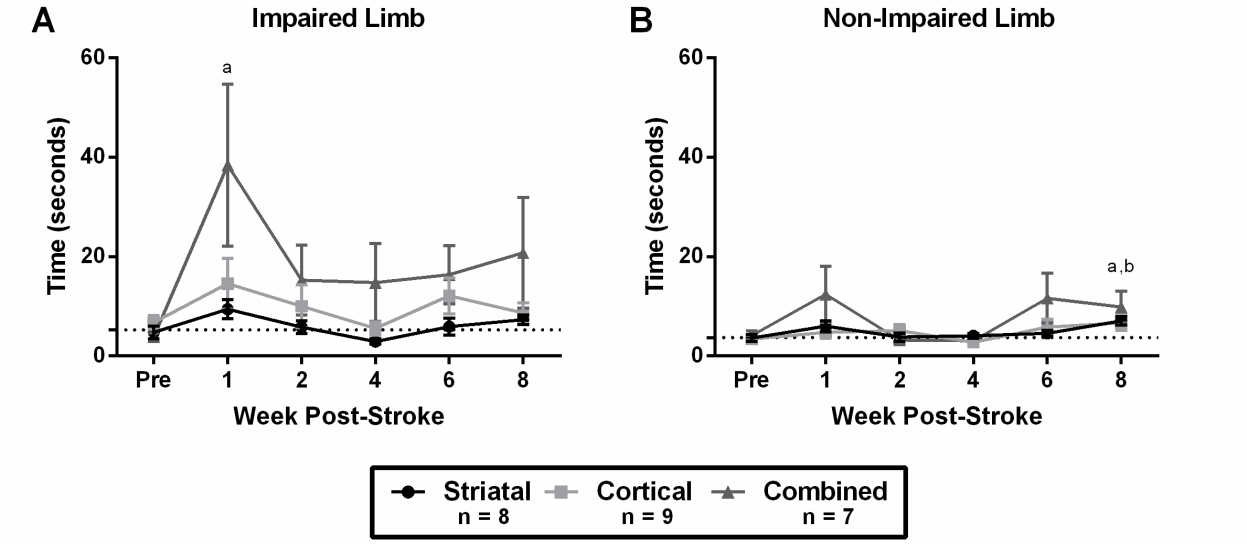

Figure 14: Post-ischemic performance on the adhesive removal test (time to contact). (A) Significant contralateral forelimb impairments could only be detected in the striatal-only group. **(B)** Both the striatal-only and cortical-only group took significantly longer to contact the tape with the ipsilateral forelimb at post-stroke week 8. Values are means ± SEM. Significance markers for pre-stroke vs. post-stroke within-group differences: a = striatal-only, b = cortical-only, c = combined; $p<0.05$.

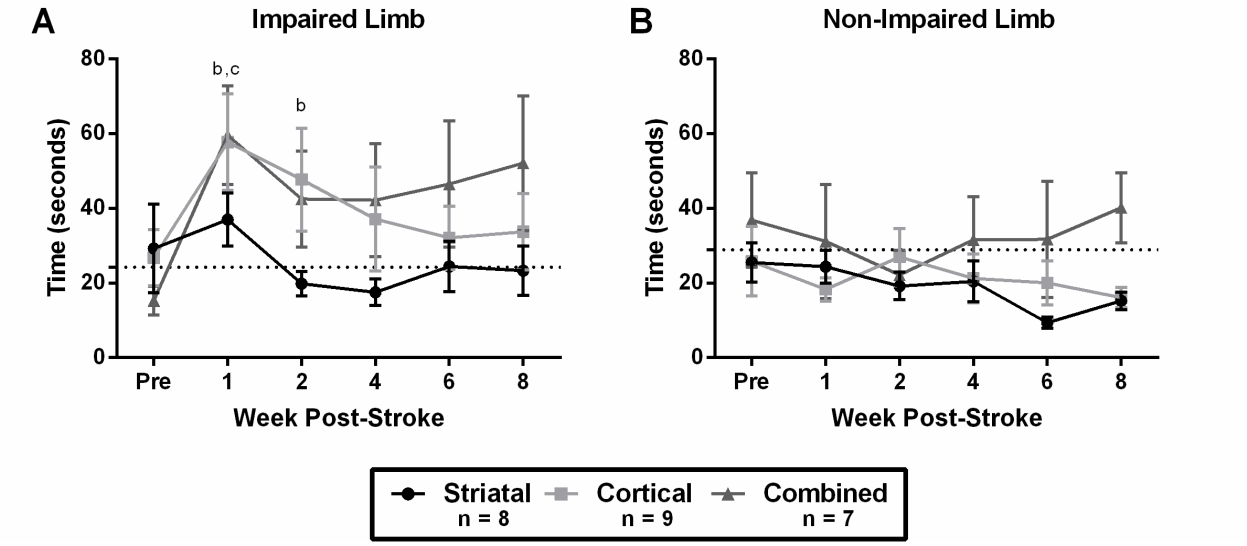

Figure 15: Post-ischemic performance on the adhesive removal test (time to remove). (A) Both the cortical-only and combined group took significantly longer to remove the tape with the contralateral forelimb, whereas the striatal-only group was unaffected. Significant impairments were detected at week 1 for the combined group and up until week 2 for the cortical-only group. **(B)** No significant impairments were observed in the use of the ipsilateral limb. Values are means ± SEM. Significance markers for pre-stroke vs. post-stroke within-group differences a = striatal-only, b = cortical-only, c = combined; $p<0.05$.

took significantly longer to remove the tape at post-stroke week 8 relative to their pre-stroke performance.

Time to Remove Tape

In the measure of time to remove tape, both the cortical-only and combined group took significantly longer to remove the tape with the contralateral forelimb following stroke ($p \leq 0.039$; Figure 15A). A significant effect of time ($F=4.24$, $p<0.005$) was observed for all post-stroke time points. Significant impairments could be detected at week 1 for the combined group and up until week 2 for the cortical-only group. Animals did not show any post-stroke impairments in the use of their ipsilateral paw to remove the tape (Figure 15B).

3.6 Relationship between Infarct Volume and Functional Outcome

To determine if there was any association between the volumes of cortical/striatal injury and severity of initial impairments (week 1 post-stroke) and the amount of recovery between post-stroke week 1 and 8 on the different tests, forward linear regression analysis was performed. Cortical and striatal infarct volumes were advanced as variables of interest to test their ability to predict the level of impairment and recovery. The analysis identified significant correlations and generated predictive models that were then used to calculate predicted impairment and recovery. Predictive model characteristics and equation for each behavioural test are presented in Supplemental Table 2.

Severity of Impairments

Regression analysis revealed that the amount of cortical damage was a significant predictor of the degree of initial impairments on the cylinder test ($r=0.40$, $p=0.044$), both forelimb ($r=0.56$, $p=0.003$) and hindlimb errors ($r=0.62$, $p=0.001$) on the beam traversal test, as well as time to contact ($r=0.47$, $p=0.02$) and remove ($r=0.41$, $p=0.047$) the tape on the adhesive removal task (Figure 16). On the staircase test, the degree of impairment could be best predicted by both the volume of striatal and cortical damage ($r=0.65$, $p<0.002$).

Recovery of Function

Lastly, regression analysis was utilized to examine whether the amount of recovery between post-stroke week 1 and 8 on each of the behavioural tests could also be predicted using cortical and/or striatal infarct volume (Figure 17; Supplemental Table 2). Regression analysis revealed that cortical damage was a significant predictor of the degree of recovery on both forelimb ($r=0.39$, $p<0.047$) and hindlimb ($r=0.53$, $p=0.005$) accuracy on the beam test as well as time to contact on the adhesive removal test ($r=0.55$, $p= 0.006$). In contrast, recovery on the cylinder test could be predicted by the amount of striatal damage ($r=0.58$, $p=0.002$). Infarct volumes were not a reliable predictor of recovery on the staircase reaching test and time to remove measure on the adhesive test.

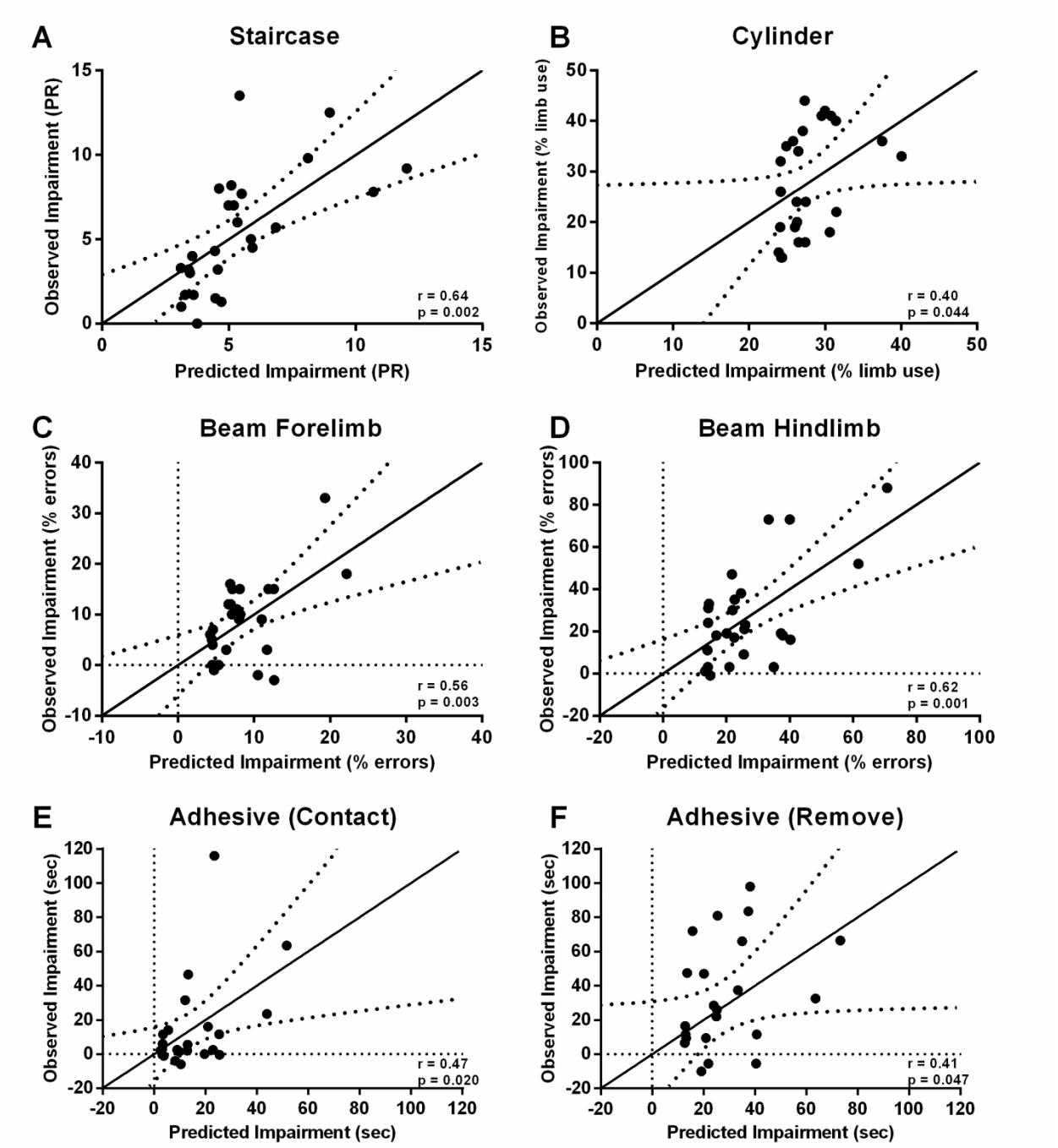

Figure 16: Prediction of impairments using infarct volumes. (A) Impairments on the staircase test (PR) could be predicted using both cortical and striatal infarct volume. Impairments on the **(B)** cylinder, **(C, D)** beam traversal and **(E, F)** adhesive removal test could be predicted by the volume of cortical damage. Predictive model characteristics for each behavioural test are presented in *Supplemental Table 2.* N = 26 for A-D and N = 24 for E, F. All graphs show regression lines with 95% confidence bands.

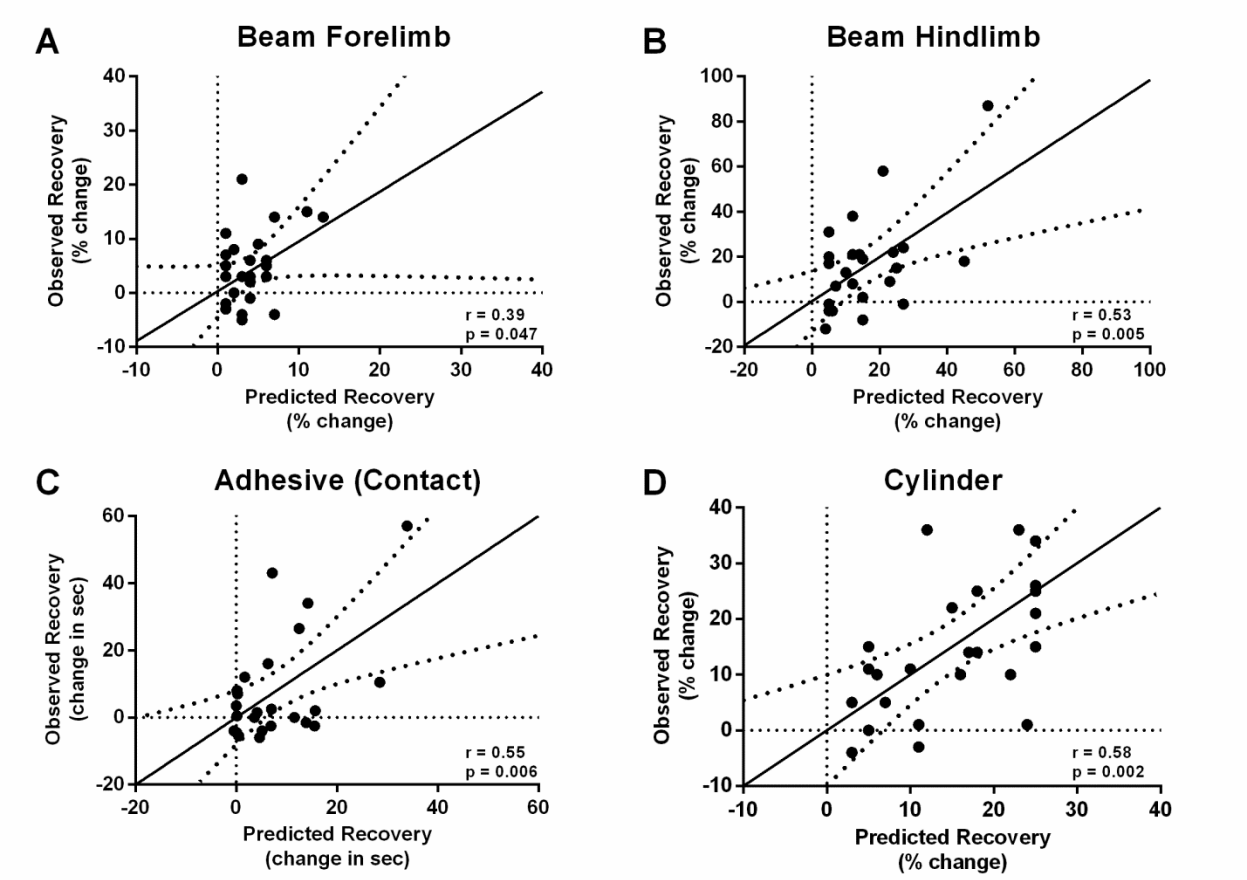

Figure 17: Prediction of recovery using infarct volumes. Cortical infarct volume significantly predicted **(A)** forelimb and **(B)** hindlimb recovery on the beam traversal test and improvement on **(C)** time to contact on the adhesive removal test. **(D)** Recovery on the cylinder test could be predicted by the amount of striatal damage. Predictive model characteristics for each behavioural test are presented in *Supplemental Table 2.* N = 26 for A, B, D and N = 24 for C. All graphs show regression lines with 95% confidence bands.

Experiment 2: Characterizing Changes in PNNs and PV

In experiment 2, all animals underwent staircase training and received the same stroke surgeries as in experiment 1. In addition, two groups of control animals (sham injection and anesthetic controls) were included for comparison. Rats were perfused at 24 hours and 7 days following stroke surgeries in order to evaluate temporal changes in PNNs and PV interneurons (Figure 18).

4.1 Infarct Volumes

The amount of cortical and striatal damage was calculated from cresyl violet stained sections. A two-way ANOVA revealed a significant effect of surgery type but not time for cortical ($F=23.4$, $p<0.001$), striatal ($F=25.8$, $p<0.001$), and total hemispheric damage ($F=20.4$, $p<0.001$; Figure 19). Post-hoc analysis indicated that the combined group had the largest total hemispheric damage compared to all other groups ($p<0.05$). There was no significant difference in the amount of cortical damage between the cortical-only (34.8 ± 5.3 mm^3) and combined group (41.4 ± 6.0 mm^3). Similarly, there was no difference in the amount of striatal damage between the striatal-only (18.6 ± 2.6 mm^3) and combined group (17.1 ± 2.4 mm^3). The infarct volumes in this experimental wave were not significantly different than that observed in experiment 1.

4.2 Post-Stroke Behavioural Assessment

Performance on the Montoya Staircase Test

Post-stroke behavioural data was obtained for animals sacrificed at 7 days. The cortical-only and combined animals were significantly impaired following stroke and retrieved fewer

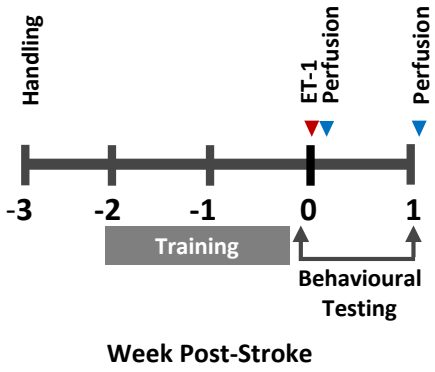

Figure 18: Timeline of experiment 2 to characterize changes in PNNs and PV following ET-1 stroke. After two weeks of behaviour training, animals underwent ET-1 stroke surgery (striatal-only, cortical-only or combined strokes). Rats were perfused at 24 hours and 7 days post-stroke. Post-stroke behaviour data was obtained for animals sacrificed at 7 days.

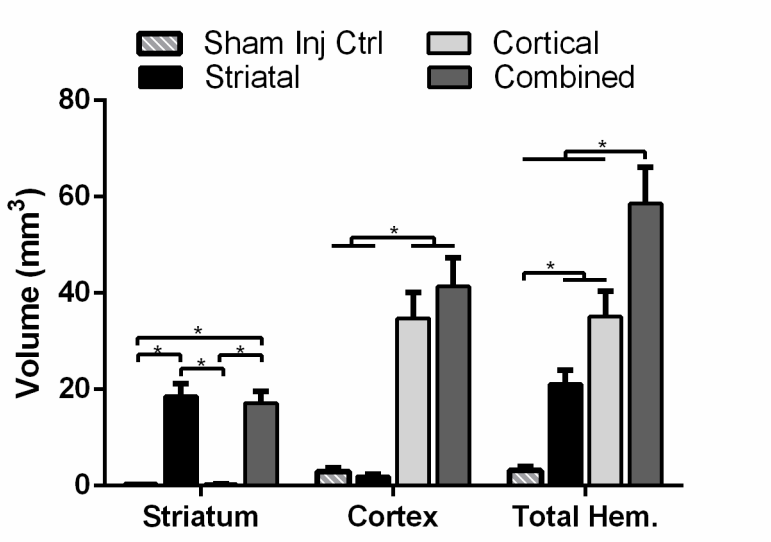

Figure 19: Infarct volumes following ET-1 induced stroke in the cortex and striatum (Exp. 2). There was a significant effect of surgery type but not time, therefore the 24 hour and 7 day time points were collapsed. The combined group had the largest total hemispheric damage. The amount of cortical damage was similar in the cortical-only and combined group. Likewise, the amount of striatal damage was similar in the striatal-only and combined group. Values are means ± SEM. * = $p<0.05$. Sham Inj Ctrl n=10; Striatal n=10; Cortical n=9; Combined n=11.

pellets on the staircase test ($p \leq 0.015$; Figure 20A). The striatal-only group also showed a drop in number of pellets eaten from 17.6 ± 1.0 to 12.7 ± 2.6 pellets; however, this was not statistically significant ($p=0.058$). A one-way ANOVA indicated a significant effect of group ($F=5.13$, $p=0.006$). The combined group was significantly more impaired than both control groups but not the other stroke groups ($p<0.05$). In addition, a between-group difference was detected between the cortical-only and sham injection animals ($p<0.05$). As expected, sham injection and anesthetic controls did not show any impairments at day 7.

Performance on the Cylinder Test

On the cylinder test, the cortical-only and combined animals displayed significant impairments and reduced their use of the contralateral forelimb ($p<0.001$) following stroke (Figure 20B). The striatal-only group also demonstrated a trend towards a decrease in the use of their impaired forelimb ($p=0.060$). There was a significant effect of group ($F=13.28$, $p<0.001$). The combined group performed significantly worse than the striatal-only, anesthetic and sham injection controls ($p<0.05$). A group difference was also observed between the cortical-only and both control groups ($p<0.05$). As with the staircase test, both control groups were not impaired on the cylinder task.

4.3 Stereological Analysis of PNNs and PV

Stereological cell counting was conducted in the perilesional cortex as well as the contralesional cortex homotopic to the infarct core. Representative images of PNN+, PV+ and co-labelled PNN+PV+ cell counts are shown in Figure 21.

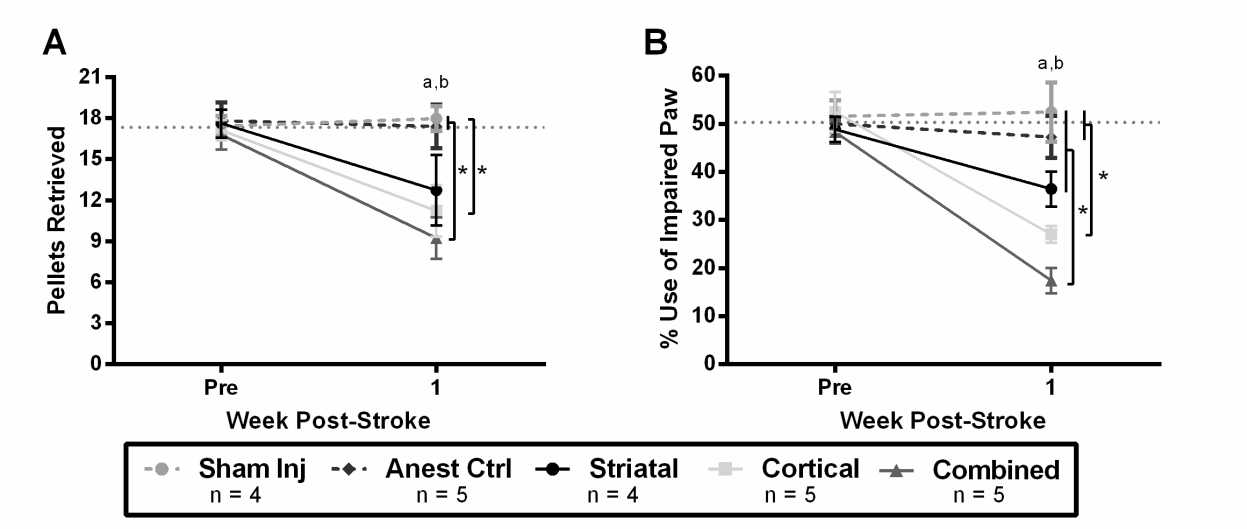

Figure 20: Post-ischemic performance on the Montoya staircase and cylinder test. (A) Skilled reaching performance on the staircase test as indicated by the number of PR. Both the cortical-only and combined group demonstrated significant impairments following stroke. Between-group differences were observed between the combined and both control groups and between the cortical-only and sham injection controls. **(B)** On the cylinder test of forelimb asymmetry both the cortical-only and combined group were significantly impaired following stroke. The combined group was significantly more impaired than the striatal-only, anesthetic and sham injection controls. Between-group differences were also detected between the cortical-only and both control groups. Sham injection and anesthetic control animals did not show any impairments on both tasks. Values are means ± SEM. Significance markers for pre-stroke vs. post-stroke within-group differences: a = cortical-only, b = combined; $p<0.05$. Between-group differences: * = $p<0.05$.

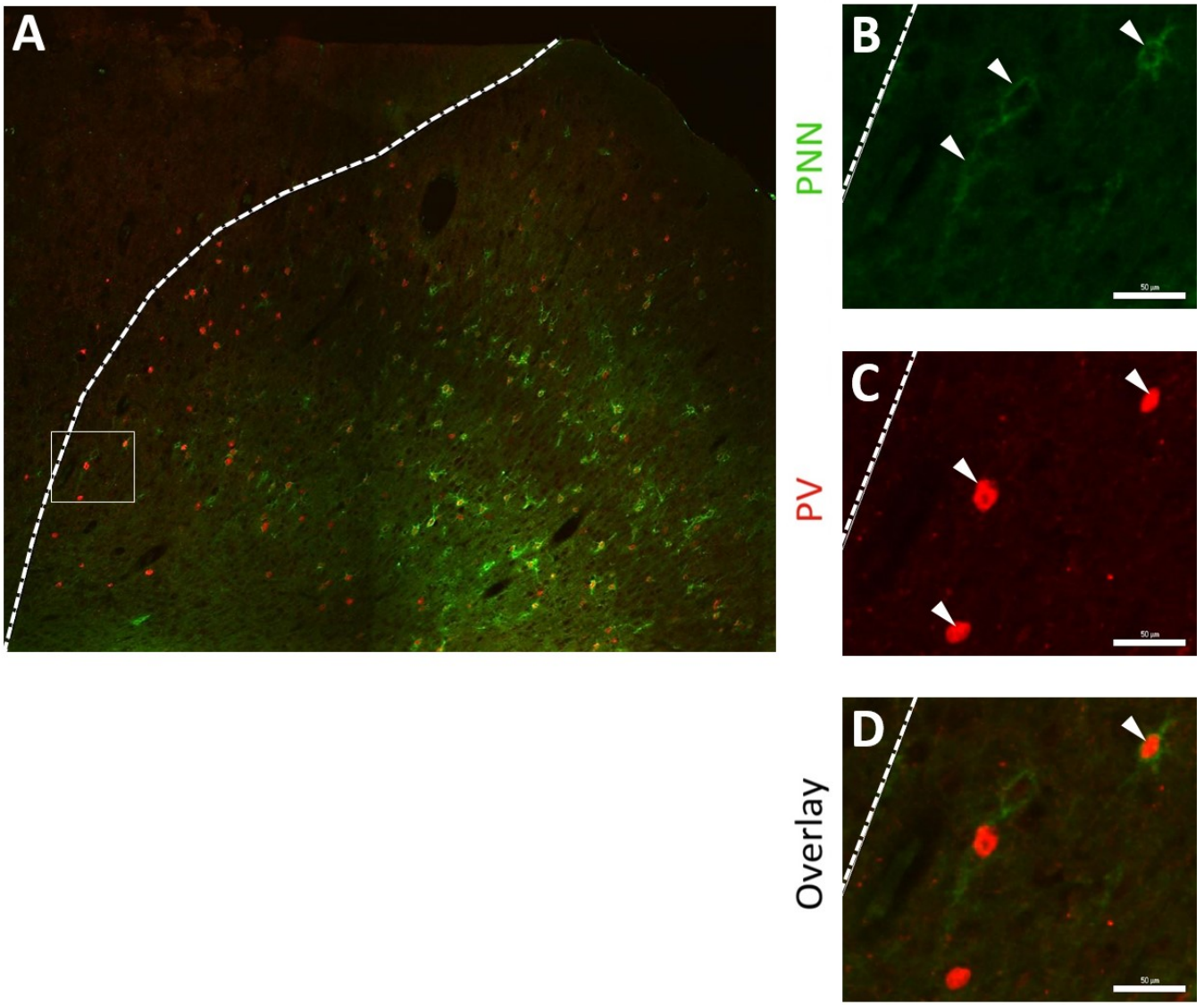

Figure 21: Representative images of PNNs, PV and co-labelled cells. **(A)** Representative image of PNN and PV staining in an animal with a combined stroke sacrificed at 24 hours. White line indicates border of infarct core. Representative images of **(B)** PNN+ **(C)** PV+, and **(D)** co-labelled PNN+PV+ cell count.

Staining and Quantification of PNNs

In SD rats, PNNs were present in all layers of the cortex except layer I, and appeared to be most abundant in layers IV–VI of the sensorimotor cortex (Supp. Figure 3). In other species such as mice, PNNs are also reported to be found throughout the striatum [105, 140], however, in SD rats, PNNs were extremely rare in this region (Supp. Figure 4). Therefore, PNNs were not counted within the striatum.

In animals that received a stroke, very few, if any, PNNs were observed in the infarct core at either post-stroke time point. Surprisingly, a distinctive pattern of non-specific WFA immunoreactivity was present in the infarct core (cortex and striatum) of all stroked animals sacrificed at the 7 day time point (Supp. Figure 5). There was an accumulation of cells that exhibited strong intracellular WFA staining and could clearly be differentiated from PNNs in these animals. It is thought that these WFA positive cells represent leukocytes that invade the infarct core and are involved in the removal of cell debris [120].

Assessment of the density of PNNs in the perilesional cortex, revealed a main effect of surgery type ($F=11.9$, $p<0.001$) but not time (Figure 22A). Post-hoc analysis indicated that the cortical-only and combined animals had significantly fewer PNNs (~25% difference) compared to anesthetic, sham injection and striatal-only group ($p<0.05$). These results suggest that it is cortical but not striatal injury that causes a reduction in PNNs in the perilesional cortex. No significant differences in the density of PNNs were found in the contralesional hemisphere homotopic to the infarct core (Figure 22B).

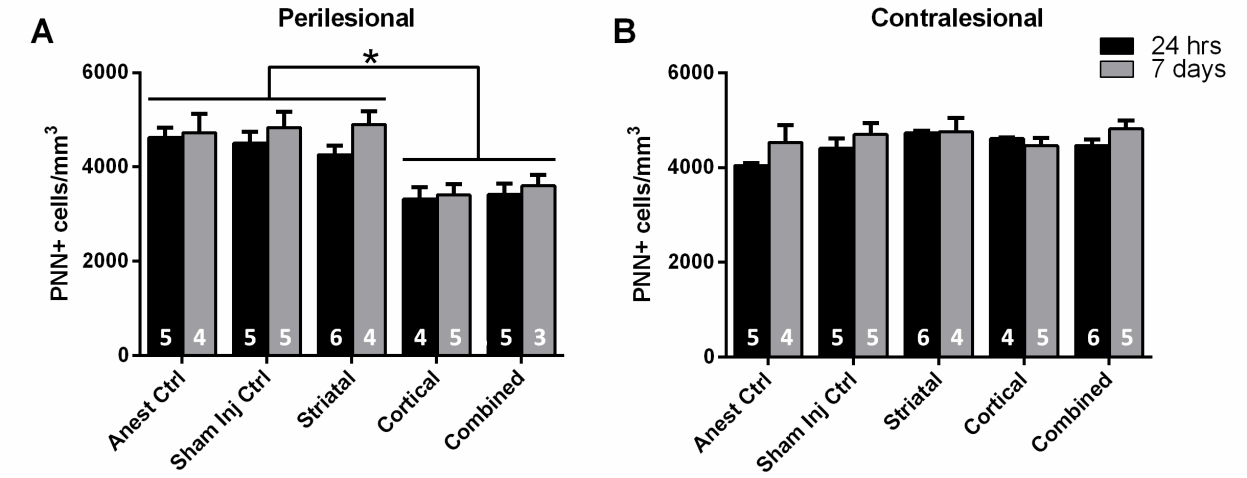

Figure 22: Density of PNNs in the perilesional and contralesional hemisphere. (A) Density of PNNs in the perilesional cortex at 24 hours and 7 days post-stroke. The cortical-only and combined groups showed a significant reduction in the density of PNNs compared to the other groups when the time points were collapsed. **(B)** No differences were observed between groups in the contralesional hemisphere. Values are means ± SEM. * = $p<0.05$. Number within each bar represents sample size.

Staining and Quantification of PV Interneurons

In SD rats, PV interneurons were distributed in all layers of the cortex except layer I (Supp. Figure 3). After stroke, there was a striking loss of PV-immunoreactivity within the infarct core of all stroked animals. However, no significant differences in the density of PV interneurons could be detected between stroke and control groups in either the perilesional and contralesional cortex (Figure 23).

Proportion of Co-labelled PV Interneurons

PNNs are known to be primarily associated with PV interneurons, therefore we assessed if reduction in PNNs was occurring around this cell type. To evaluate this, the proportion of co-labelled PV cells was calculated by dividing the density of co-labelled cells (PNN+PV+) by the density of PV interneurons. This revealed that approximately 70% of all PV interneurons in the control animals (sham injection and anesthetics) were surrounded by PNNs.

In the perilesional cortex, two-way ANOVA indicated a main effect of group ($F=4.3$, $p<0.01$) but not time (Figure 24A). Post-hoc analysis identified that both the combined and cortical-only animals had a significantly lower proportion of co-labelled PV cells compared to the striatal-only group ($p<0.05$). The combined group also had a significantly lower proportion of co-labelled PV interneurons than the sham injection group ($p<0.05$). These results show that PNNs are reduced around PV interneurons in the perilesional cortex following a cortical injury. In contrast, no significant differences in the proportion of co-labelled PV cells were observed between groups in the contralesional cortex (Figure 24B).

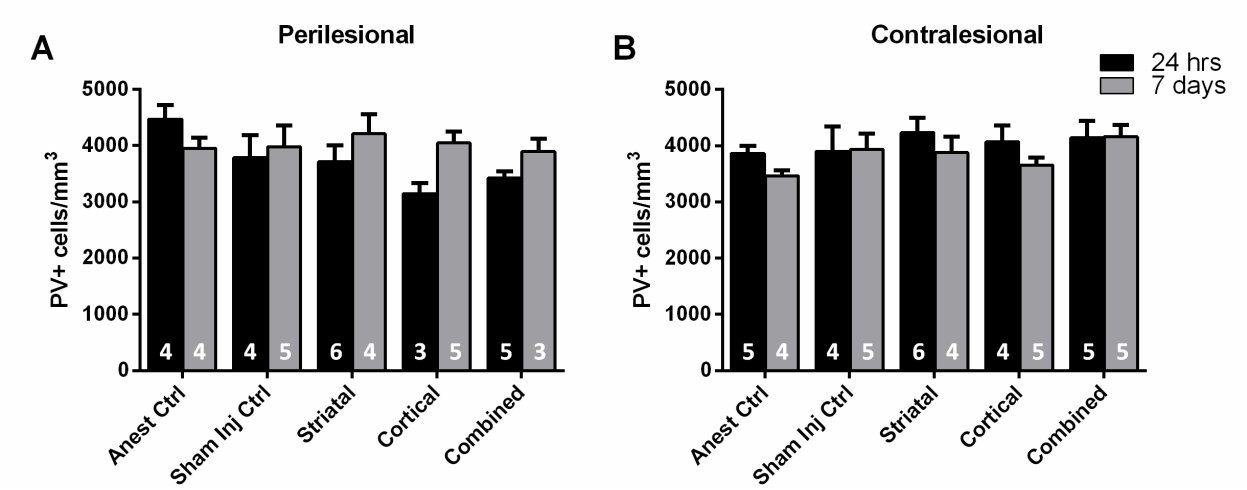

Figure 23: Density of PV interneurons in the perilesional and contralesional hemisphere. There were no significant differences in PV density between stroked and control groups in both the **(A)** perilesional and **(B)** contralesional hemisphere. Values are means ± SEM. Number within each bar represents sample size.

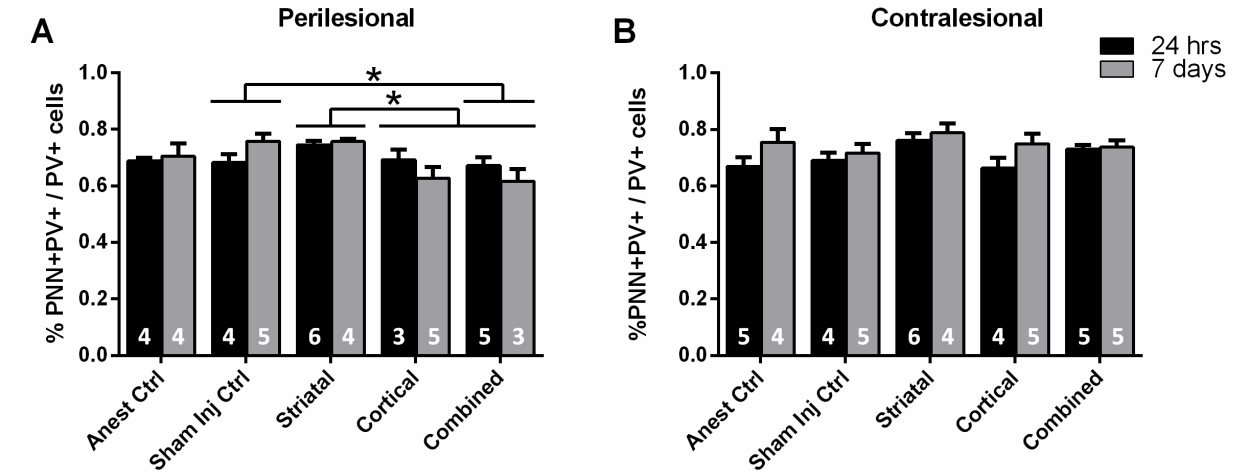

Figure 24: Proportion of co-labelled PV cells in the perilesional and contralesional hemisphere. (A) A significant effect of group was detected in the perilesional cortex. The cortical-only and combined groups showed a significant reduction in the proportion of co-labelled PV cells compared to the striatal-only group when the time points were collapsed. The combined group also had a significantly lower proportion than the sham injection group. **(B)** There were no differences between groups in the contralesional hemisphere. Values are means ± SEM. * = $p<0.05$. Number within each bar represents sample size.

Proportion of Co-labelled PNN Cells

Although PNNs mainly enwrap GABAergic PV interneurons, they are also found surrounding other cell types (e.g. pyramidal neurons). To determine whether PNN reduction is confined primarily to PV interneurons or other cell types following stroke, the proportion of co-labelled PNNs was compared between groups. This measure was calculated by dividing the density of co-labelled cells by the density of PNNs. In the control groups approximately 60% of all PNNs were associated with PV interneurons. This suggests that the remaining 30% surround other cell types in the cortex.

No significant differences in the proportion of co-labelled PNNs were observed between stroked and controls groups in either the perilesional or contralesional hemisphere (Figure 25). This indicates that the reduction of PNNs observed in the perilesional cortex was not exclusively around PV interneurons, but was also occurring around other cell types.

4.4 Distribution of PNNs and PV as a Function of Distance from Infarct

To assess if the distribution of PNNs and PV interneurons varied as a function of distance from infarct, the locus analysis probe in StereoInvestigator was used. The distance of every counted PNN and PV cell within the perilesional cortex was measured from the infarct border and distribution of the cells within the first 800 μm was examined.

No significant differences in the distribution of PNNs and PV were observed between groups (Figure 26). In the stroked groups, PNNs and PV interneurons could be found even at the very edge of the traced infarct border (0 μm from infarct). This suggests that the observed post-stroke reduction in PNNs was occurring uniformly throughout the perilesional cortex and was not localized to a narrow band near the infarct.

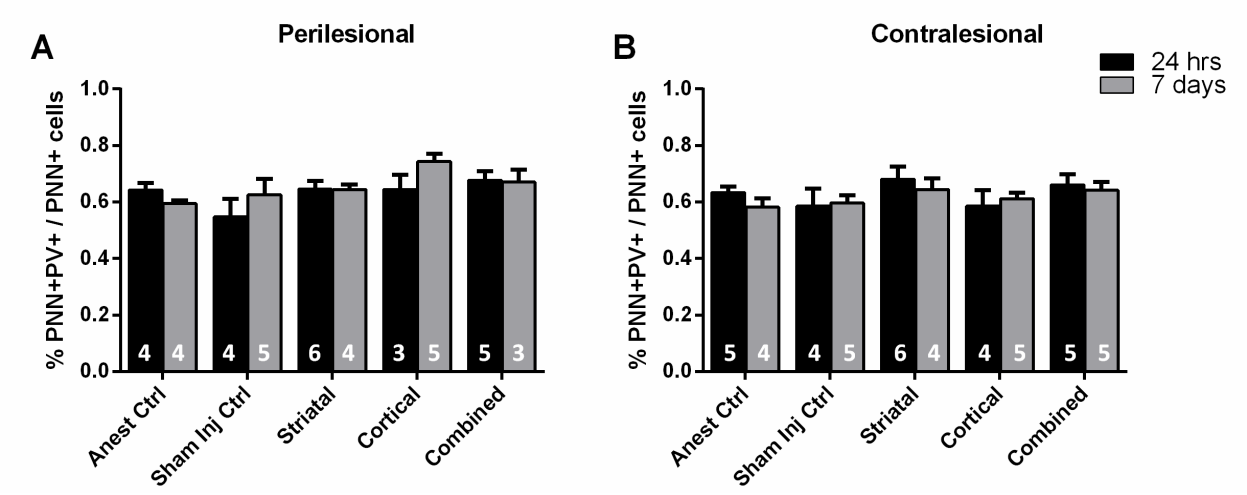

Figure 25: Proportion of co-labelled PNNs in the perilesional and contralesional hemisphere. There were no significant differences between stroked and control groups in both the **(A)** perilesional and **(B)** contralesional hemisphere. Values are means ± SEM. Number within each bar represents sample size.

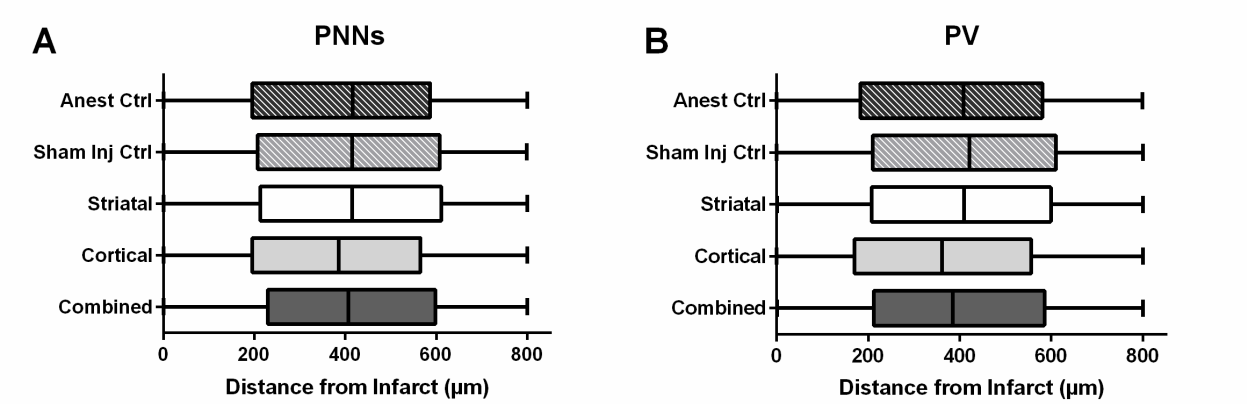

PNNs: Anest Ctrl n=9; Sham Inj Ctrl n=10; Striatal n=10; Cortical n=9; Combined n=8

PV: Anest Ctrl n=8; Sham Inj Ctrl n=9; Striatal n=10; Cortical n=8; Combined n=8

Figure 26: Distribution of PNNs and PV interneurons as a function of distance from the infarct. Box plot representation of the distribution of **(A)** PNNs and **(B**) PV interneurons in the different groups. The box represents the lower quartile (25%) and upper quartile (75%). The whiskers represent the minimum (0 µm) and maximum distance (800 µm) of counted cells from the infarct border. Vertical line in the box shows the median distance. The distribution of PNNs and PV cells relative to the infarct border were similar between all groups.

4.5 Relationship between Infarct Volume and Cellular Changes

The results of the stereological analysis suggest that it was cortical and not striatal injury that caused cellular changes in the perilesional cortex. Therefore, possible relationships between the volume of damage and the density/proportion of PNNs and PV cells were evaluated. Animals from all groups were included in this analysis.

A significant negative correlation was observed between cortical infarct volume and PNN density ($r=-0.75$, $p<0.001$), PV density ($r=-0.37$, $p=0.014$) and proportion of co-labelled PV cells ($r=-0.41$, $p=0.007$) in the perilesional cortex (Figure 27). In addition, a significant positive correlation was found between the amount of cortical damage and the proportion of co-labelled PNNs ($r=0.35$, $p=0.021$). In contrast to cortical damage, there was no association between the volume of striatal damage and the density/proportion of PNNs and PV in the perilesional cortex (Figure 27). The difference in results between the correlation analysis and ANOVA suggests that the experiment may not have had enough statistical power to detect a between-group effect in the density of PV interneurons.

There was no significant relationship between volume of striatal/cortical damage and density/proportion of PNNs and PV cells in the contralesional cortex.

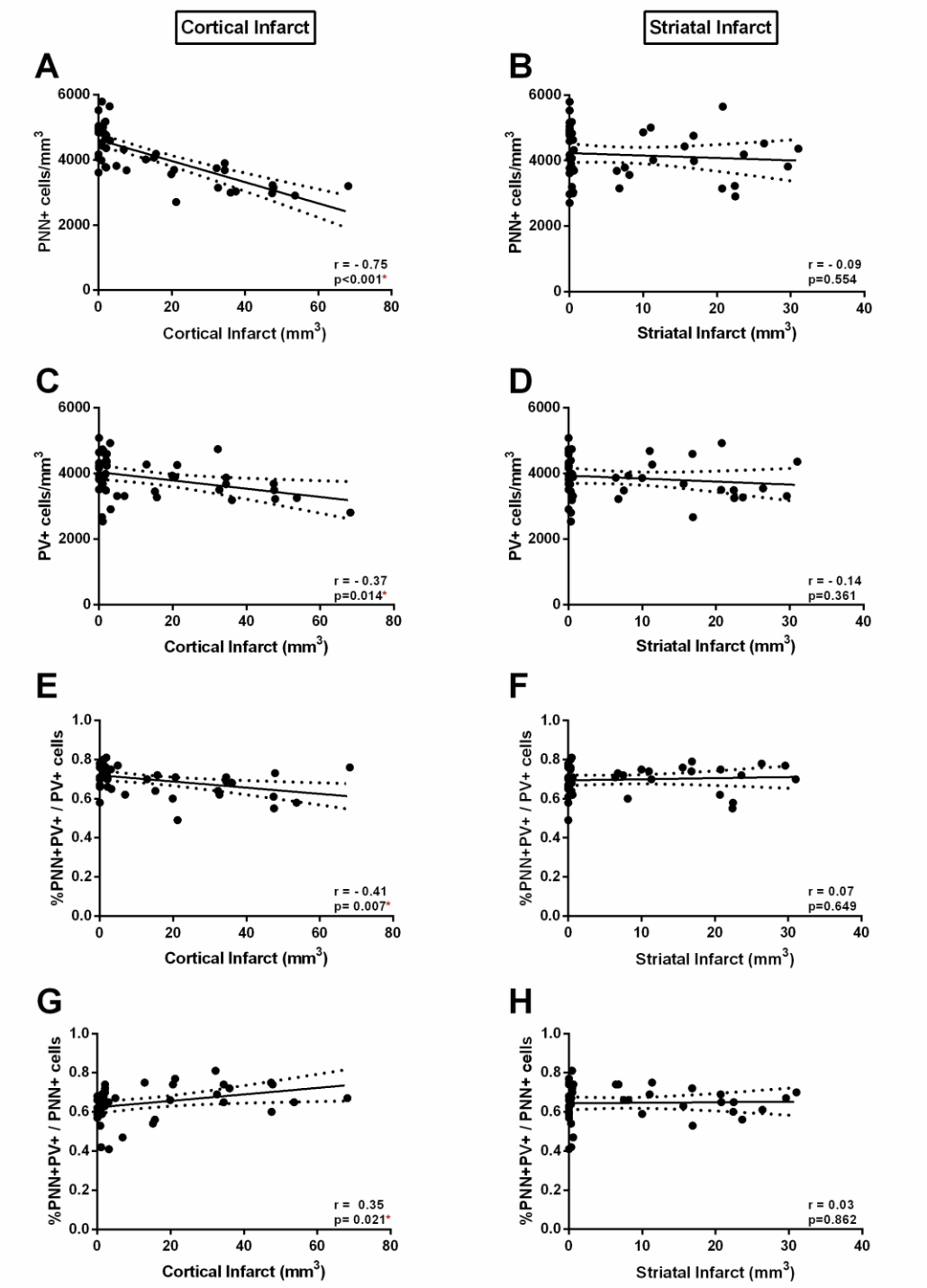

Figure 27: Relationship between infarct volume and density/proportion of PNNs and PV cells in the perilesional cortex. Plots showing relationship between stereological outcome measures and cortical (left column) and striatal (right column) infarct volume. The outcome measures were **(A, B)** PNN density, **(C, D)** PV density, **(E, F)** proportion of co-labelled PV cells and **(G, H)** proportion of co-labelled PNN cells. There was a significant correlation between cortical infarct volume and all outcome measures. N = 46 for A, B and N = 43 for C-H. All graphs show regression lines with 95% confidence bands.

Discussion

Experiment 1

In both humans and animals, varying degrees of spontaneous functional recovery are observed following stroke. This recovery process is especially difficult to study in humans as most stroke survivors receive rehabilitation. The present study sought to determine how the location of injury affects recovery of motor function up to 2 months after stroke. We produced focal strokes in the FMC, equivalent to the primary motor cortex (M1) and/or the DLS which is homologous to the human basal ganglia. Our results confirm our hypothesis that the lesion location does affect functional outcome following stroke. Stroke to the FMC and/or DLS resulted in significant functional impairments on most of the behavioural tests. Interestingly, our data demonstrated that recovery is not only dependent on the lesion volume but also on the lesion location and the behavioural test used to assess function.

Motor recovery is dependent on infarct location and varies with different behavioural tests

In this study we used a battery of behavioural tests to assess functional outcome following stroke. In the cylinder test of spontaneous forelimb use, both the striatal-only and combined group displayed limited recovery and remained impaired throughout the testing period. In contrast, the cortical-only group demonstrated significantly greater recovery and returned to pre-stroke performance levels by week 6. These results indicate that striatal involvement is important for performance on this test, which was further confirmed by regression analysis that identified striatal damage to be a significant predictor of the amount of recovery. Our finding is in line with clinical evidence that patients with subcortical strokes show poorer upper limb motor recovery than those with injuries confined to the cortex [17, 18]. It is thought that better outcome

in patients with cortical-only strokes may be due to the redundancy of the cortical motor system with spared cortical regions taking over function of the damaged site [17]. Others have hypothesized that poor functional outcome following strokes isolated to the striatum may be due to dysfunctional cortical-striatal interactions that impede recovery [18].

In the staircase test of skilled forelimb reaching, animals in all groups displayed significant impairments in their ability to retrieve pellets that persisted even at 2 months following stroke. Interestingly, while both the striatal-only and combined group exhibited difficulty in reaching pellets from the lower steps, the cortical-only group was not affected on this measure. The dorsolateral region of the striatum that we targeted is involved in skilled motor control [141] which may explain the deficits seen in the groups with striatal damage. Clinically, it is accepted that patients with milder impairments are likely to show both rapid and complete recovery than those with severe deficits [52]. Despite having mild deficits (~80% of baseline performance), animals in the striatal-only group did not achieve complete recovery. In addition, the striking recovery seen in the cortical-only group in the cylinder test was not evident in the staircase test. This difference between tasks suggests that recovery of gross motor skills may occur spontaneously whereas recovery of fine motor function may require intervention.

In contrast to the staircase and cylinder test, we were unable to detect robust long-term deficits on the adhesive removal task. Groups that were initially impaired recovered to pre-stroke levels by week 2. Our results differ from other studies that observed long-term impairments, as late as 6 months following stroke on the adhesive test [142, 143]. This may be due to differences in size and location of injury and strain of rats between studies. It is also important to note that both the cortical-only and the combined groups showed a high degree of within-group variability in performance on this task, which may have prevented us from detecting significant deficits. We

noticed a few animals starting to use compensatory strategies to contact and remove the tape on their impaired forelimb which may explain the large variability in performance. Due to the transient deficits, we do not believe that this test is a sensitive measure in our stroke model.

We found the beam traversal test to be more sensitive in detecting impairments of hindlimb function than that of the forelimb. Regardless of stroke location, animals in all groups made significantly more contralateral hindlimb foot faults following surgery. Although our stereotaxic coordinates targeted forelimb areas, the hindlimb representation area in both the striatum and the cortex lies in close proximity to the forelimb area [29, 144]. As a result, animals in our study had strokes that extended into the hindlimb regions causing these hindlimb deficits. As with the staircase and cylinder test, the striatal-only and combined group displayed limited recovery on the task and had significant impairments throughout the testing period. In comparison, the cortical-only group recovered to pre-stroke levels by week 8. This finding lends further support to previous studies that have shown that subcortical strokes result in poorer functional outcome than cortical strokes [17, 18].

Significant and chronic impairments can result even with small strokes

In the present study we wanted to capture the clinical characteristics of stroke with respect to both location and size. As previously reported by Carmichael and colleagues, “human strokes are mostly small in size” with lesions ranging from 4.5-14% of the ipsilesional hemisphere [35]. However, the majority of preclinical stroke studies have utilized models that result in the destruction of a greater proportion of the ipsilesional hemisphere than is typically observed in the clinical population [28]. This mismatch between preclinical and clinical research may impair translational efforts.

The infarct volumes obtained in our study correspond to ipsilesional hemispheric damage of 1.9% in the striatal group and range up to 6.1% in the combined group. Despite these relatively small strokes, our animals showed chronic motor impairments as a result of strokes targeting specific cortical and striatal regions involved in motor control. A problem for pre-clinical researchers is the occurrence of rapid and complete recovery in many stroke models [53]. This is especially challenging when evaluating new interventions, since spontaneous recovery may prevent the detection of a treatment effect. The chronic impairments resulting from the stroke models described in this thesis will be valuable for future research evaluating new adjunct therapies.

Animals demonstrated similar patterns of recovery to that seen in humans

Overall, the pattern of recovery observed on the different behavioural tasks in this study was similar to the non-linear curve described in humans [54]. Most of the spontaneous recovery appeared to take place between post-stroke weeks 1 and 2. Resolution of edema and diaschisis may be a likely mechanism that contributes to recovery during this early phase. After approximately 4 to 6 weeks following stroke, recovery on most of the behavioural tests reached a plateau. There is compelling preclinical evidence for the existence of a critical period of increased neuroplasticity in the days to weeks following stroke [8]. The plateau observed in the behavioural tests in our study may reflect the closure of this critical period. The second experiment in this thesis was aimed at investigating one potential cellular mechanism that might be responsible for this recovery plateau.

Limitations

One limitation of the present study is that we cannot differentiate true spontaneous recovery from improvement due to behavioural compensation. It is conceivable that some amount of improvement we observed in the behavioural tests may have resulted from animals using new adaptive strategies to perform a task in a different manner than they did prior to stroke. This was especially evident in the adhesive removal test where some animals were "cheating" by using their non-impaired paw to hold the impaired paw to aid in removal of the tape. Compensation may also exist in other tasks such as the staircase test where animals may be making more subtle changes in posture and forelimb movements to retrieve pellets. In future studies, the use of kinematic analysis and comparison of pre- and post-stroke movement patterns will help identify such changes and confirm the use of behavioural compensation.

Implications of the study

Our results highlight the importance of using multiple and varying behavioural tests when assessing functional outcome following stroke. Most pre-clinical studies use only one or two tests to evaluate functional outcome. Here, we demonstrate that the degree of recovery that animals show on one test may not necessarily be similar in another test. For example, if we had only used the cylinder test we would not have seen the chronic reaching impairments that the cortical-only group revealed in the Montoya staircase test. Moreover, researchers must carefully select tasks that are sensitive to the particular injury model and species.

This experiment also has clinical implications. Stroke is a heterogeneous condition; therefore a "one-size-fits-all" approach to stroke rehabilitation might not be the most effective. Recently, there has been a lot of interest in trying to identify biomarkers to predict stroke

recovery and optimize current rehabilitation. Several different biomarkers have been investigated including the use of anatomical (e.g. lesion size), physiological (e.g. motor evoked potential) and behavioural measures (e.g. initial level of impairment on Fugl-Meyer assessment) to predict recovery [145]. In the present study, we evaluated whether cortical/striatal infarct volume could be used to predict the degree of initial impairment and amount of motor recovery after stroke. Regression analysis showed that these measures are significant predictors of functional outcome on several of the behavioural tests, accounting for ~12-37% of the variance. Thus, our findings lend support to the use of infarct volume and location as biomarkers of functional outcome following stroke. Clinicians should consider these measures when developing and prescribing interventions for stroke survivors.

Experiment 2

This experiment was conducted as a follow up to experiment 1, to investigate one mechanism known to regulate critical period plasticity [116] that could also be important for neuroplasticity and recovery following stroke. We sought to understand how plasticity limiting PNNs and associated PV+ GABAergic interneurons change in the days following an ischemic injury. A limited number of studies have previously investigated changes in PNNs and PV using the PT or MCAO stroke model [80, 120–123]. However, these studies have yielded conflicting results. To the best of our knowledge, ours is the first study to characterize changes in these cell types following injury to different brain regions using the ET-1 stroke model. Our results demonstrated a significant reduction of PNNs in the perilesional cortex of animals that received a cortical-only or combined cortical-striatal stroke. Interestingly, the same was not observed in the striatal-only group. Although we did not observe significant between-group differences in the

density of PV interneurons, a significant negative correlation existed between PV density and cortical infarct volume. Our results suggest that PNNs are reduced not only around PV interneurons but also around other cell types. In contrast to the perilesional cortex, we did not observe any cellular changes in the contralesional hemisphere. Together, these results support our initial hypothesis that stroke triggers neuroplastic changes in the injured brain that vary depending on the location of injury.

Reduction of PNNs in the perilesional cortex following a cortical-only/combined stroke but not a striatal-only stroke

Several studies have shown that the perilesional cortex undergoes cortical reorganization and is crucial for functional recovery, thus prompting us to analyze this region [146, 147]. Here, we observed a ~25% reduction in the density of PNNs following either cortical-only or combined stroke at both 24 hours and 7 days post-stroke. These results are similar to the findings of two other groups that had previously reported a reduction of PNNs in this region using PT and pMCAO models [121, 122]. However, in the study using the PT model the authors noted a more striking reduction of PNNs (~90%) at 24 hours which then continued to increase over time [122]. One possible explanation for this disparity may have been the difference in the region sampled. Our perilesional counting box extended much further (1 mm) from the infarct in comparison to the other study (200 μm). This led us to consider whether the reduction in PNNs was more pronounced in regions closer to the infarct. We examined how PNNs in our perilesional area were distributed as a function of distance from the infarct border. The results of this locus analysis indicated that the reduction of PNNs in our ET-1 model was uniform throughout the perilesional cortex and not localized to a narrow region directly adjacent to the infarct.

Our findings also differ from the results reported by Carmichael and colleagues (2005) who noted an increase in staining for PNN associated components in the region immediately adjacent to the infarct core, and a reduction in staining in the area more distant (2 mm) from the infarct following pMCAO [80]. The differences between our results and other studies are likely attributed to the stroke model itself. Indeed, there is evidence that expression of molecules associated with plasticity can differ depending on the type of method used to produce the lesion [148]. One notable difference between our model and that of others is the occurrence of reperfusion in the ET-1 model, resulting in a different injury profile. Future research involving a direct comparison between models (e.g. PT vs. ET-1) can provide more insight as to why such differences exist. Other possible explanations for discordant results between studies include differences in species/strain (e.g. mouse vs. rat) and the quantification approach (e.g. qualitative vs. stereological).

There is some evidence for cortical plasticity and reorganization following subcortical strokes [149, 150], thus we wanted to examine whether PNNs in the cortex undergo remodelling following a subcortical injury. In contrast to cortical injuries, striatal-only strokes did not lead to a reduction of PNNs in the ipsilesional cortex. One simple explanation for this result could be that remodeling of PNNs may only occur in proximity to the stroke site or within the same region. However, this is unlikely as others have reported significant changes in PNNs density in areas distant from the lesion [122]. Although we did not observe changes in the cortex it is possible that striatal strokes may have induced PNN reduction in other motor-related structures such as the substantia nigra or red nucleus which are abundant in PNNs. Our results are in agreement with past research which found that stroke induced neuroplastic changes can differ

depending on the location of the injury [151]. Taken together, our findings suggest that different mechanisms may underlie functional recovery following cortical and striatal strokes.

Inverse relationship between cortical infarct volume and density of PV interneurons in the perilesional cortex

Previous studies that have looked at post-stroke changes in PV have reported conflicting findings. For example, significant reduction of PV interneurons was observed following pMCAO whereas no early changes in PV were seen following PT stroke [121, 123–125]. Similar to PNNs, these discrepancies are most likely due to differences in stroke models used in the studies. In the present study, we did not find a significant difference in the density of PV interneurons between stroke and control groups. Nonetheless, the correlational analysis in which all animals were included indicated a significant inverse relationship between cortical infarct volume and density of PV interneurons in the perilesional cortex. This led us to consider the possibility that we may not have had enough power in this experiment to detect a potential between-group effect of stroke on the density of PV interneurons. A post-hoc power analysis revealed that in order for a between-group effect of this size to be detected (80% chance), a total sample of 78 animals (~8 per group) would be needed. This can easily be achieved with one replication of this experiment. Thus, our results indicate that both PNNs and PV are affected by stroke, however the effect of stroke on PNNs ($f = 1.15$) is far more pronounced than on PV interneurons ($f = 0.40$).

PNNs are not exclusively reduced around PV interneurons

Although past studies investigated post-stroke changes in PNN and PV separately, we are the first to examine the association between both. In our control animals, approximately 60% of

all PNNs were associated with PV interneurons which is in line with reports that PNNs primarily enwrap PV interneurons [107, 108]. Our analysis of the proportion of co-labelled PV and PNN cells suggests that PNNs are reduced around PV interneurons in the perilesional cortex following a cortical and combined stroke. However, the reduction of PNNs is not exclusive to PV interneurons but also to other cell types. In addition to PV interneurons, PNNs are also known to enwrap non-GABAergic pyramidal neurons [108]. Our findings suggest that future studies investigating post-stroke changes in PNNs should not solely focus on PV interneurons, but also distinguish the other cell types that PNNs enwrap. Further studies are needed to determine how the reduction in PNNs affect the activity of the neurons they surround in the perilesional cortex.

No cellular changes observed in the contralesional cortex

In addition to the perilesional cortex, more remote regions to the infarct, such as the contralesional cortex, have been shown to undergo neuroplastic changes following stroke [152, 153]. Thus, we hypothesized that cellular changes may have been evident in the contralesional cortex. Interestingly, stereological analysis did not reveal any significant changes in the density or proportion of PNNs or PV interneurons in the contralesional cortex. Our results are in agreement with most of the previous literature that evaluated post-stroke changes of PNNs/PV [120, 121, 123, 125]. However, our findings differ from the study by Karetko-Sysa and colleagues (2011) who reported a significant reduction of PNNs (by ~40%) in the contralesional hemisphere, following cortical PT strokes. This notable difference between studies further supports our premise that the mechanisms responsible for the reduction of PNNs may differ across stroke models. Another possible explanation for this notable change in the contralesional

cortex, may be due to damage to the corpus callosum which was observed in animals in the study by Karetko-Sysa and colleagues.

Mechanisms underlying the reduction of PNNs

The mechanisms underlying PNN remodeling in the cortex following stroke remains unclear. In their study, Karetko-Sysa and colleagues (2011) used markers for necrotic and degenerating cells and showed that the reduction of PNNs they observed was not associated with cell death [122]. This suggests that other regulatory mechanisms may exist which control PNN expression following injury. Indeed, there is an upregulation of enzymes such as matrix metalloproteinases (MMPs) and hyaluronidase following stroke [154–156]. MMPs are a family of proteolytic enzymes that are known to cleave ECM molecules including components of PNNs [157]. Likewise, the enzyme hyaluronidase degrades HA, the main backbone of PNNs [156]. Thus, it is conceivable that stroke-induced elevation of these enzymes contributes to the degradation of PNNs. Further studies are needed to clarify the association between these enzymes and PNN degradation following ischemic injury.

Association between cellular changes and functional recovery

CSPGs, which are a major component of PNNs, restrict plasticity and neuronal repair in the adult brain [99, 100]. In models of spinal cord injury, digestion of PNNs with the enzyme chABC has been associated with sprouting of new fibers and improved functional outcome [89, 92]. Likewise, administration of chABC in the peri-infarct region following stroke enhances functional outcome when combined with motor training [94]. The post-stroke reduction of PNNs that we observed might be an endogenous response to create a permissive environment for

regenerative processes such as axonal sprouting. Indeed axonal sprouting in the peri-infarct region has been causally associated with functional recovery following stroke [147].

Moreover, recent findings indicate that PNNs modulate the activity of the inhibitory PV interneurons that they surround [119]. Thus, post-stroke reduction in PNNs may also affect the activity of associated PV interneurons, subsequently altering the E/I balance in the brain leading to decreased inhibition. Alterations in the E/I balance of the cortex has been shown to underlie critical period plasticity and has also been implicated in stroke recovery [116]. For example, pharmacological reduction of excessive GABAergic inhibition has been shown to improve functional recovery following stroke [158, 159].

Future work is needed to further extend the findings of this study. While the present experiment provides insight into how PNNs change early after stroke, it is important to determine whether the reduction of PNNs observed in our ET-1 model decreases further, stays at the same level, or increases in the following weeks. Furthermore, an important question yet to be answered is, what do the post-stroke changes in PNNs mean for spontaneous functional recovery? To address this, a long-term study with behavioural assessment is currently underway to investigate the association between temporal changes in PNNs and functional recovery. We hypothesize that PNNs in the perilesional cortex will begin to recover over time, thereby leading to the plateau in spontaneous functional recovery.

Conclusion

Using the ET-1 stroke model, we compared spontaneous motor recovery following a cortical-only, striatal-only and combined cortical-striatal stroke. Our findings demonstrate that functional outcome is dependent not only on the lesion volume but also on the lesion location and the behavioural test employed. The models described in this thesis could be of significant value for future studies assessing novel, adjunctive post-stroke therapies due to their resultant chronic impairments. Moreover, we demonstrate that plasticity-limiting PNNs are reduced in the perilesional cortex following strokes targeting the cortex but not the striatum. These results suggest that different mechanisms may underlie recovery following cortical and subcortical strokes, thus different interventions may be necessary for treating various stroke subtypes. Further investigation into how the changes in PNNs correlate with functional recovery will provide more insight into the mechanisms underlying spontaneous motor recovery.

References

1. Heart & Stroke Foundation: *Heart & Stroke Foundation 2016 Stroke Report*. 2016.

2. Krueger H, Koot J, Hall RE, O'Callaghan C, Bayley M, Corbett D: **Prevalence of individuals suffering from the effects of stroke in Canada: Trends and projections**. *Stroke* 2015, **46**:2226–2231.

3. Mittmann N, Seung SJ, Hill MD, Phillips SJ, Hachinski V, Coté R, Buck BH, Mackey A, Gladstone DJ, Howse DC, Shuaib A, Sharma M: **Impact of disability status on ischemic stroke costs in Canada in the first year**. *Can J Neurol Sci* 2012, **39**:793–800.

4. Andersen KK, Olsen TS, Dehlendorff C, Kammersgaard LP: **Hemorrhagic and ischemic strokes compared: stroke severity, mortality, and risk factors**. *Stroke* 2009, **40**:2068–72.

5. Mozaffarian D, Benjamin EJ, Go AS, Arnett DK, Blaha MJ, Cushman M, De Ferranti S, Després JP, Fullerton HJ, Howard VJ, Huffman MD, Judd SE, Kissela BM, Lackland DT, Lichtman JH, Lisabeth LD, Liu S, Mackey RH, Matchar DB, McGuire DK, Mohler ER, Moy CS, Muntner P, Mussolino ME, Nasir K, Neumar RW, Nichol G, Palaniappan L, Pandey DK, Reeves MJ, et al.: **Heart disease and stroke statistics-2015 update : A report from the American Heart Association**. *Circulation* 2015, **131**:e29–e39.

6. Murphy TH, Li P, Betts K, Liu R: **Two-photon imaging of stroke onset in vivo reveals that NMDA-receptor independent ischemic depolarization is the major cause of rapid reversible damage to dendrites and spines**. *J Neurosci* 2008, **28**:1756–72.

7. Hossmann KA: **Pathophysiology and therapy of experimental stroke**. *Cell Mol Neurobiol* 2006, **26**:1057–1083.

8. Murphy TH, Corbett D: **Plasticity during stroke recovery: from synapse to behaviour**. *Nat Rev Neurosci* 2009, **10**:861–72.

9. Hakim AM: **Ischemic penumbra: the therapeutic window**. *Neurology* 1998, **51**(3 Suppl 3):S44–S46.

10. Jauch EC, Saver JL, Adams HP, Bruno A, Connors JJB, Demaerschalk BM, Khatri P, McMullan PW, Qureshi AI, Rosenfield K, Scott PA, Summers DR, Wang DZ, Wintermark M, Yonas H: **Guidelines for the early management of patients with acute ischemic stroke: a guideline for healthcare professionals from the American Heart Association/American Stroke Association**. *Stroke* 2013, **44**:870–947.

11. Iadecola C, Anrather J: **Stroke research at a crossroad: asking the brain for directions**. *Nat Neurosci* 2011, **14**:1363–1368.

12. Saver JL, Goyal M, van der Lugt A, Menon BK, Majoie CBLM, Dippel DW, Campbell BC, Nogueira RG, Demchuk AM, Tomasello A, Cardona P, Devlin TG, Frei DF, du Mesnil de Rochemont R, Berkhemer OA, Jovin TG, Siddiqui AH, van Zwam WH, Davis SM, Castaño C, Sapkota BL, Fransen PS, Molina C, van Oostenbrugge RJ, Chamorro Á, Lingsma H, Silver FL, Donnan GA, Shuaib A, Brown S, et al.: **Time to treatment with endovascular thrombectomy and outcomes from ischemic stroke: A meta-analysis**. *JAMA* 2016, **316**:1279.

13. Teasell R, Hussein N, Foley N, Cotoi A: *The Efficacy of Stroke Rehabilitation: An Evidence-Based Review of Stroke Rehabilitation*. 2016.

14. Ramsey LE, Siegel JS, Lang CE, Strube M, Shulman GL, Corbetta M: **Behavioural clusters and predictors of performance during recovery from stroke**. *Nat Hum Behav* 2017, **1**:38.

15. Krakauer JW: **Arm function after stroke: from physiology to recovery**. *Semin Neurol* 2005, **25**:384–95.

16. Lang CE, Bland MD, Bailey RR, Schaefer SY, Birkenmeier RL: **Assessment of upper extremity impairment, function, and activity after stroke: foundations for clinical decision making**. *J Hand Ther* 2013, **26**:104–115.

17. Shelton FN, Reding MJ: **Effect of lesion location on upper limb motor recovery after stroke**. *Stroke* 2001, **32**:107–12.

18. Miyai I, Blau AD, Reding MJ, Volpe BT: **Patients with stroke confined to basal ganglia have diminished response to rehabilitation efforts**. *Neurology* 1997, **48**:95–101.

19. Krebs HI, Volpe BT, Aisen ML, Hogan N: **Increasing productivity and quality of care: robot-aided neuro-rehabilitation**. *J Rehabil Res Dev* 2000, **37**:639–52.

20. Feys H, Hetebrij J, Wilms G, Dom R, De Weerdt W: **Predicting arm recovery following stroke: value of site of lesion**. *Acta Neurol Scand* 2000, **102**:371–377.

21. Dromerick A, Reding MJ: **Functional outcome for patients with hemiparesis, hemihypesthesia, and hemianopsia. Does lesion location matter?** *Stroke* 1995, **26**:2023–2026.

22. Pantano P, Formisano R, Ricci M, Piero V Di, Sabatini U, Pofi B Di, Rossi R, Bozzao L, Lenzi GL: **Motor recovery after stroke**. *Brain* 1996, **119**:1849–1857.

23. Corbetta M, Ramsey L, Callejas A, Baldassarre A, Hacker CD, Siegel JS, Astafiev S V, Rengachary J, Zinn K, Lang CE, Connor LT, Fucetola R, Strube M, Carter AR, Shulman GL: **Common behavioral clusters and subcortical anatomy in stroke**. *Neuron* 2015, **85**:927–941.

24. Kang D-W, Chalela JA, Ezzeddine MA, Warach S: **Association of ischemic lesion patterns on early diffusion-weighted imaging with TOAST stroke subtypes**. *Arch Neurol* 2003, **60**:1730.

25. Wessels T, Wessels C, Ellsiepen A, Reuter I, Trittmacher S, Stolz E, Jauss M: **Contribution of diffusion-weighted imaging in determination of stroke etiology**. *Am J Neuroradiol* 2006, **27**:35–39.

26. Lazar RM, Marshall RS: **24 – Middle Cerebral Artery Disease**. In *Stroke*; 2011:384–424.

27. Seitz RJ, Donnan GA: **Role of neuroimaging in promoting long-term recovery from ischemic stroke**. *J Magn Reson Imaging* 2010, **32**:756–772.

28. Edwardson MA, Wang X, Liu B, Ding L, Lane CJ, Park C, Nelsen MA, Jones TA, Wolf SL, Winstein CJ, Dromerick AW: **Stroke lesions in a large upper limb rehabilitation trial cohort rarely match lesions in common preclinical models**. *Neurorehabil Neural Repair* 2017, **31**:509–520.

29. Paxinos G, Watson C: **The rat brain in stereotaxic coordinates**. 2007.

30. Casals JB, Pieri NCG, Feitosa MLT, Ercolin ACM, Roballo KCS, Barreto RSN, Bressan FF, Martins DS, Miglino MA, Ambrósio CE: **The use of animal models for stroke research: A review**. *Comparative Medicine* 2011:305–313.

31. Fluri F, Schuhmann MK, Kleinschnitz C: **Animal models of ischemic stroke and their application in clinical research**. *Drug Des Devel Ther* 2015, **9**:3445–54.

32. Whishaw IQ, Pellis SM, Gorny BP: **Skilled reaching in rats and humans: evidence for parallel development or homology**. *Behav Brain Res* 1992, **47**:59–70.

33. Livingston-Thomas JM, Tasker RA: **Animal models of post-ischemic forced use rehabilitation: methods, considerations, and limitations**. *Exp Transl Stroke Med* 2013, **5**:2.

34. Ng YS, Stein J, Ning M, Black-Schaffer RM: **Comparison of clinical characteristics and functional outcomes of ischemic stroke in different vascular territories**. *Stroke* 2007, **38**:2309–2314.

35. Carmichael ST: **Rodent models of focal stroke: Size, mechanism, and purpose**. *NeuroRX* 2005, **2**:396–409.

36. Li F, Omae T, Fisher M, Dietrich WD, Kuluz JW: **Spontaneous hyperthermia and its mechanism in the intraluminal suture middle cerebral artery occlusion model of rats**. *Stroke* 1999, **30**:2464–2471.

37. Braeuninger S, Kleinschnitz C: **Rodent models of focal cerebral ischemia: procedural pitfalls and translational problems**. *Exp Transl Stroke Med* 2009, **1**:8.

38. Watson BD, Dietrich WD, Busto R, Wachtel MS, Ginsberg MD: **Induction of reproducible brain infarction by photochemically initiated thrombosis**. *Ann Neurol* 1985, **17**:497–504.

39. Labat-gest V, Tomasi S: **Photothrombotic ischemia: a minimally invasive and reproducible photochemical cortical lesion model for mouse stroke studies**. *J Vis Exp* 2013.

40. Windle V, Szymanska A, Granter-Button S, White C, Buist R, Peeling J, Corbett D: **An analysis of four different methods of producing focal cerebral ischemia with endothelin-1 in the rat**. *Exp Neurol* 2006, **201**:324–334.

41. Fuxe K, Bjelke B, Andbjer B, Grahn H, Rimondini R, Agnati LF: **Endothelin-1 induced lesions of the frontoparietal cortex of the rat. A possible model of focal cortical ischemia**. *Neuroreport* 1997, **8**:2623–2629.

42. Nguemeni C, Gomez-Smith M, Jeffers MS, Schuch CP, Corbett D: **Time course of neuronal death following endothelin-1 induced focal ischemia in rats**. *J Neurosci Methods* 2015, **242**:72–76.

43. Biernaskie J, Corbett D, Peeling J, Wells J, Lei H: **A serial MR study of cerebral blood flow changes and lesion development following endothelin-1-induced ischemia in rats**. *Magn Reson Med* 2001, **46**:827–30.

44. Frost SB, Barbay S, Mumert ML, Stowe AM, Nudo RJ: **An animal model of capsular infarct: Endothelin-1 injections in the rat**. *Behav Brain Res* 2006, **169**:206–211.

45. Windle V, Corbett D: **Fluoxetine and recovery of motor function after focal ischemia in rats.** *Brain Res* 2005, **1044**:25–32.

46. Macrae IM, Robinson MJ, Graham DI, Reid JL, McCulloch J: **Endothelin-1-induced reductions in cerebral blood flow: dose dependency, time course, and neuropathological consequences**. *J Cereb Blood Flow Metab* 1993, **13**:276–284.

47. Horie N, Maag A-L, Hamilton SA, Shichinohe H, Bliss TM, Steinberg GK: **Mouse model of**

focal cerebral ischemia using endothelin-1. *J Neurosci Methods* 2008, **173**:286–290.

48. Wiley KE, Davenport AP: **Endothelin receptor pharmacology and function in the mouse: comparison with rat and man**. *J Cardiovasc Pharmacol* 2004, **44 Suppl 1**(November):S4-6.

49. Willette RN, Ohlstein EH, Pullen M, Sauermelch CF, Cohen A, Nambi P: **Transient forebrain ischemia alters acutely endothelin receptor density and immunoreactivity in gerbil brain**. *Life Sci* 1993, **52**:35–40.

50. Bian L-G, Zhang T-X, Zhao W-G, Shen J-K, Yang G-Y: **Increased endothelin-1 in the rabbit model of middle cerebral artery occlusion**. *Neurosci Lett* 1994, **174**:47–50.

51. Kwakkel G, Buma FE, Selzer ME: **Understanding the mechanisms underlying recovery after stroke**. In *Textbook of Neural Repair and Rehabilitation*. Edited by Selzer M, Clarke S, Cohen LG, Kwakkel G, Miller R. Cambridge: Cambridge University Press; :7–24.

52. Cramer SC: **Repairing the human brain after stroke: I. Mechanisms of spontaneous recovery**. *Ann Neurol* 2008, **63**:272–287.

53. Corbett D, Jeffers M, Nguemeni C, Gomez-Smith M, Livingston-Thomas J: **Lost in translation: Rethinking approaches to stroke recovery**. *Prog Brain Res* 2015, **218**(April):413–434.

54. Langhorne P, Bernhardt J, Kwakkel G: **Stroke rehabilitation**. *Lancet* 2011, **377**:1693–1702.

55. Kwakkel G, Kollen B, Twisk J: **Impact of time on improvement of outcome after stroke**. *Stroke* 2006, **37**:2348–2353.

56. Desmond DW, Moroney JT, Sano M, Stern Y: **Recovery of cognitive function after stroke**. *Stroke* 1996, **27**:1798–803.

57. Lendrem W, Lincoln NB: **Spontaneous recovery of language in patients with aphasia between 4 and 34 weeks after stroke**. *J Neurol Neurosurg Psychiatry* 1985, **48**:743–8.

58. Twitchell TE: **The restoration of motor function following hemiplegia in man**. *Brain* 1951, **74**:443–480.

59. Wade DT, Langton-Hewer R, Wood VA, Skilbeck CE, Ismail HM: **The hemiplegic arm after stroke: measurement and recovery**. *J Neurol Neurosurg Psychiatry* 1983, **46**:521–524.

60. Duncan PW, Goldstein LB, Horner RD, Landsman PB, Samsa GP, Matchar DB: **Similar motor recovery of upper and lower extremities after stroke**. *Stroke* 1994, **25**:1181–1188.

61. Duncan PW, Goldstein LB, Matchar D, Divine GW, Feussner J: **Measurement of motor recovery after stroke. Outcome assessment and sample size requirements**. *Stroke* 1992, **23**:1084–9.

62. Prabhakaran S, Zarahn E, Riley C, Speizer A, Chong JY, Lazar RM, Marshall RS, Krakauer JW: **Inter-individual variability in the capacity for motor recovery after ischemic stroke**. *Neurorehabil Neural Repair* 2007, **22**:64–71.

63. Winters C, van Wegen EEH, Daffertshofer A, Kwakkel G: **Generalizability of the proportional recovery model for the upper extremity after an ischemic stroke**. *Neurorehabil Neural Repair* 2015, **29**:614–622.

64. Byblow WD, Stinear CM, Barber PA, Petoe M a, Ackerley SJ: **Proportional recovery after**

stroke depends on corticomotor integrity. *Ann Neurol* 2015, **78**:1–12.

65. Feng W, Wang J, Chhatbar PY, Doughty C, Landsittel D, Lioutas VA, Kautz SA, Schlaug G: **Corticospinal tract lesion load: An imaging biomarker for stroke motor outcomes**. *Ann Neurol* 2015, **78**:860–870.

66. Lazar RM, Minzer B, Antoniello D, Festa JR, Krakauer JW, Marshall RS: **Improvement in aphasia scores after stroke is well predicted by initial severity**. *Stroke* 2010, **41**:1485–8.

67. Winters C, van Wegen EEH, Daffertshofer A, Kwakkel G: **Generalizability of the maximum proportional recovery rule to visuospatial neglect early poststroke**. *Neurorehabil Neural Repair* 2017, **31**:334–342.

68. Zarahn E, Alon L, Ryan SL, Lazar RM, Vry MS, Weiller C, Marshall RS, Krakauer JW: **Prediction of motor recovery using initial impairment and fMRI 48 h poststroke**. *Cereb Cortex* 2011, **21**:2712–2721.

69. Krakauer J, Marshall R: **The proportional recovery rule for stroke revisited**. *Ann Neurol* 2015, **78**:845–847.

70. Krakauer JW: **Motor learning: its relevance to stroke recovery and neurorehabilitation**. *Curr Opin Neurol* 2006, **19**:84–90.

71. Feeney DM, Baron JC: **Diaschisis**. *Stroke* 1986, **17**:817–30.

72. Warraich Z, Kleim JA: **Neural plasticity: the biological substrate for neurorehabilitation**. *PM&R* 2010, **2**:S208–S219.

73. Seitz RJ, Azari NP, Knorr U, Binkofski F, Herzog H, Freund H-J: **The Role of Diaschisis in Stroke Recovery**. *Stroke* 1999, **30**:1844–1850.

74. Dancause N, Nudo RJ: **Shaping plasticity to enhance recovery after injury**. *Prog Brain Res* 2011, **192**:273–295.

75. Cirstea MC: **Compensatory strategies for reaching in stroke**. *Brain* 2000, **123**:940–953.

76. Alaverdashvili M, Whishaw IQ: **Compensation aids skilled reaching in aging and in recovery from forelimb motor cortex stroke in the rat**. *Neuroscience* 2010, **167**:21–30.

77. Nudo RJ: **Neural bases of recovery after brain injury**. *Journal of Communication Disorders* 2011:515–520.

78. Kwakkel G, Kollen B, Lindeman E: **Understanding the pattern of functional recovery after stroke: facts and theories**. *Restor Neurol Neurosci* 2004, **22**:281–299.

79. Biernaskie J: **Efficacy of Rehabilitative Experience Declines with Time after Focal Ischemic Brain Injury**. *J Neurosci* 2004, **24**:1245–1254.

80. Carmichael ST, Archibeque I, Luke L, Nolan T, Momiy J, Li S: **Growth-associated gene expression after stroke: evidence for a growth-promoting region in peri-infarct cortex**. *Exp Neurol* 2005, **193**:291–311.

81. Carmichael ST: **Cellular and molecular mechanisms of neural repair after stroke: Making waves**. *Ann Neurol* 2006, **59**:735–742.

82. Li S, Carmichael ST: **Growth-associated gene and protein expression in the region of axonal sprouting in the aged brain after stroke**. *Neurobiol Dis* 2006, **23**:362–373.

83. Karetko M, Skangiel-Kramska J: **Diverse functions of perineuronal nets**. *Acta Neurobiologiae Experimentalis* 2009:564–577.

84. Pizzorusso T, Medini P, Berardi N, Chierzi S, Fawcett JW, Maffei L: **Reactivation of ocular dominance plasticity in the adult visual cortex**. *Science* 2002, **298**:1248–51.

85. Morawski M, Brückner MK, Riederer P, Brückner G, Arendt T: **Perineuronal nets potentially protect against oxidative stress**. *Exp Neurol* 2004, **188**:309–315.

86. Cabungcal J-H, Steullet P, Morishita H, Kraftsik R, Cuenod M, Hensch TK, Do KQ: **Perineuronal nets protect fast-spiking interneurons against oxidative stress**. *Proc Natl Acad Sci U S A* 2013, **110**:9130–5.

87. Brückner G, Brauer K, Härtig W, Wolff JR, Rickmann MJ, Derouiche A, Delpech B, Girard N, Oertel WH, Reichenbach A: **Perineuronal nets provide a polyanionic, glia-associated form of microenvironment around certain neurons in many parts of the rat brain**. *Glia* 1993, **8**:183–200.

88. McRae PA, Rocco MM, Kelly G, Brumberg JC, Matthews RT: **Sensory deprivation alters aggrecan and perineuronal net expression in the mouse barrel cortex.** *J Neurosci* 2007, **27**:5405–13.

89. Bradbury EJ, Moon LDF, Popat RJ, King VR, Bennett GS, Patel PN, Fawcett JW, McMahon SB: **Chondroitinase ABC promotes functional recovery after spinal cord injury**. *Nature* 2002, **416**:636–640.

90. Gogolla N, Caroni P, Lüthi A, Herry C: **Perineuronal nets protect fear memories from erasure**. *Science* 2009, **325**:1258–61.

91. Pizzorusso T, Medini P, Landi S, Baldini S, Berardi N, Maffei L: **Structural and functional recovery from early monocular deprivation in adult rats**. *Proc Natl Acad Sci* 2006, **103**:8517–8522.

92. Cafferty WBJ, Bradbury EJ, Lidierth M, Jones M, Duffy PJ, Pezet S, McMahon SB: **Chondroitinase ABC-mediated plasticity of spinal sensory function**. *J Neurosci* 2008, **28**:11998–2009.

93. Soleman S, Yip PK, Duricki D a, Moon LDF: **Delayed treatment with chondroitinase ABC promotes sensorimotor recovery and plasticity after stroke in aged rats**. *Brain* 2012, **135**(Pt 4):1210–23.

94. Gherardini L, Gennaro M, Pizzorusso T: **Perilesional treatment with chondroitinase ABC and motor training promote functional recovery after stroke in rats**. *Cereb Cortex* 2015, **25**:202–12.

95. Kwok JCF, Dick G, Wang D, Fawcett JW: **Extracellular matrix and perineuronal nets in CNS repair**. *Dev Neurobiol* 2011, **71**:1073–89.

96. Galtrey CM, Fawcett JW: **The role of chondroitin sulfate proteoglycans in regeneration and plasticity in the central nervous system**. *Brain Research Reviews* 2007:1–18.

97. de Winter F, Kwok JCF, Fawcett JW, Vo TT, Carulli D, Verhaagen J: **The chemorepulsive protein semaphorin 3A and perineuronal net-mediated plasticity**. *Neural Plast* 2016, **2016**:1–14.

98. Tsien RY: **Very long-term memories may be stored in the pattern of holes in the perineuronal net**. *Proc Natl Acad Sci U S A* 2013, **110**:12456–61.

99. Corvetti L: **Degradation of chondroitin sulfate proteoglycans induces sprouting of intact purkinje axons in the cerebellum of the adult rat**. *J Neurosci* 2005, **25**:7150–7158.

100. Barritt AW, Davies M, Marchand F, Hartley R, Grist J, Yip P, McMahon SB, Bradbury EJ: **Chondroitinase ABC promotes sprouting of intact and injured spinal systems after spinal cord injury**. *J Neurosci* 2006, **26**:10856–67.

101. Adams I, Brauer K, Arélin C, Härtig W, Fine A, Mäder M, Arendt T, Brückner G: **Perineuronal nets in the rhesus monkey and human basal forebrain including basal ganglia**. *Neuroscience* 2001, **108**:285–298.

102. Mauney SA, Athanas KM, Pantazopoulos H, Shaskan N, Passeri E, Berretta S, Woo TUW: **Developmental pattern of perineuronal nets in the human prefrontal cortex and their deficit in schizophrenia**. *Biol Psychiatry* 2013, **74**:427–435.

103. Balmer TS, Carels VM, Frisch JL, Nick TA: **Modulation of perineuronal nets and parvalbumin with developmental song learning.** *J Neurosci* 2009, **29**:12878–85.

104. Bertolotto A, Manzardo E, Guglielmone R: **Immunohistochemical mapping of perineuronal nets containing chondroitin unsulfate proteoglycan in the rat central nervous system**. *Cell Tissue Res* 1996, **283**:283–295.

105. Lee H, Leamey C a, Sawatari A: **Perineuronal nets play a role in regulating striatal function in the mouse**. *PLoS One* 2012, **7**:e32747.

106. Sorg BA, Berretta S, Blacktop JM, Fawcett JW, Kitagawa H, Kwok JCF, Miquel M: **Casting a wide net: Role of perineuronal nets in neural plasticity**. *J Neurosci* 2016, **36**:11459–11468.

107. Härtig W, Brauer K, Brückner G: **Wisteria floribunda agglutinin-labelled nets surround parvalbumin-containing neurons**. *Neuroreport* 1992, **3**:869–72.

108. Wegner F, Härtig W, Bringmann A, Grosche J, Wohlfarth K, Zuschratter W, Brückner G: **Diffuse perineuronal nets and modified pyramidal cells immunoreactive for glutamate and the GABAA receptor α1 subunit form a unique entity in rat cerebral cortex**. *Exp Neurol* 2003, **184**:705–714.

109. Wang D, Fawcett J: **The perineuronal net and the control of CNS plasticity**. *Cell Tissue Res* 2012, **349**:147–160.

110. Vo T, Carulli D, Ehlert EME, Kwok JCF, Dick G, Mecollari V, Moloney EB, Neufeld G, de Winter F, Fawcett JW, Verhaagen J: **The chemorepulsive axon guidance protein semaphorin3A is a constituent of perineuronal nets in the adult rodent brain**. *Mol Cell Neurosci* 2013, **56**:186–200.

111. Frischknecht R, Heine M, Perrais D, Seidenbecher CI, Choquet D, Gundelfinger ED: **Brain extracellular matrix affects AMPA receptor lateral mobility and short-term synaptic plasticity**. *Nat Neurosci* 2009, **12**:897–904.

112. Rudy B, Fishell G, Lee S, Hjerling-Leffler J: **Three groups of interneurons account for nearly 100% of neocortical GABAergic neurons**. *Dev Neurobiol* 2011, **71**:45–61.

113. Kawaguchi Y, Kubota Y: **GABAergic cell subtypes and their synaptic connections in rat frontal cortex**. *Cereb Cortex* 1997, **7**:476–486.

114. Markram H, Toledo-Rodriguez M, Wang Y, Gupta A, Silberberg G, Wu C: **Interneurons of the neocortical inhibitory system**. *Nat Rev Neurosci* 2004, **5**:793–807.

115. Hu H, Gan J, Jonas P: **Interneurons. Fast-spiking, parvalbumin^{+} GABAergic interneurons: from cellular design to microcircuit function**. *Science* 2014, **345**:1255263.

116. Hensch TK: **Critical period plasticity in local cortical circuits**. *Nat Rev Neurosci* 2005, **6**:877–88.

117. del Rio J, de Lecea L, Ferrer I, Soriano E: **The development of parvalbumin-immunoreactivity in the neocortex of the mouse**. *Dev Brain Res* 1994, **81**:247–259.

118. Härtig W, Derouiche A, Welt K, Brauer K, Grosche J, Mäder M, Reichenbach A, Brückner G: **Cortical neurons immunoreactive for the potassium channel Kv3.1b subunit are predominantly surrounded by perineuronal nets presumed as a buffering system for cations**. *Brain Res* 1999, **842**:15–29.

119. Balmer TS: **Perineuronal nets enhance the excitability of fast-spiking neurons**. *eNeuro* 2016, **3**:e0112–16.2016.

120. Bidmon HJ, Jancsik V, Schleicher A, Hagemann G, Witte OW, Woodhams P, Zilles K: **Structural alterations and changes in cytoskeletal proteins and proteoglycans after focal cortical ischemia**. *Neuroscience* 1998, **82**:397–420.

121. Hobohm C, Günther A, Grosche J, Roßner S, Schneider D, Brückner G: **Decomposition and long-lasting downregulation of extracellular matrix in perineuronal nets induced by focal cerebral ischemia in rats**. *J Neurosci Res* 2005, **80**:539–548.

122. Karetko-Sysa M, Skangiel-Kramska J, Nowicka D: **Disturbance of perineuronal nets in the perilesional area after photothrombosis is not associated with neuronal death**. *Exp Neurol* 2011, **231**:113–26.

123. Alia C, Spalletti C, Lai S, Panarese A, Micera S, Caleo M: **Reducing GABAA-mediated inhibition improves forelimb motor function after focal cortical stroke in mice**. *Sci Rep* 2016, **6**:37823.

124. Zeiler SR, Gibson EM, Hoesch RE, Li MY, Worley PF, O'Brien RJ, Krakauer JW: **Medial premotor cortex shows a reduction in inhibitory markers and mediates recovery in a mouse model of focal stroke**. *Stroke* 2013, **44**:483–489.

125. Cheatwood JL, Emerick AJ, Schwab ME, Kartje GL: **Nogo-A expression after focal ischemic stroke in the adult rat**. *Stroke* 2008, **39**:2091–2098.

126. Hobohm C, Härtig W, Brauer K, Brückner G: **Low expression of extracellular matrix components in rat brain stem regions containing modulatory aminergic neurons**. *J Chem Neuroanat* 1998, **15**:135–142.

127. Montoya CP, Campbell-Hope LJ, Pemberton KD, Dunnett SB: **The "staircase test": a measure of independent forelimb reaching and grasping abilities in rats**. *J Neurosci Methods* 1991, **36**:219–228.

128. Schallert T, Fleming SM, Leasure JL, Tillerson JL, Bland ST: **CNS plasticity and**

assessment of forelimb sensorimotor outcome in unilateral rat models of stroke, cortical ablation, parkinsonism and spinal cord injury. *Neuropharmacology* 2000, **39**:777–787.

129. Bouet V, Boulouard M, Toutain J, Divoux D, Bernaudin M, Schumann-Bard P, Freret T: **The adhesive removal test: a sensitive method to assess sensorimotor deficits in mice**. *Nat Protoc* 2009, **4**:1560–4.

130. Schallert T, Woodlee MT, Fleming SM, Schallert T, Woodlee MT FS: **Disentangling multiple types of recovery from brain injury recovery of function**. *Pharmacol Cereb Ischemia* 2002(January 2002):201–216.

131. Kolb B, Whishaw IQ: **Dissociation of the contributions of the prefrontal, motor, and parietal cortex of the control of movement in the rat: An experimental review**. *Can J Psychol Can Psychol* 1983, **37**:211–232.

132. Jeffers MS, Hoyles A, Morshead C, Corbett D: **Epidermal growth factor and erythropoietin infusion accelerate functional recovery in combination with rehabilitation**. *Stroke* 2014, **45**:1856–8.

133. Clarke J, Langdon KD, Corbett D: **Early poststroke experience differentially alters periinfarct layer II and III cortex**. *J Cereb Blood Flow Metab* 2014, **34**:630–637.

134. West MJ, Slomianka L, Gundersen HJ: **Unbiased stereological estimation of the total number of neurons in thesubdivisions of the rat hippocampus using the optical fractionator.** *Anat Rec* 1991, **231**:482–97.

135. Slomianka L, West MJ: **Estimators of the precision of stereological estimates: An example based on the CA1 pyramidal cell layer of rats**. *Neuroscience* 2005, **136**:757–767.

136. Faul F, Erdfelder E, Lang A-G, Buchner A: **G*Power 3: a flexible statistical power analysis program for the social, behavioral, and biomedical sciences**. *Behav Res Methods* 2007, **39**:175–91.

137. Cammermeyer J: **Is the solitary dark neuron a manifestation of postmortem trauma to the brain inadequately fixed by perfusion?** *Histochemistry* 1978, **56**:97–115.

138. Jortner BS: **The return of the dark neuron. A histological artifact complicating contemporary neurotoxicologic evaluation**. *Neurotoxicology* 2006, **27**:628–34.

139. Lin TN, He YY, Wu G, Khan M, Hsu CY: **Effect of brain edema on infarct volume in a focal cerebral ischemia model in rats**. *Stroke* 1993, **24**:117–121.

140. Lee H, Leamey CA, Sawatari A: **Rapid reversal of chondroitin sulfate proteoglycan associated staining in subcompartments of mouse neostriatum during the emergence of behaviour**. *PLoS One* 2008, **3**:e3020.

141. Pisa M: **Motor functions of the striatum in the rat: Critical role of the lateral region in tongue and forelimb reaching**. *Neuroscience* 1988, **24**:453–463.

142. Justicia C, Ramos-Cabrer P, Hoehn M: **MRI detection of secondary damage after stroke: chronic iron accumulation in the thalamus of the rat brain**. *Stroke* 2008, **39**:1541–7.

143. Rewell SSJ, Churilov L, Sidon TK, Aleksoska E, Cox SF, Macleod MR, Howells DW: **Evolution of ischemic damage and behavioural deficit over 6 months after MCAo in the rat: Selecting the optimal outcomes and statistical power for multi-centre preclinical trials**.

PLoS One 2017, **12**:e0171688.

144. Brown LL, Sharp FR: **Metabolic mapping of rat striatum: somatotopic organization of sensorimotor activity**. *Brain Res* 1995, **686**:207–222.

145. Milot M-H, Cramer SC: **Biomarkers of recovery after stroke**. *Curr Opin Neurol* 2008, **21**:654–659.

146. Castro-Alamancos MA, Borrell J: **Functional recovery of forelimb response capacity after forelimb primary motor cortex damage in the rat is due to the reorganization of adjacent areas of cortex**. *Neuroscience* 1995, **68**:793–805.

147. Li S, Nie EH, Yin Y, Benowitz LI, Tung S, Vinters H V, Bahjat FR, Stenzel-Poore MP, Kawaguchi R, Coppola G, Carmichael ST: **GDF10 is a signal for axonal sprouting and functional recovery after stroke**. *Nat Neurosci* 2015, **18**:1737–1745.

148. Szele FG, Alexander C, Chesselet MF: **Expression of molecules associated with neuronal plasticity in the striatum after aspiration and thermocoagulatory lesions of the cerebral cortex in adult rats.** *J Neurosci* 1995, **15**:4429–48.

149. Zhang J, Meng L, Qin W, Liu N, Shi FD, Yu C: **Structural damage and functional reorganization in Ipsilesional M1 in well-recovered patients with subcortical stroke**. *Stroke* 2014, **45**:788–793.

150. Thickbroom GW, Byrnes ML, Archer SA, Mastaglia FL: **Motor outcome after subcortical stroke correlates with the degree of cortical reorganization**. *Clin Neurophysiol* 2004, **115**:2144–2150.

151. Shimada IS, Peterson BM, Spees JL: **Isolation of locally derived stem/progenitor cells from the peri-infarct area that do not migrate from the lateral ventricle after cortical stroke**. *Stroke* 2010, **41**:e552-60.

152. Touvykine B, Mansoori BK, Jean-Charles L, Deffeyes J, Quessy S, Dancause N: **The effect of lesion size on the organization of the ipsilesional and contralesional motor cortex**. *Neurorehabil Neural Repair* 2016, **30**:280–92.

153. Jones TA, Schallert T: **Overgrowth and pruning of dendrites in adult rats recovering from neocortical damage**. *Brain Res* 1992, **581**:156–160.

154. Romanic AM, White RF, Arleth AJ, Ohlstein EH, Barone FC: **Matrix metalloproteinase expression increases after cerebral focal ischemia in rats: inhibition of matrix metalloproteinase-9 reduces infarct size.** *Stroke* 1998, **29**:1020–30.

155. Rosell A, Ortega-Aznar A, Alvarez-Sabín J, Fernández-Cadenas I, Ribó M, Molina CA, Lo EH, Montaner J: **Increased brain expression of matrix metalloproteinase-9 after ischemic and hemorrhagic human stroke**. *Stroke* 2006, **37**:1399–1406.

156. Al'Qteishat A, Gaffney J, Krupinski J, Rubio F, West D, Kumar S, Kumar P, Mitsios N, Slevin M: **Changes in hyaluronan production and metabolism following ischaemic stroke in man**. *Brain* 2006, **129**:2158–2176.

157. Slaker M, Blacktop JM, Sorg BA: **Caught in the net: Perineuronal nets and addiction**. *Neural Plasticity* 2016:1–8.

158. Clarkson AN, Huang BS, Macisaac SE, Mody I, Carmichael ST: **Reducing excessive**

GABA-mediated tonic inhibition promotes functional recovery after stroke. *Nature* 2010, **468**:305–9.

159. Lake EM, Chaudhuri J, Thomason L, Janik R, Ganguly M, Brown M, McLaurin J, Corbett D, Stanisz GJ, Stefanovic B: **The effects of delayed reduction of tonic inhibition on ischemic lesion and sensorimotor function**. *J Cereb Blood Flow Metab* 2015, **35**:1601–1609.

Appendix

Supplemental Table 1: List of staining materials.

Primary Antibody	**Company**	**Catalogue #**	**Concentration**
Biotinylated Wisteria Floribunda Lectin (WFA)	Vector	B-1355	1:500
Mouse-Anti-Parvalbumin Monoclona Antibody	Sigma	SAB4200545	1:600
Secondary Antibody	**Company**	**Catalogue #**	**Concentration**
Alexa Fluor® 594 AffiniPure Donkey Anti-Mouse IgG (H+L)	Jackson ImmunoResearch	715-585-150	1:250
Alexa Fluor® 488 Streptavidin	Jackson ImmunoResearch	016-540-084	1:250
Blocking Solutions	**Company**	**Catalogue #**	**% Solution**
Carbo-Free blocking solution	Vector	SP-5040	10%
Normal Donkey Serum	Jackson ImmunoResearch	017-000-121	10%

Supplemental Table 2: Predictors of impairment and recovery on the different behavioural tests. Predictive model characteristics for *Figures 16* and *17* as determined by forward linear regression analysis.

Predicting Impairments on Motor Tests						
Determinant	**Predictor**	**Unstandardized B**	**Std. Error**	**p-value**	**R**	**Adjusted R Square**
Staircase	Intercept	2.15	0.988	0.04	0.646	0.367
	Cortical Infarct Volume	0.078	0.027	0.008		
	Striatal Infarct Volume	0.17	0.072	0.027		
$Y = 0.078X_1 + 0.17X_2 + 2.15$; where X_1 is cortical infarct volume and X_2 is striatal infarct volume						
Cylinder	Intercept	0.239	0.026	0	0.397	0.123
	Cortical Infarct Volume	0.002	0.001	0.044		
$Y = 0.002X + 0.239$; where X is cortical infarct volume						
Beam Forelimb	Intercept	0.042	0.018	0.031	0.564	0.29
	Cortical Infarct Volume	0.002	0.001	0.003		
$Y = 0.002X + 0.042$; where X is cortical infarct volume						
Beam Hindlimb	Intercept	0.133	0.051	0.016	0.621	0.36
	Cortical Infarct Volume	0.007	0.002	0.001		
$Y = 0.007X + 0.133$; where X is cortical infarct volume						
Adhesive Contact	Intercept	2.402	6.951	0.733	0.473	0.188
	Cortical Infarct Volume	0.584	0.232	0.02		
$Y = 0.584X + 2.402$; where X is cortical infarct volume						
Adhesive Remove	Intercept	11.933	10.345	0.261	0.41	0.13
	Cortical Infarct Volume	0.728	0.345	0.047		
$Y = 0.728X + 11.933$; where X is cortical infarct volume						
Predicting Recovery on Motor Tests						
Determinant	**Predictor**	**Unstandardized B**	**Std. Error**	**p-value**	**R**	**Adjusted R Square**
Staircase	No significant predictors					
Cylinder	Intercept	0.249	0.036	0	0.578	0.306
	Striatal Infarct Volume	-0.01	0.003	0.002		
$Y = -0.01X + 0.249$; where X is striatal infarct volume						
Beam Forelimb	Intercept	0.012	0.019	0.52	0.393	0.119
	Cortical Infarct Volume	0.001	0.001	0.047		
$Y = 0.001X + 0.012$; where X is cortical infarct volume						
Beam Hindlimb	Intercept	0.045	0.054	0.412	0.531	0.252
	Cortical Infarct Volume	0.006	0.002	0.005		
$Y = 0.006X + 0.045$; where X is cortical infarct volume						
Adhesive Contact	Intercept	-0.43	3.982	0.915	0.547	0.268
	Cortical Infarct Volume	0.408	0.133	0.006		
$Y = 0.408X - 0.43$; where X is cortical infarct volume						
Adhesive Remove	No significant predictors					

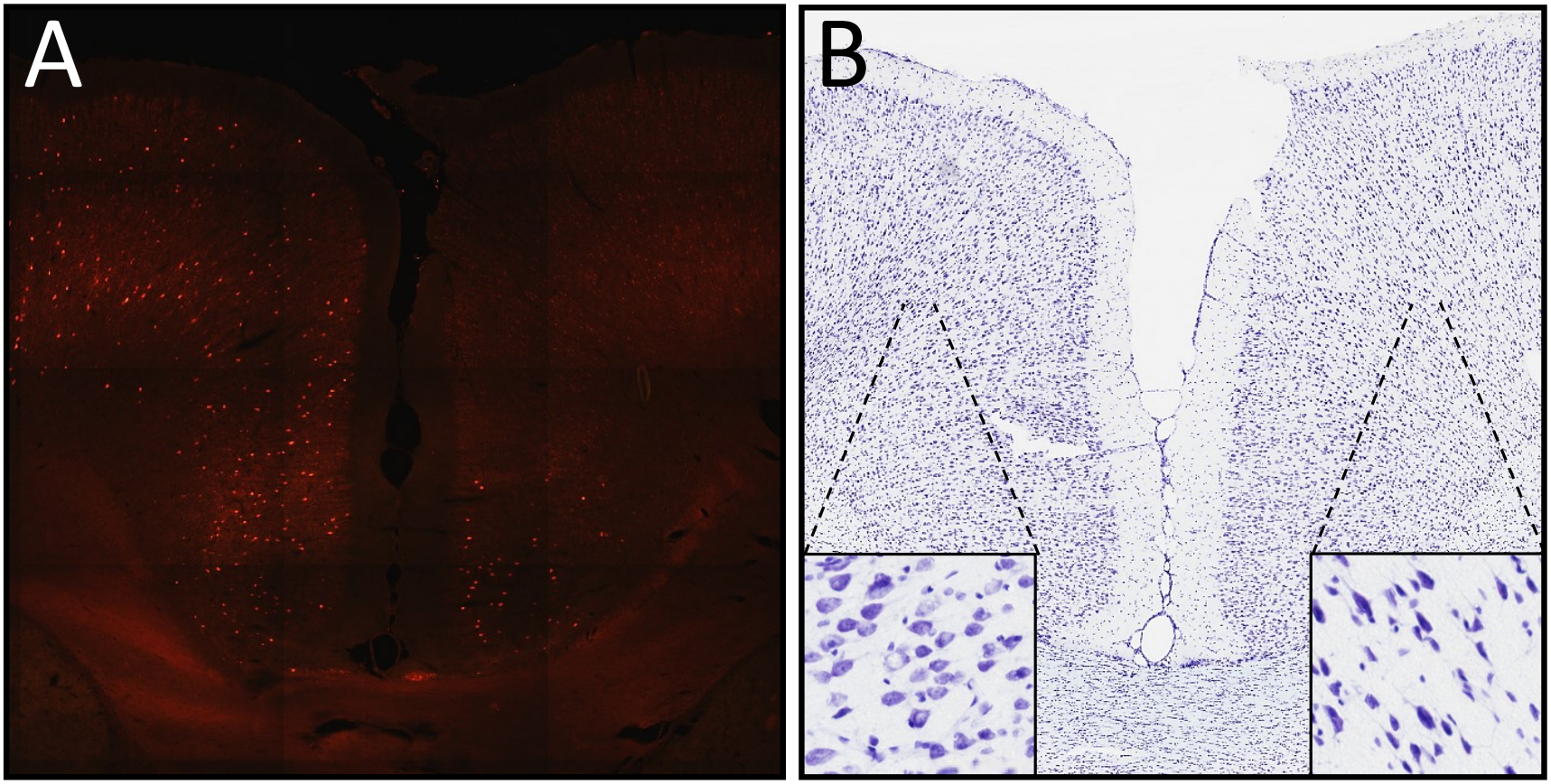

Supplemental Figure 1: The "dark neuron" staining artifact. (A) Example of the "dark neuron" artifact in a sham animal. There was an absence of PV staining in the medial region of the right hemisphere due to this artifact. **(B)** Corresponding cresyl violet stained section showing the appearance of neurons in the affected and non-affected hemisphere. The "dark neurons" present in the right hemisphere were shrunken and intensely stained.

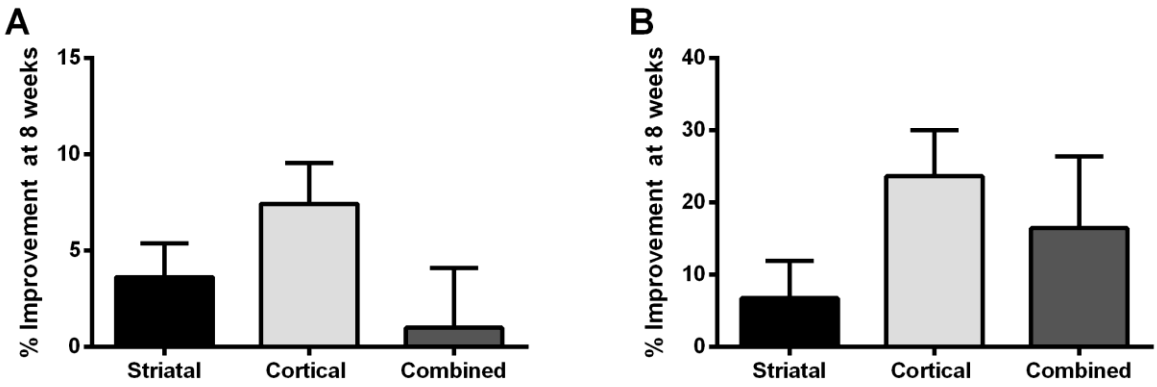

Supplemental Figure 2: Improvement on the beam-traversal test. The percentage of improvement was calculated by taking the difference between performance at post-stroke week 8 and week 1. There was no significant difference in the amount of improvement in **(A)** forelimb and **(B)** hindlimb paw placement accuracy between groups. Values are means ± SEM. n = 8; striatal-only, n = 9; cortical-only and n = 9; combined group.

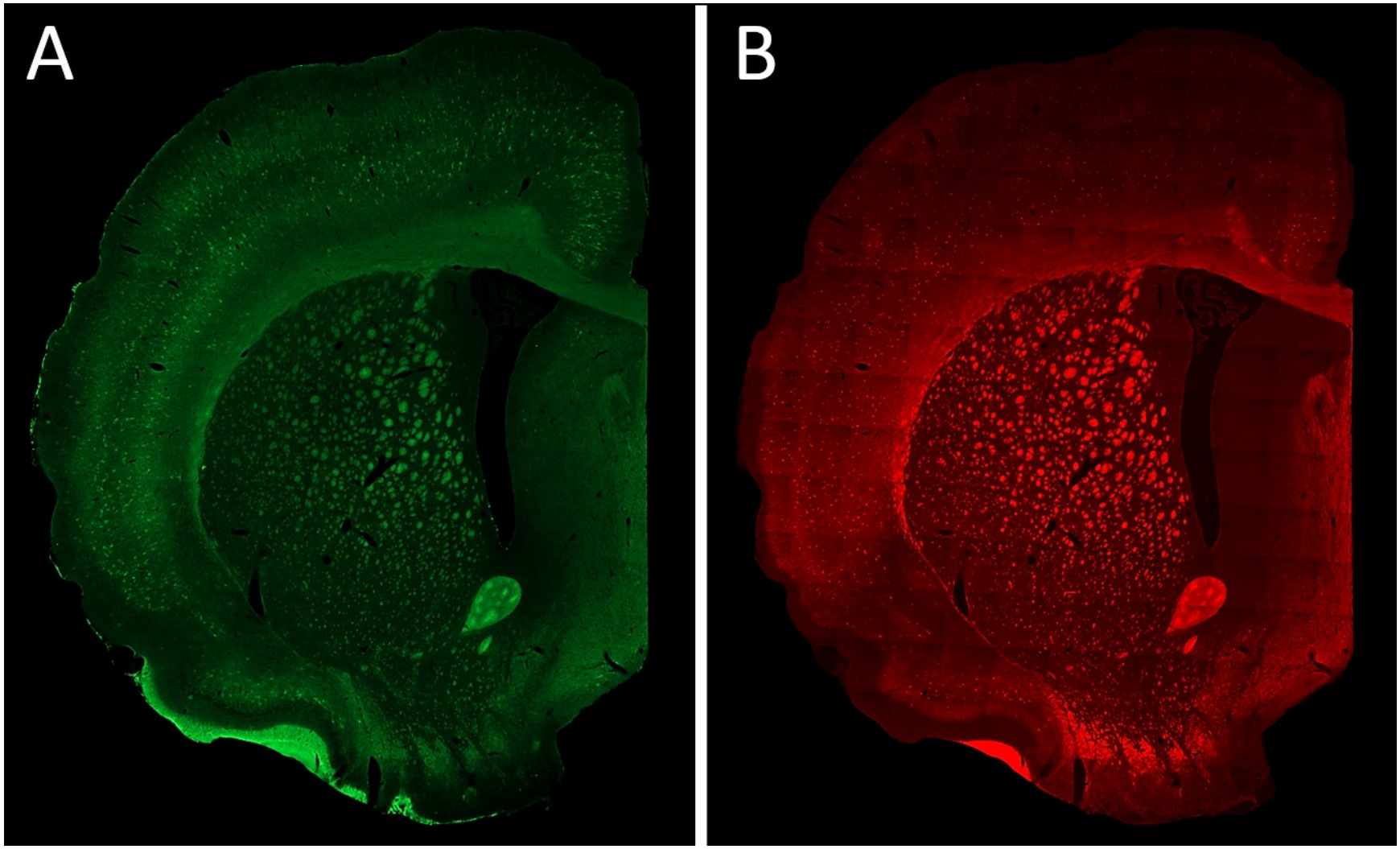

Supplemental Figure 3: Distribution of PNNs and PV interneurons in the SD rat. Staining for **(A)** PNNs and **(B)** PV interneurons in a sham anesthetic rat. Both PNNs and PV were visible in all layers of the rat cortex except for layer I.

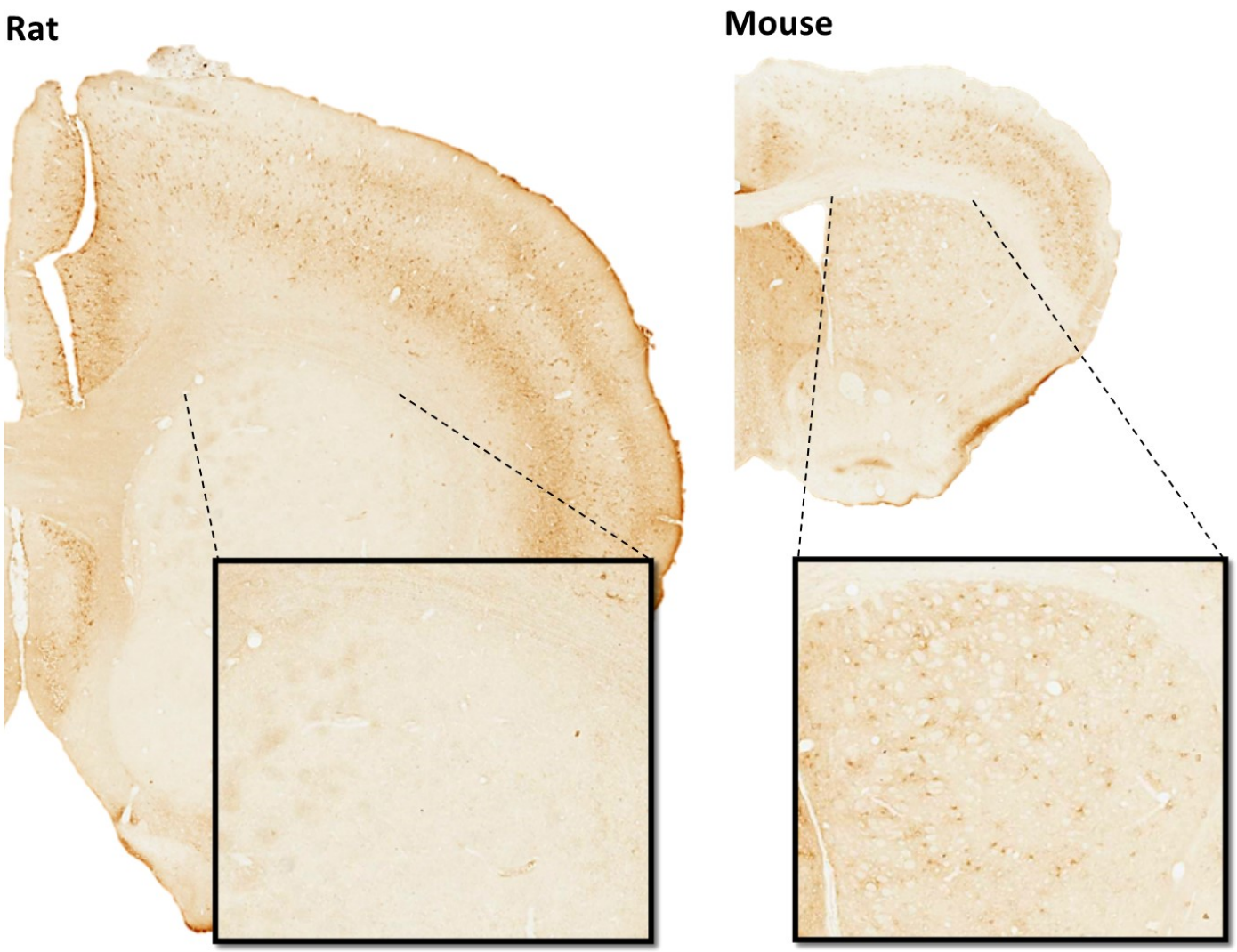

Supplemental Figure 4: PNNs in the rat and mouse striatum. Comparison of WFA DAB staining in a rat and mouse brain. PNNs are abundant in the mouse striatum but are scarce in the rat striatum.

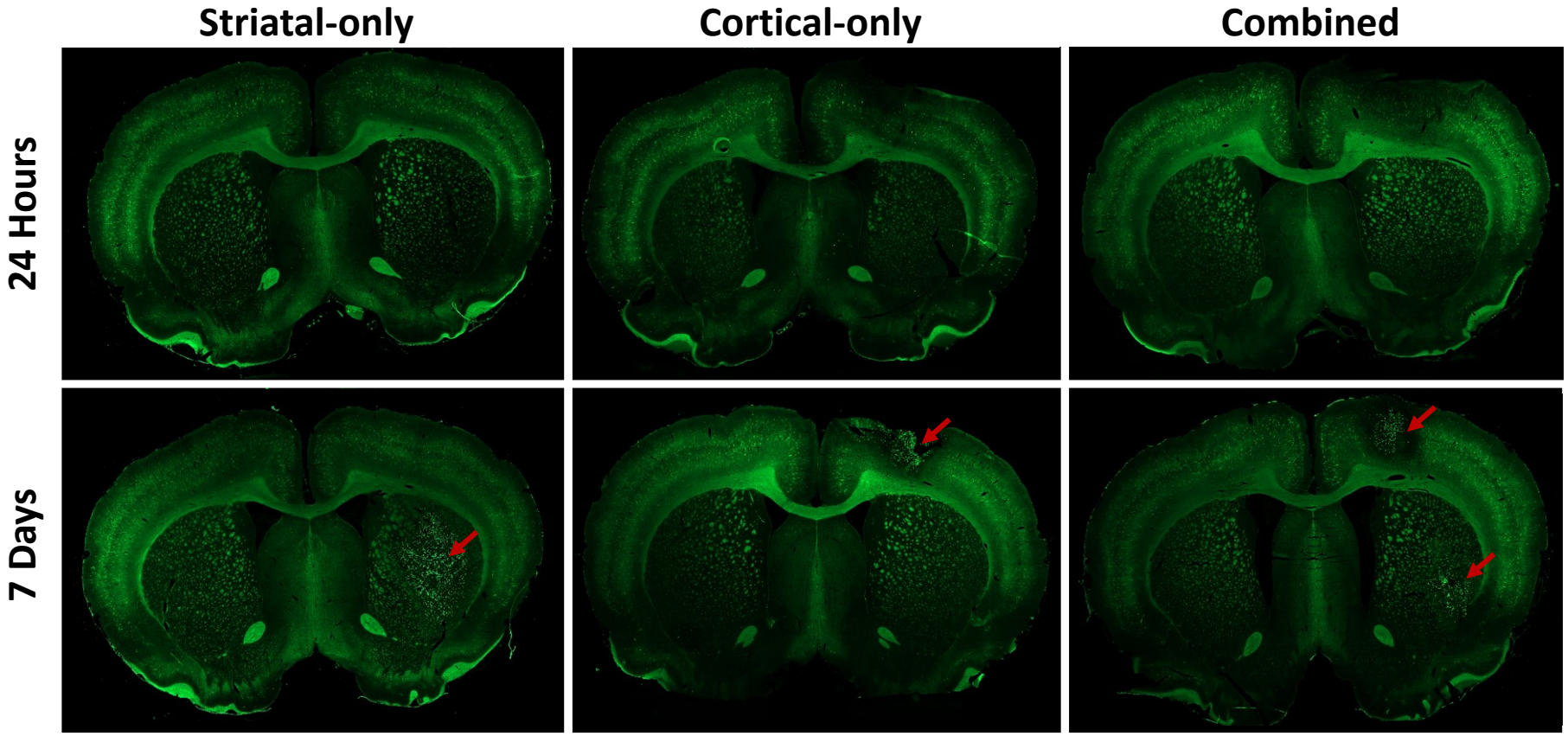

Supplemental Figure 5: WFA staining following stroke. Comparison of WFA staining at 24 hours and 7 days post-stroke. An accumulation of cells that exhibited strong intracellular WFA staining (red arrow) was observed within the infarct core of all stroked animals at 7 days following stroke.